EPIGENETIC DRUG COMBINATION OVERCOMES BONE MARROW MICROEVNIRONMENT-INDUCED CHEMOPROTECTION IN PEDIATRIC ACUTE LYMPHOBLASTIC LEUKEMIA VIA MODULATION OF CD81 AND BTK

by

Anthony Joseph Quagliano

A dissertation submitted to the Faculty of the University of Delaware in partial fulfillment of the requirements for the degree of Doctor of Philosophy in Biological Sciences

Summer 2020

EPIGENETIC DRUG COMBINATION OVERCOMES BONE MARROW MICROEVNIRONMENT-INDUCED CHEMOPROTECTION IN PEDIATRIC ACUTE LYMPHOBLASTIC LEUKEMIA VIA MODULATION OF CD81 AND BTK

by

Anthony Joseph Quagliano

Approved: _____
Velia M. Fowler, Ph.D.
Chair of the Department of Biological Sciences

Approved: _____
John A. Pelesko, Ph.D.
Dean of the College of Arts and Sciences

Approved: _____
Douglas J. Doren, Ph.D.
Interim Vice Provost for Graduate and Professional Education and Dean of the Graduate College

I certify that I have read this dissertation and that in my opinion it meets the academic and professional standard required by the University as a dissertation for the degree of Doctor of Philosophy.

Signed: _____

Erica M. Selva, Ph.D.
Professor in charge of dissertation

I certify that I have read this dissertation and that in my opinion it meets the academic and professional standard required by the University as a dissertation for the degree of Doctor of Philosophy.

Signed: _____

Sonali P. Barwe, Ph.D.
Member of dissertation committee

I certify that I have read this dissertation and that in my opinion it meets the academic and professional standard required by the University as a dissertation for the degree of Doctor of Philosophy.

Signed: _____

Randall L. Duncan, Ph.D.
Member of dissertation committee

I certify that I have read this dissertation and that in my opinion it meets the academic and professional standard required by the University as a dissertation for the degree of Doctor of Philosophy.

Signed: _____

John H. Slater, Ph.D.
Member of dissertation committee

I certify that I have read this dissertation and that in my opinion it meets the academic and professional standard required by the University as a dissertation for the degree of Doctor of Philosophy.

Signed: _____

Donna S. Woulfe, Ph.D.
Member of dissertation committee

I certify that I have read this dissertation and that in my opinion it meets the academic and professional standard required by the University as a dissertation for the degree of Doctor of Philosophy.

Signed: _____

Shou Wei, Ph.D.
Member of dissertation committee

ACKNOWLEDGMENTS

I first wanted to extend my utmost gratitude to my advisor, Dr. Sonali Barwe. Back in January of 2015, I was scrambling to find a lab to do my master's thesis in. Dr. Barwe was incredibly inviting and offered me an excellent opportunity to work on a project that was completely in-line with my interests. Throughout these past five and a half years, she has been an amazing mentor and one of my favorite people to talk science with. One of the fondest memories I will hold on to from my doctoral training will be our in-depth conversations where we freely speculated on datasets and imagined new and different experiments we could try. Some of the best experiments I performed and data I obtained came as a direct result of those conversations, and they never ceased to make me excited about what was coming next in our work.

I also wanted to thank my co-mentor, Dr. Anilkumar Gopalakrishnapillai. You have an incredible knack for lighting a fire underneath me when I most needed it. Your passion for research inspires me and your enthusiasm when we made a big breakthrough was infectious. I appreciate all of your encouragement throughout these five and a half years and know that I could not have achieved what I have without your assistance.

I would be remised if I didn't specifically mention the assistance I received from Dr. Randy Duncan. From the time I stepped into his classroom for "Advanced Physiology", he challenged me. I have the utmost respect for you Dr. Duncan, and will be forever grateful for your assistance in the classroom, on my committee, and with writing my recommendation letters to medical school.

I would also like to express my gratitude to the rest of my dissertation committee: Dr. Donna Woulfe, Dr. Shou Wei, Dr. John Slater, and Dr. Erica Selva, for your incredible assistance throughout my tenure. You all continually challenged me in my committee meetings, and your feedback was invaluable. Without your assistance, I could not have taken my project the levels I was able to.

To my mother, Debi, and my father, Dick, I wanted to say I love you both very much and thank you for your unending support. I've been away from home for nearly 10 years now, yet it never feels like that. Both of you are just a phone call away whenever I need to talk things through or just talk about something to distract me from the stress. I am appreciative to always have your hands at my back, and I look forward to continuing making you proud in the future.

To all of my labmates and the SNERPs, both past and present, thank you as well. The journey of a doctoral student is never complete without having close colleagues you can rely on. I wish you all the success and happiness the world can offer each and every one of you.

To my best friends: Dexter, Alex, and Collin, you live all over the country and we don't see each other nearly enough. But I know that you all are just a phone call away. When times get tough, I appreciate having you boys to turn to for a laugh or a distraction.

And finally, I need to mention my better half, Claire. You were there for me through all of my struggles, frustrations, and late nights. No matter how my day went, having you to lean on and talk to was the best support I could have ever asked for. There aren't any words I can use to properly describe how I feel about you and everything you've done for me, so I'll just say thank you and I love you.

TABLE OF CONTENTS

LIST OF TABLES

LIST OF FIGURES

ABSTRACT

Acute Lymphoblastic Leukemia (ALL) is the most commonly diagnosed cancer in pediatric patients in the United States. While recent advances have improved remission rates to upwards of 95%, ALL is still plagued by relapse in nearly 20% of patients. Patients in relapse are more likely to be refractory and have higher mortality rates (50%). The occurrence of these relapse events can be attributed to the accumulation of epigenetic alterations during leukemogenesis. Modulations in DNA methylation and modification of histone proteins can result in an increased occurrence of chemoresistance. A chemoresistant state can be achieved when malignant cells interact with elements within the bone marrow microenvironment. This is referred to as bone marrow microenvironment-induced chemoprotection (BMC) and is prevalent in hematologic malignancies like ALL.

In this study, I investigate the use of the epigenetic modifiers azacitidine (DNA methyltransferase inhibitor) and panobinostat (histone deacetylase inhibitor) in overcoming the effects of BMC in ALL. I identify that these two drugs in combination (aza/pano) have a synergistic killing effect and are not subject to chemoprotective effects when treating ALL cells in direct co-culture with osteoblast-like cells. Minimally cytotoxic concentrations of aza/pano sensitize ALL cells to chemotherapy through a reduction in the surface expression of the tetraspanin protein CD81 and its associated pro-survival signaling through BTK and p53. One cycle of aza/pano treatment *in vivo* potentiates the effectiveness of subsequent chemotherapy by mobilizing leukemic cells from the bone marrow into the peripheral blood. This study

identifies a novel method of improving treatment of ALL via the use of epigenetic sensitization and modulation of CD81 surface expression.

Chapter 1

INTRODUCTION

1.1 Acute Lymphoblastic Leukemia

Acute lymphoblastic leukemia (ALL) is a hematologic malignancy that is characterized by the accumulation of immature white blood cells in the bone marrow (Hunger and Mullighan, 2015). ALL is the most commonly diagnosed cancer in pediatric patients, accounting for over 3,000 new cases annually in the United States and is the leading cause of cancer deaths amongst children despite having initial remission rates over 90%. The development of these cells is disrupted due to the presence of chromosomal translocations and/or mutations in key proteins. The accumulation of these cells within the bone marrow can inhibit the production of healthy and functional blood cells. Due to this, patients with ALL commonly present with anemia and are at higher risks of infection. The malignant cells can also exit the bone marrow and proliferate in other organs throughout the body; the most common of which are the liver, spleen, and lymph node.

ALL is classified into two different subtypes based on the specific precursor cell that is predominantly affected (T-cell: T-ALL; B-cell: B-ALL) (Chiaretti et al., 2014). B-ALL accounts for nearly 85% of patients while T-ALL only affects 15%. B-ALL is further subclassified by the specific progenitor cell that is affected. Pro/pre- B-ALL shows alterations in the pro/pre-B progenitor cell, while common ALL originates from mutated mature B-cells. Pro/pre B-ALL have similar

prognoses, both of which are more favorable than common B-ALL. T-ALL has a worse prognosis than B-ALL because it is more difficult to treat. Cytogenetic markers such as chromosomal translocations and other genetic abnormalities can also further subclassify ALL. Patients with hyperdiploidy (non-random gain in at least five chromosomes) have more favorable outcomes, while patients presenting with hypodiploidy (fewer than 44 chromosomes) are more adverse. Patients with chromosomal translocations such as t(9;22)(q34;q11)(*BCR-ABL1* or "Philadelphia chromosome") are identified as adverse risk, while patients with translocation such as t(12;21)(p13;q22)(ETV6-RUNX1 or *TEL-AML1*) are highlighted as good prognosis.

1.2 Treatment of ALL

Treatment of ALL is separated into three phases: induction, consolidation, and maintenance. The induction phase consists of treatment with a combination of chemotherapeutic drugs such as vincristine, dexamethasone, and daunorubicin (a topoisomerase II inhibitor). Depending on cytogenetic markers and risk stratification, patients can also receive higher intensity chemotherapy such as cytarabine (disrupts DNA synthesis by incorporating into DNA), or targeted therapies such as imatinib (inhibits the Bcr/Abl kinase in Philadelphia chromosome positive patients). The aim for induction therapy is the complete removal of all traces of leukemia from the bone marrow and a return of normal blood counts. The continued presence of leukemic cells in the bone marrow following completion of treatment is referred to as minimal residual disease

(MRD) (Campana, 2010). While induction therapy can often achieve remission by itself, the patient has not necessarily been cured.

Following completion of induction therapy, patients move into the second phase of treatment: consolidation. This phase often consists of drugs similar to induction, but this time they are given at higher doses in an effort to remove any remaining traces of leukemia from the body. Proper consolidation therapy is crucial for minimizing or eliminating MRD and preventing secondary recurrences of ALL in patients (Campana, 2010; Health Quality, 2016; Stow et al., 2010).

The final phase of treatment is maintenance. Patients typically receive chemotherapeutics such as methotrexate which can be combined with the drugs used in previous phases (such as vincristine and dexamethasone). Maintenance therapy lasts for about two additional years in an effort to prevent relapse.

1.3 Chemoresistance and the Role of Epigenetics in ALL

Despite having initial remission rates over 90%, patients with ALL continue to battle with relapse. Nearly 20% of patients will have some form of a secondary recurrence of this malignancy, which is often more aggressive and leads to higher rates of mortality (50%) (Locatelli et al., 2012). One of the primary causes of relapse is the resistance of leukemic cells to chemotherapy. Resistance of ALL cells to chemotherapeutics can come in a multitude of forms (Table 1.1) and can often be the result of epigenetic aberrations (Burke and Bhatla, 2014).

The term “epigenetics” refers to the modification of gene expression independent of changes in the genetic code itself (Dupont et al., 2009). It often

involves heritable changes in DNA methylation (addition of methyl group to the nucleotide cytosine) or histone modifications such as acetylation (addition of an acetyl group to lysine residues on histone proteins near the histone tail) or methylation (addition of a methyl group to amino acids such as lysine or arginine in histones), as a way to turn the expression of specific genes "on" or "off" (Bannister and Kouzarides, 2011; Berger et al., 2009; Jin et al., 2011).

Chemoresistance mechanism	**Example protein/pathway**	**Example description and drugs affected**	**Reference**
Drug receptor down-regulation	Glucocorticoid receptors	Insufficient expression of glucocorticoid receptors prevents induction of apoptosis	(Geley et al., 1996)
Drug receptor modifications	Glucocorticoid receptors	Receptor mutations, decreased activity, or internalization prevents uptake of drugs (like glucocorticoids) into the cell	(Catts et al., 2001)
Intracellular drug efflux	MRP1	Mediate transport of a broad spectrum of drugs	(Winter et al., 2013)
Intracellular drug degradation	5' Nucleotidase II	Enzyme inactivation of nucleoside analogues	(Tzoneva et al., 2013)
Gene deletion/mutation	DCK/FPGS	Genetic deletions of DCK and FPGS prevent drug activation and lead to resistance against both cytarabine and methotrexate respectively	(Nowak et al., 2015)
Targeted protein modification	BCR/ABL	BCR/ABL kinase domain mutations confer resistance to imatinib treatments	(Pfeifer et al., 2007)
Upregulation of proliferative proteins	A20	Overexpression of A20 leads to increased proliferation and anti-apoptotic effects in conjunction with Erk signaling and p53 to confer chemoresistance	(Chen et al., 2015)
Cellular quiescence	Exit to G_0	Intracellular signaling causes an exit from cell cycle to G_0 and resistance to multiple drugs that rely on cells to be actively proliferating to be effective	(Redner et al., 1990)
Overexpression of "-" regulators of apoptosis	GSTM1	Overexpression prevents the activity of apoptotic regulators like Bim	(Hosono et al., 2010)

Ion flux	hERG1	hERG1 channel activity increased pro-survival signaling and conferred multidrug resistance	(Pillozzi et al., 2011)
Redox adaptation	Antioxidant production and MCL-1	Increased mitochondrial calcium influx increase levels of reactive oxygen species, leading to an adaptation process that increases antioxidant and MCL-1 levels to induce multidrug resistance	(Liu et al., 2015)
Abnormal glucose metabolism	GLUT1	Increase in transporter expression increases glucose uptake and prevents cells from undergoing metabolic stress and defends against chemotherapy	(Liu et al., 2014)
Unfolded protein response	XBP1	Expression of XBP1 protects cells from ER stress and leads to chemoresistance	(Kharabi Masouleh et al., 2014)
Increased protein expression of DNA repair proteins	Alt-NHEJ pathway	Increased activity of DNA repair pathway allows cells to repair more readily and protect against chemotherapy	(Hahnel et al., 2014)
Protein stabilization	p73	p73 stabilization by Kpm/Lats2 phosphorylation of YAP2 protected cells from DNA damaging chemotherapeutics	(Kawahara et al., 2008)
MicroRNA aberrations	miR125b/100/99a	Dysregulation of miRNAs can alter expression patterns of key proteins and lead to resistance against chemotherapy drugs like vincristine	(Akbari Moqadam et al., 2013)
Cell adhesion-mediated drug resistance	Cell-cell/matrix adhesion	Binding of cellular adhesion molecules on the surface of ALL cells to other cells or the ECM in the BM stimulate a chemoprotective effect	(Hazlehurst and Dalton, 2001; Li and Dalton, 2006)

Table 1.1 Mechanisms of Chemoresistance in ALL

During leukemogenesis, it is known that ALL cells undergo drastic changes in their epigenetic profiles (Burke and Bhatla, 2014; Figueroa et al., 2013; Navarrete-Meneses and Perez-Vera, 2017; Newton et al., 2014). Changes in DNA methylation patterns and modification of histone proteins can not only be a driver of ALL development, but can also

induce chemoresistance (Figure 1.1). Patients in relapse often have drastically different epigenetic profiles compared to their samples at initial diagnosis (Burke and Bhatla, 2014).

1.3.1 Epigenetic modifiers

Due to the role of epigenetic modifications in leukemogenesis and the development of chemoresistance, epigenetic modifiers such as DNA methyltransferase inhibitors (DNMTi), histone deacetylase inhibitors (HDACi), and others have been used to combat these aberrations.

In this study, I use the DNMTi azacitidine and the HDACi panobinostat. Azacitidine functions by trapping DNMT (DNMT1: maintenance of methylation patterns; DNMT3a/b: De Novo methylation) and preventing its progression along DNA. This leads to hypomethylation of DNA promoters, thereby increasing associated gene expression. However, there is some evidence to support that demethylation of gene bodies can actually decrease gene expression (Yang et al., 2014).

Panobinostat is a non-selective HDACi. By preventing the deacetylation of histone proteins, lysine residues remain with a net neutral charge instead of net positive charge. This causes the histone protein to dissociate from the negatively charged DNA strands and unwind DNA, providing access of transcriptional machinery to DNA.

The use of epigenetic modifiers like azacitidine and panobinostat has had some preliminary success either alone or in combination with one another. However,

their greatest efficacy is achieved when they are combined with traditional chemotherapeutics, where the modifiers can potentiate the effects of chemotherapy through a variety of mechanisms (Quagliano, 2020).

1.4 Bone Marrow Microenvironment

1.4.1 Bone Marrow Microenvironment-Induced Chemoprotection

The bone marrow (BM) in healthy individuals is the site of hematopoiesis, where hematopoietic stem cells (HSCs) undergo differentiation to give rise to blood cells. Within the BM is also a collection of other cells such as osteoblasts and mesenchymal stem cells which can secrete extracellular matrix (ECM) proteins and soluble factors. In normal hematopoiesis, HSCs interact directly with these supporting cells and their secreted ECM proteins and soluble factors to help foster survival and proper differentiation into functional blood cells (Birbrair and Frenette, 2016).

However, ALL cells can exploit these same interactions as a mechanism to induce pro-survival signaling and resist chemotherapy (Meads et al., 2008).This phenomenon is known as bone marrow microenvironment-induced chemoprotection (BMC) and can be a driving force in promoting relapse in ALL.

1.4.2 Cellular Adhesion Molecules and Their Role

While the binding of soluble factors present in the BM to their cognate receptors on ALL cells can be responsible for the development of the chemoresistant states associated with BMC, many of the effects of BMC are mediated through direct cell-cell or cell-matrix contacts within the BM

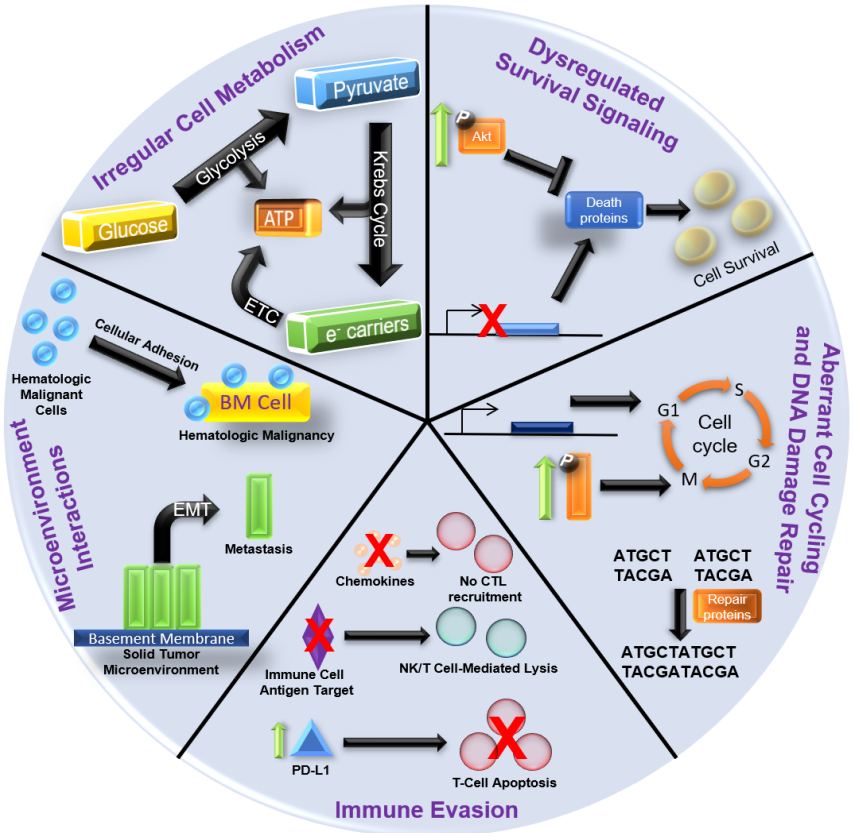

Figure 1.1 Hallmarks of Epigenetic-Induced Chemoresistance Epigenetic dysregulation is a driving force in oncogenesis and the development of chemoresistance. Silencing of tumor suppressor genes or genes related to drug transport or metabolism can render cancer cells resistant to therapies. Dysregulated survival signaling (over-activation of pro-survival or inhibition of cell death signaling) can occur via increased/decreased expression of genes associated with specific pathways. Aberrant cell cycling can be caused by the over/under-expression of proliferative/checkpoint proteins, or increased activation of signaling pathways related to proliferation. DNA damage repair can be augmented by an increased expression of repair proteins and disruption of checkpoint signaling. Augmented intracellular signaling pathways can alter cytokine expression and cause immunosuppression, while aberrant antigen expression can disrupt immune cell targeting and activation. Epigenetic alterations in cellular adhesion mediate interactions within the tumor microenvironment, the detailed consequences of which are described in more detail in figure 2. Resistance mechanisms are not restricted to just one of the categories, and there is often crossover to multiple categories.

(Barwe et al., 2017). These interactions occur through the binding of cellular adhesion molecules (CAMs) on ALL cells to target CAMs on BM cells or epitopes on ECM proteins. Upon binding of these CAMs to their targets, associated downstream pathways can be altered within ALL cells, often times resulting in a resistance to cell death.

Due to their ability to induce BMC, CAMs have become prime targets for inhibitors in an effort to circumvent their chemoprotective effects. The most widely studied adhesion molecule in hematologic malignancies like ALL is very-late antigen 4 (VLA-4: Integrin $\alpha_4\beta_1$). Two such inhibitors have been developed: 1) a monoclonal antibody (natalizumab) which acts as a competitive inhibitor to VLA-4 targets such as vascular cellular adhesion molecule 1 (VCAM1) and 2) a tellurium compound (AS101) that reduces thiols in the extracellular domains to prevent successful adhesion (Figure 1.2) (Hsieh et al., 2013; Layani-Bazar et al., 2014). Anti-CAM therapies against targets like VLA-4 and others have had moderate successes in clinical models, however, due to the large variety of CAMs that can elicit BMC and the ability of multiple CAMs to function simultaneously, these targeted therapies can sometimes lack efficiency.

1.5 Tetraspanins

1.5.1 Structure and Function

Beyond integrins, other classes of cell surface proteins can also be responsible for mediating cellular adhesion. One such example is the transmembrane 4 superfamily (tetraspanins, TSPANs). Proteins in this family are characterized by

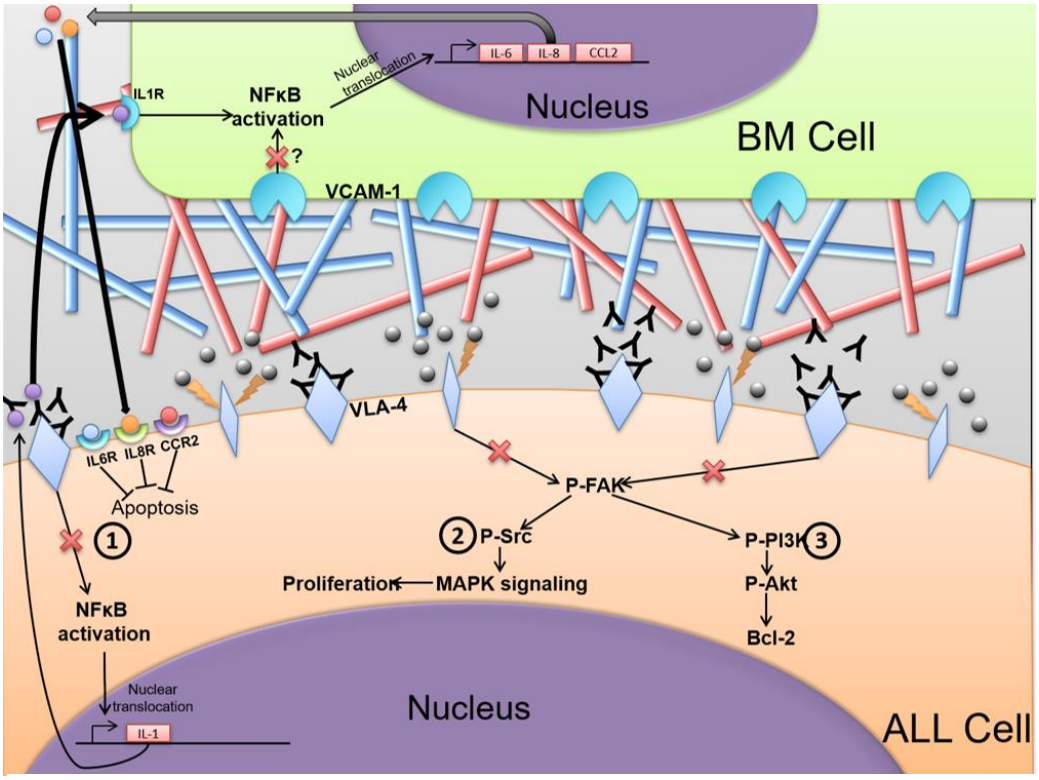

Figure 1.2 VLA-4 induces chemoprotection through a variety of mechanisms and can be inhibited by Natalizumab and AS101 VLA-4 binds to its target VCAM-1 on bone marrow stromal cells or to ECM proteins such as osteopontin and fibronectin. This interaction activates pro-survival signaling pathways such as (1) NF-κb, (2) Src/MAPK, and (3) PI3K/Akt. Disruption of these interactions by Natalizumab (black Ys), a monoclonal antibody that targets VLA-4, or AS101 (black spheres), which oxidizes adjacent thiol residues in the exofacial domain of VLA-4 molecules. This prevents target binding and causes cytoskeletal and conformational changes in the VLA-4 molecule, results in inhibition of these pathways (shown by red crosses).

the presence of four transmembrane domains, intracellular N- and C-termini, and two extracellular loops: a small 13-30 amino acid loop (EC1) and a large 200-300 amino acid loop (EC2) (Figure 1.3) (Charrin et al., 2014). Though TSPANs are not known to act as typical receptors, there is extensive support for their role in mediating the organization of other cell surface proteins, cytoskeletal proteins, and

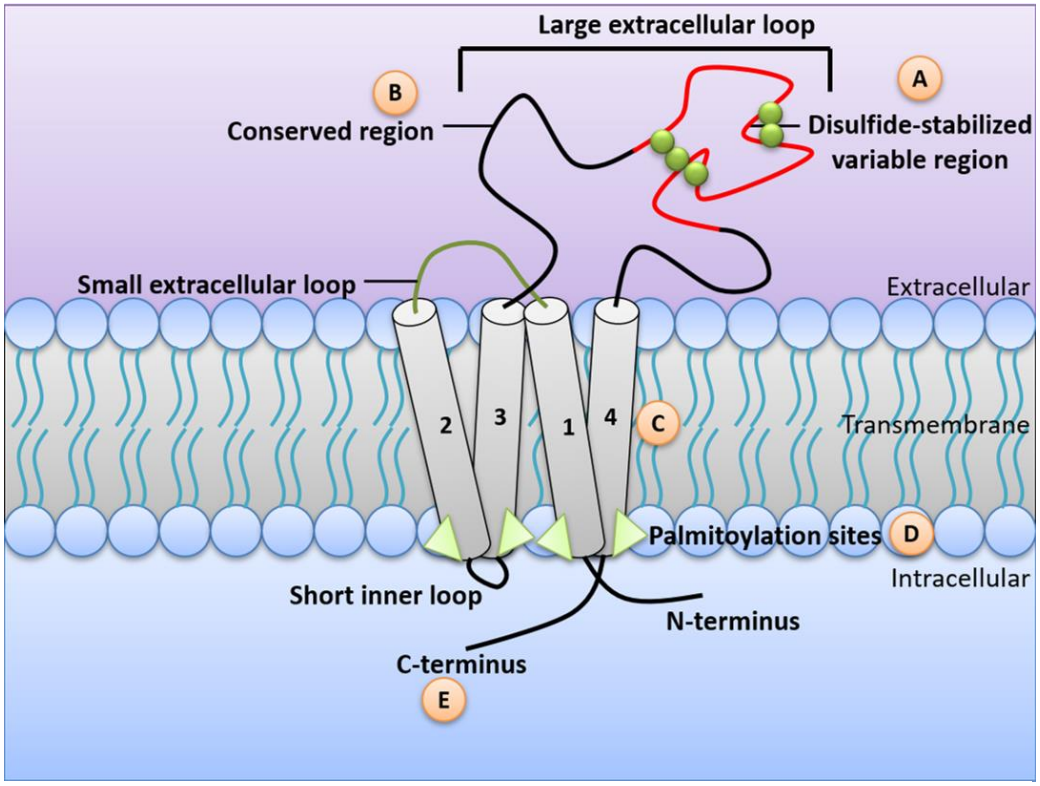

Figure 1.3: Structure and domain functions of TSPANs TSPANs are characterized by the presence of 4 transmembrane domains (1-4). There are multiple regions within the protein that mediate key effects A) Disulphide stabilized variable region of the large extracellular loop (EC2) which is responsible for the unique interactions specific to each TSPAN. B) The Conserved region of the EC2 loop mediates homodimerization. C) Transmembrane regions are important for the formation of tetraspanin enriched microdomains (TEMs). D) Palmitoylation sites are crucial to the proper formation of new TEMs and also play a role in signaling. E) The c-terminus is responsible for interacting with signaling and cytoskeletal proteins.

intracellular signaling proteins, leading to changes in cellular adhesion and survival.

There are four major functional domains within TSPAN proteins (Stipp et al., 2003). The EC2 loop contains two separate regions: a disulfide-stabilized

hypervariable region responsible for mediating the specific interaction of each individual TSPAN, and a highly conserved region which is responsible for homodimerization (Higginbottom et al., 2000; Kitadokoro et al., 2001; Seigneuret et al., 2001). Transmembrane regions are responsible for the formation of the "TSPAN web" or "Tetraspanin-enriched microdomains (TEMs)", which will be discussed more below. The transmembrane domains mediate a multitude of in hydrophobic interactions and hydrogen bonding, creating a tightly formed and stable TEMs (Stipp et al., 2003). TSPANs also have intracellular palmitoylation sites which play a role in signaling and TEM formation (Berditchevski et al., 2002; Charrin et al., 2002; Delandre et al., 2009; Zhou et al., 2004). Finally, the intracellular C-terminus mediates both signaling and interactions with the cytoskeleton (Berditchevski and Odintsova, 1999; Berditchevski et al., 1997; Carloni et al., 2004; Delaguillaumie et al., 2002; Rous et al., 2002; Termini and Gillette, 2017).

1.5.2 Tetraspanin-Enriched Microdomains

Tetraspanin-enriched microdomains (TEMs) are membrane formations that assemble functionally related proteins to potentiate their effects (Hemler, 2005). TEMs consist of TSPAN proteins, which act as the scaffolding for the microdomain, and can also include adhesion molecules, like integrins or IgSF members, and other signaling receptors like G-proteins and tyrosine kinases (Figure 1.4) (Yanez-Mo et al., 2009).

TEMs share many similarities with lipid rafts, however, there are a few key differences to note between the two. Specifically, TEMs are not subject to cholesterol breakdown and do not typically present with GPI-linked proteins or caveolin (Le Naour et al., 2006).

TEM formation relies on redundancies present within the functional domains of TSPANs mentioned above (Stipp et al., 2003). Palmitoylation regions are

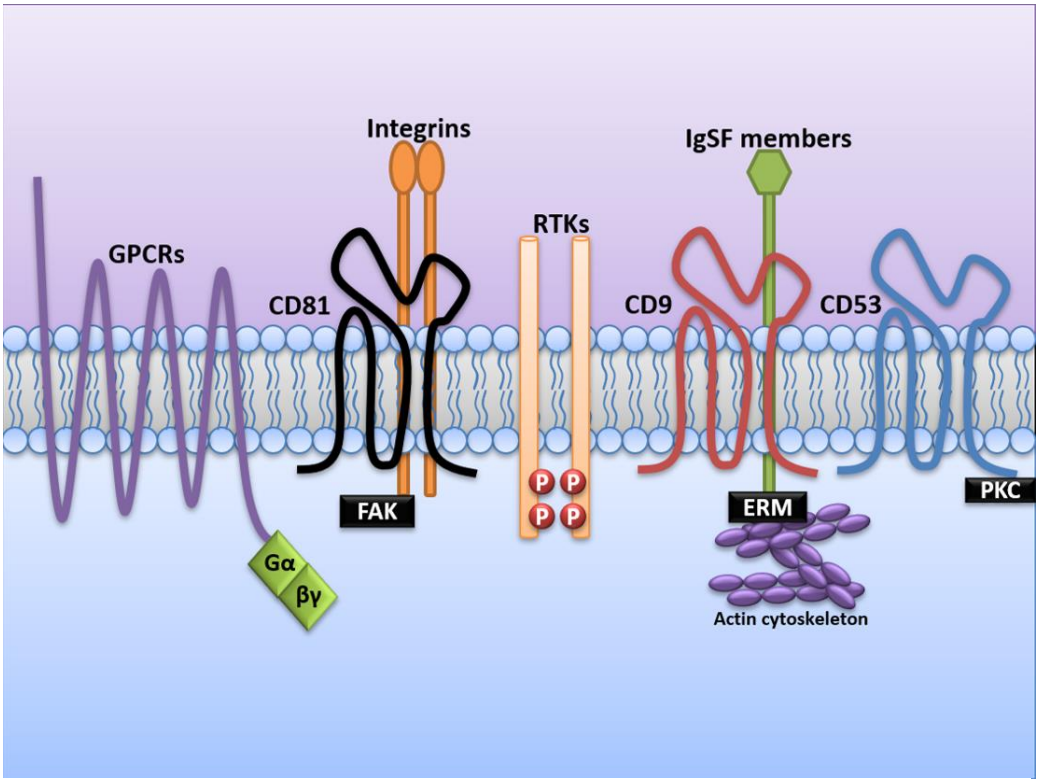

Figure 1.4: Tetraspanin enriched microdomains play a key role in TSPAN function Tetraspanin enriched microdomains (TEMs) are dynamic membrane entities that play a key role in mediating interactions with the BM. TSPANs act as scaffolding proteins to bring together many proteins with similar functions such as CAMs (like integrins and IgSF members) and signaling receptors (GPCRs and RTKs). The cross-linking of TSPANs creates a large secondary signaling network which can effectively transduce extracellular stimuli inside to intracellular signaling pathways.

responsible for the formation of new TEMs on the cell surface, while transmembrane domains are important for the tight, strong packing of the proteins together. The multiple regions of the EC2 loop are responsible for the selectivity of individual TEMs, and thereby, their functional consequences. Due to the strong interactions of individual TSPANs with one another, large secondary signaling networks can be formed within TEMs (Hemler, 2005).

1.5.3 Microenvironmental Interactions and CD81

Though evidence has yet to be provided on the function of TSPANs as receptors or adhesion molecules, their regulation of cell surface dynamics has consequences on interactions with microenvironments. Much of the understanding of TSPANs and their microenvironmental functions comes from studies in solid tumors (Table 1.2) (Yang et al., 2016). Little progress has been made on the understanding of TSPANs and their role in hematologic cells and malignancies,. Since it is the focus of this project, an in-depth characterization of the role of CD81 in hematologic cells and malignancies is provided below. A more exhaustive list of other specific TSPAN interactions and functions is described in table 1.3.

CD81 is known to be a poor prognostic marker in AML, where it controls cellular adhesion, migration, BM homing, and drug resistance (Boyer et al., 2016; Gonzales et al., 2017b). While not much is known about its function in B-ALL, its transcript level is nearly five-fold increased compared to healthy samples. It is also known to interact with VLA-4 and other integrins, the interaction of which is

Protein	Cell type	Function	Reference
CD9	Breast cancer	• Interactions with P-FAK, p38, MAPK, JNK, and talin1 (regulates integrin activity) • Mediates invasiveness and metastasis • Crosstalk with mesenchymal stem cells confers chemoresistance • Complexes with CD81 to mediate VLA-3 adhesion • Interacts with EWI-2	(Powner et al., 2011) (Rappa et al., 2015) (Ullah et al., 2019) (Gustafson-Wagner and Stipp, 2013) (Stipp et al., 2001)
	Breast carcinoma		
	Melanoma		
CD63	Fibrosarcoma	• Complexes with VLA-3 and PI4K in focal complexes at cell periphery	(Berditchevski et al., 1997)
CD81	Breast cancer	• Complexes with CD9 to regulate VLA-3 adhesion via PKCα • Regulates motility through Rac-GTPase • Metastasis inducer • Increases cell motility via MT1-MMP expression through Akt and Sp1 signaling pathways • Linked to ERK/MAPK signaling through Shc • Interacts with EWI-2 • Inhibits metastasis through MMP signaling via ERK • Mediates growth and metastasis through ERK/Akt signaling and MMP expression	(Gustafson-Wagner and Stipp, 2013) (Tejera et al., 2013) (Uretmen Kagiali et al., 2019) (Hong et al., 2014) (Carloni et al., 2004) (Stipp et al., 2001) (Park et al., 2019) (Mizoshiri et al., 2019)
	Melanoma		
	Liver tumor		
	Melanoma		
	Bladder cancer		
	Osteosarcoma		
CD82	Non-small cell lung cancer	• Strengthens E-cadherin adhesion and reduces tyrosine phosphorylation of β-catenin • Inhibits cellular migration through actin organization • Represses TGF-β1 and Wnt signaling associated with epithelila to mesenchymal transition and metastasis • Inhibits fibronectin adhesion-induced epithelial to messenchymal transition by suppressing integrin signaling • Metastasis suppressor • Inhibits invasion and metastasis via regulation of TGF-β1	(Abe et al., 2008) (Liu et al., 2012) (Lee et al., 2019) (Lee et al., 2017) (Liu and Zhang, 2006) (Zeng et al., 2018)
	Prostate cancer		
	Multiple cancers		
	Esophageal cancer		
CD151	Breast cancer	• Links VLA-3 to other TSPANs • Loss impairs cell motility • Promotes metastasis via TGF-β1/Smad signaling • Mediates communication with osteoblasts (loss abolishes pro-migratory/survival signals) • Stimulates adhesion-dependent activation of Ras, Rac, and Cdc42 by facilitating integrin β1 association with small GTPases	(Gustafson-Wagner and Stipp, 2013) (Winterwood et al., 2006) (Zhao et al., 2018) (Grudowska et al., 2017) (Hong et al., 2012) (Wang et al., 2016) (Sadej et al., 2014)
	Prostate cancer		
	Melanoma		
	Osteosarcoma		
	Multiple cancers		

	Kidney cancer	• Interactions with Akt, p38, NFκB, FAK, and integrin β1 • Regulates post-adhesion events and the involved with the process of metastasis • Mediates integrin-independent drug resistance • Promotes proliferation and migration through GSK3β/p21/cyclin D signaling	(Hwang et al., 2019) (Wang et al., 2019)
TSPAN 15	Oral squamous cell carcinoma	• Positively regulates development and promotes metastasis through B-catenin signaling and increased ADAM10 expression • Interacts with BTRC to promote cancer metastasis through NFκB signaling	(Hiroshima et al., 2019) (Zhang et al., 2018)
TSPAN 7	Lung cancer	• Promotes migration and proliferation via epithelial to mesenchymal transition	(Wang et al., 2018a)
TSPAN 1	Cholangiocarcinoma	• Promotes epithelial to mesenchymal transition and metastasis via PI3K/Akt signaling	(Wang et al., 2018b)

Table 1.2: Key microenvironmental interactions of TSPANs in solid tumors TSPANs have been widely characterized in many different solid tumors. Their various effects could shed light on possible roles they may play in hematologic

Protein	Cell type	Function/Interaction	Reference
CD9	B-cells	• Associates with CD19/CD21 complex to lower threshold of activation and enhance signaling • Facilitates VLA-4 binding to dendritic cells	(Horvath et al., 1998) (Yoon et al., 2014) (Barrena et al., 2005)
	T-cells HSCs B-ALL	• Loss of expression associated with mature B-cells being ready to migrate and leave the BM • Modulates TCR signaling by interaction with CD3 and CD4 • Bone marrow homing	(Tai et al., 1996) (Leung et al., 2011) (Arnaud et al., 2015) (Rubinstein et al., 1996) (Yamazaki et al., 2011)
	ALL	• Modulates CXCR-4-mediated cell migration through RAC1 signaling	(Komada and Sakurai, 1994) (Yoon et al., 2010)
	MM and Lymphoma Lymphoma	• Interacts with VLA-4 and VLA-5 • Regulates LSC activity • Possible shedding during relapse • Inverse correlation of expression with survival	(Hu et al., 2014) (Machado-Pineda et al., 2018)
	MM AML HSCs	• Hypermethylation leads to a decrease in bortezomib sensitivity • Controls VLA-5 mediated cell adhesion by modulating association with ADAM17 • Enhances susceptibility to cell-mediated cytolysis	(Shallal and Kornbluth, 2000) (Touzet et al., 2019) (Leung et al., 2015)

		• Relevant marker for MRD and targeting of LSCs • Regulates engraftment and mobilization of CD34+ stem cells and modulates VLA-4 activity	
CD37	T-cells CLL Plasma cells Neutrophils	• Regulates proliferation • Antigen presentation • Mediates pro-survival signaling via PI3K through "ITAM" motif in C-terminus • Induces SHP1-dependent apoptotic signaling through "ITIM-like" motif in N-terminus • Clusters VLA-4 and activates Akt for survival signaling • Promote adhesion and recruitment via cytoskeletal functions downstream of integrin-mediated adhesion	(van Spriel et al., 2004) (Sheng et al., 2009) (Lapalombella et al., 2012) (Lapalombella et al., 2012) (van Spriel et al., 2012) (Wee et al., 2015)
CD53	T-cells Lymphoma B and T-cells NK cells	• Co-stimulatory signal to CD3 for activation of T-cells • Increases Bcl-XL and decreases bax expression via activation of Akt • Interacts with VLA-4 • Induces adhesion through PI3K and PKC signaling • Mediates binding of LFA-1 to ICAM-1 • Shifts cells from effectors to a proliferation phase	(Lagaudriere-Gesbert et al., 1997) (Yunta and Lazo, 2003) (Mannion et al., 1996) (Lazo et al., 1997) (Cao et al., 1997) (Todros-Dawda et al., 2014)
CD63	T-cells HPCs	• Interacts with VLA-4 • Mediates binding to osteoblasts by being taken up into osteoblasts, inhibiting Smad signaling and increasing SDF-1 secretion	(Mannion et al., 1996) (Gillette and Lippincott-Schwartz, 2009)
CD81	T-cells B-cells HSCs Erythroblasts Monocytes B-ALL MM AML	• Interacts with CD4/CD8 to co-stimulate T-cells through PLCγ, CD3ζ, SLP76, P-Lck, and cytoskeletal rearrangements • Sustains activation • Highly enriched in the formation of tunneling nanotubes (TNTs) • Complexes with CD19/CD21 to make up the B-cell co-receptor and initiates signaling through Syk/Ezrin to cause actin polymerization • Regulates expression of CD19 during development • Loss of expression associated with mature B-cells being ready to migrate and leave the BM • Inhibits proliferation, allowing cells to stay in quiescence and maintain their self-renewing capabilities • Facilitates VLA-4 adhesion to VCAM-1 • Strengthens VLA-4 and VLA-5 adhesion under shear flow • Interacts with VLA-4 and VLA-6	(Sagi et al., 2012) (Rocha-Perugini et al., 2013) (Lachambre et al., 2014) (Cherukuri et al., 2004) (Shoham et al., 2003) (Barrena et al., 2005) (Lin et al., 2011) (Spring et al., 2013) (Feigelson et al., 2003) (Rubinstein et al., 1996) (Tohami et al., 2007) (Gonzales et al., 2017a)

		• Overexpression induces cell death and reduces cell adhesion to fibronectin • Controls cellular adhesion, migration, BM homing, and drug resistance	
CD82	T-cells HSCs Erythroblasts AML B-ALL MM Macrophages	• Co-stimulation through Rho-GTPase-mediated cytoskeletal rearrangements • Enhances LFA-1 adhesion to ICAM-1 • Maintains LT-HSCs by interacting with DARC on macrophages. Induces PKCα which increases autocrine TGF-β1 and inhibits CDKs • Regulates bone marrow homing and engraftment • Facilitates VLA-4 adhesion to VCAM-1 • Regulates VLA-4 density, clustering, and stability • Bone marrow homing via N-cadherin organization • LSC adhesion and survival through STAT5/IL-10 • Akt regulation of BCL2L12 • Increases expression of EZH2 by inhibiting p38 activity • Promotes survival via activation of Wnt/β-catenin signaling • Interacts with VLA-4 and VLA-6 • Overexpression induces cell death and reduces cell adhesion to fibronectin • Associates with TLR9 to modulate nuclear translocation of NFκB for inflammatory cytokine production	(Delaguillaumie et al., 2002) (Shibagaki et al., 1999) (Hur et al., 2016) (Saito-Reis et al., 2018) (Spring et al., 2013) (Termini et al., 2014) (Marjon et al., 2016) (Nishioka et al., 2014) (Nishioka et al., 2015a) (Nishioka et al., 2015b) (Ji et al., 2019) (Rubinstein et al., 1996) (Tohami et al., 2007) (Khan et al., 2019)
TSPAN3	AML MM	• Critical for AML disease progression • Key regulator of AML cell interactions with the microenvironment • Forms fusion protein with ROS1	(Kwon et al., 2015) (Kwon et al., 2015) (He et al., 2016)

Table 1.3: Interactions and effects of TSPANs on normal and malignant hematologic cells TSPANs have a large variety of interacting partners and can mediate many different cellular processes.

known to facilitate and strengthen adhesion to targets like VCAM-1 (Feigelson et al., 2003; Mannion et al., 1996). Prior study also identified that the loss of CD81 surface expression on mature B-cells was associated with exit from the BM and entry into the blood, suggesting a role in BM homing and retention (Barrena et al., 2005).

CD81 is also known to be responsible for the proper membrane trafficking of CD19, a key component of the B-cell co-receptor along with CD21 (Cherukuri et al., 2004; Shoham et al., 2003). The B-cell co-receptor is responsible for lowering the threshold of activation of the B-cell receptor, specifically, CD19 is responsible for prolonging and amplifying the activation of BTK signaling (Fujimoto et al., 2002). Transgenic $CD81^{-/-}$ mice had reduced CD19 and showed diminished antibody responses following stimulation (Tsitsikov et al., 1997; van Zelm et al., 2010). Therefore, CD81 could be an important mediator of B-cell receptor signaling and the associated survival and adhesive affects.

Due to their ability to mediate microenvironmental interactions, TSPANs are intriguing targets for study in hematologic malignancies. Moreover, due to its interaction with CD19, CD81 could be an important mediator of the survival and progression of B-cell malignancies.

1.6 Hypothesis

Due to the significant role of epigenetics aberrations in leukemogenesis and chemoresistance, I hypothesize that treatment with the epigenetic modifiers azacitidine (DNMTi) and panobinostat (HDACi) can sensitize bone marrow microenvironment chemoprotected cells to chemotherapy. This sensitization will likely occur via modulation of the expression of cell surface proteins, and thereby, disruption of their associated survival signaling mechanisms.

Chapter 2

AZACITIDINE AND PANOBINOSTAT HAVE A SYNERGISTIC KILLING EFFECT AND SENSITIZE ALL CELLS TO CHEMOTHERAPY UNDER BMC CONDITIONS

2.1 Introduction

Relapse remains a consistent impediment to improving the efficacy of treatment in ALL and can arise through a multitude of chemoresistance mechanisms. The root cause of this chemoresistance can often be traced to underlying epigenetic aberrations that are accumulated during leukemogenesis (Burke and Bhatla, 2014; Figueroa et al., 2013; Navarrete-Meneses and Perez-Vera, 2017; Newton et al., 2014). Alterations in the epigenetic landscape of DNA methylation patterns and/or modification of histone proteins can change the expression levels of key genes, thereby shifting ALL cells into chemoresistant states.

Due to this, the use of epigenetic modifiers such as DNMTi and HDACi have become more prevalent. By targeting the machinery that drives epigenetic aberrations in leukemia, epigenetic modifiers can revert these chemoresistant effects to eliminate malignant cells (Quagliano, 2020). Moreover, these modifiers can also be used in conjunction with traditional chemotherapeutics to sensitize/potentiate the effects of chemotherapy. These effects make epigenetic modifier/chemotherapeutic combination treatments a potent approach to overcoming chemoresistance, and thereby relapse, in ALL.

Recent studies have also shed light on how epigenetic dysregulation in cancer can affect cellular adhesion. In solid tumors, this dysregulation can actually decrease microenvironmental interactions as a method to increase metastasis. In hematologic malignancies like multiple myeloma, epigenetic alterations can be a driving force to increase CAM-mediated BMC (Furukawa and Kikuchi, 2016). In leukemia, the epigenetic landscapes of patients in relapse show aberrant activation of adhesion related pathways, promoting relapse and further progression (Zampini et al., 2018). This data supports the use of epigenetic modifiers as a mechanism to combat the effects of BMC.

In this study, I focus on the use of two epigenetic modifying drugs, azacitidine (DNMTi) and panobinostat (HDACi). These individual drugs are known to induce leukemic cell death on their own as well as in conjunction with chemotherapy, however, their combination with one another has yet to be extensively studied. Due to the multiple forces that can drive the development of epigenetic aberrations, examining the efficacy of a combination of two drugs targeting different epigenetic mechanisms could provide a new mechanism to improve overall survival in ALL patients.

2.2 Materials and Methods

2.2.1 Cell Lines and Maintenance

REH (CRL-8286), CCRF-CEM (CCL-119), Nalm6 (CRL-3273), and Saos-2 (HTB-85) cells were obtained from American Type Culture Collection (ATCC), Manassas, VA. Leukemic cell lines were cultured in RPMI-1640 culture medium

supplemented with 10% fetal bovine serum (FBS), 2 mM/L L-glutamine, 25 U/mL penicillin, and 25 μg/mL streptomycin. Cells were monitored daily and kept at a density of 5 x 10^5-1 x 10^6 cells/mL. Saos-2 cells were cultured in DMEM/F12 (1:1) culture medium with the supplements described above. Cells were monitored daily and split when they reached 90% confluency. All cells were cultured at 37ºC and 5% CO_2.

Primary ALL samples isolated from bone marrow aspirates or peripheral blood of patients treated at Nemours/Alfred I. duPont Hospital for Children are banked by the Nemours BioBank. Samples were collected under a Nemours Delaware Institutional Review Board (IRB) protocol approval by the Nemours Office of Human Subjects Protection. Generation of mouse passaged patient-derived xenograft (PDX) lines was described previously (Gopalakrishnapillai et al., 2016).

2.2.2 Chemicals

Azacitidine (S1782), panobinostat (S1030), cytarabine (Ara-C)(S1648), and daunorubicin (S1648) were obtained from Selleckchem (Houston, TX). Powder was dissolved in DMSO to appropriate concentrations.

2.2.3 Chemoprotection Assay

10,000 Saos-2 cells were plated in wells of a 96-well plate and left to adhere overnight. Media was removed and 30,000 leukemic cells were added to wells with RPMI-1640 for monoculture or co-culture with Saos-2 cells. Corresponding drugs were diluted to proper concentrations in RPMI-1640 and added to necessary wells. Viability was determined after 48 h via flow cytometry (NovoCyte Flow

Cytometer; ACEA Biosciences; San Diego, CA) using forward scatter (FSC) x side scatter (SSC) gating (previously confirmed by propidium iodide staining).

2.2.4 Determination of EC50 and Synergy

For determination of EC50, 30,000 leukemic cells were plated in wells of a 96-well plate and treated with varying concentrations of azacitidine and panobinostat alone. Drugs were diluted in RPMI-1640 to the proper starting concentration, then serial diluted to the lowest concentration and added to corresponding wells. Viability was determined via flow cytometry after 48 h. Viabilities were then input into GraphPad Prism and a corresponding curve was generated using a non-linear regression (curve fit): log(inhibitor) vs. response – variable slope (four parameters), constrained to 100, interpolating an unknown of 50 using a confidence interval of 95% to determine the EC50 value.

To determine synergy, 30,000 leukemic cells were plated in wells of a 96-well plate and treated with EC50 concentrations of azacitidine and panobinostat both alone and in combination. Viability was determined via flow cytometry after 48 h. Synergy was calculated using a relative risk ratio (RRR = [Percentage of viable cells in sample treated with combination]/[[Percentage of viable cells in treatment 1 x Percentage of viable cells in treatment 2]/100]). Values < 1.00 indicate synergy.

2.2.5 Sensitization Assay

For *in vitro* sensitization, leukemic cells were cultured in a 12-well plate at a density of 200,000 cells/mL in RPMI-1640 and pre-treated with

azacitidine/panobinostat for 48 h in monoculture. After 24 h, 10,000 Saos-2 cells were plated in wells of a 96-well plate and left to adhere overnight. After completion of the 48 h pre-treatment, media was removed from Saos-2 cells and 100 μL of pre-treated leukemic cells (in RPMI1640) were transferred into co-culture with Saos-2 cells. 50 μL of drug containing chemotherapeutic (diluted to proper concentration in RPMI1640) was then added to corresponding wells. Viability was determined via flow cytometry after 48 h.

For *ex vivo* sensitization, Saos-2 cells were plated in wells of a 96-well plate and left to adhere overnight. Media was removed and 150,000 PDX cells were co-cultured with Saos-2 cells in RPMI-1640. Cells were pre-treated for 24 h with azacitidine/panobinostat. 100 μL of sample was then transferred to fresh monolayers of Saos-2 cells in a 96-well plate and 50 μL of corresponding drug was added. Viability was determined via flow cytometry after 48 h.

2.2.6 Statistical Analysis

Statistical analysis was performed using a t-test: two sample assuming unequal variance to evaluate the variance between two data points captured from a minimum of three trials. A p-value < 0.05 was considered statistically significant.

2.3 Results

2.3.1 Saos-2 Cells Induce Chemoprotection via Direct Cell-Cell Contact with Leukemic Cells

To begin this study, I developed a model of BMC. Three different ALL cell lines (REH, Nalm6, and CCRF-CEM) were cultured alone, in direct contact (cellular adhesion) with monolayers of Saos-2 cells (osteoblast-like to mimic the BM), or suspended above Saos-2 monolayers in 0.4 micron Transwell filters (to study the effects of diffusible soluble factors alone). These conditions were then treated with cytarabine (Ara-C) for 48 h. ALL cells treated in monoculture and in transwells had similar viabilities, while cells treated in direct contact with Saos-2 monolayers had significant ($p < 0.05$) increases in cell survival (Figure 2.1). This highlights the development of a successful BMC model that is reliant upon direct cell-cell contact.

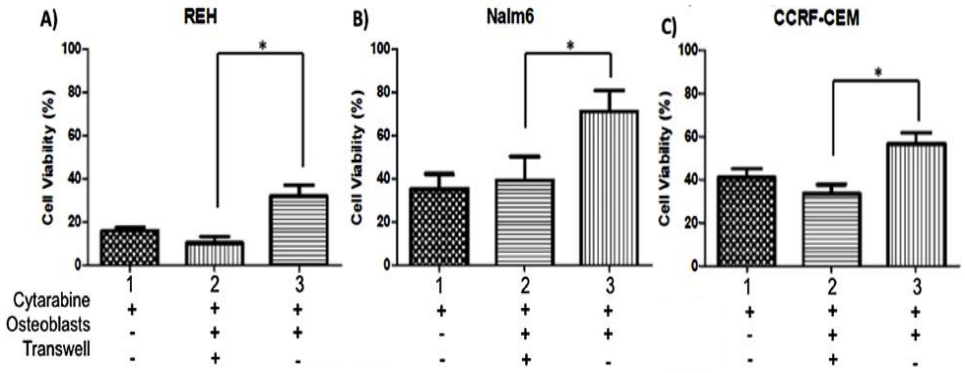

Figure 2.1 Development of a Chemoprotection Model B-ALL (REH and Nalm6) or T-ALL (CCRF-CEM) cell lines were plated either directly on top of Saos-2 cells (osteoblast-like) or suspended above in 0.4 µm Transwell filters and treated with cytarabine (600 nM for REH and CCRF-CEM, 800 nM for Nalm6) for 48 h. Error bars denote standard deviation of the mean from 3 independent experiments. *$p < 0.05$ indicates statistical significance.

2.3.2 Azacitidine and Panobinostat in Combination Have a Synergistic Killing Effect and Are Not Subject to the Same Chemoprotection as Cytarabine

Epigenetic modifiers like DNMTi and histone deacetylase inhibitors HDACi have been used previously in hematologic malignancies as a method to overcome chemoresistance and sensitize malignant cells to chemotherapy. In this study, I wanted to determine the efficacy of the DMNTi azacitidine and the HDACi panobinostat in my BMC model. I first determined the EC50 concentration of each individual drug in the three ALL cell lines (Figure 2.2).

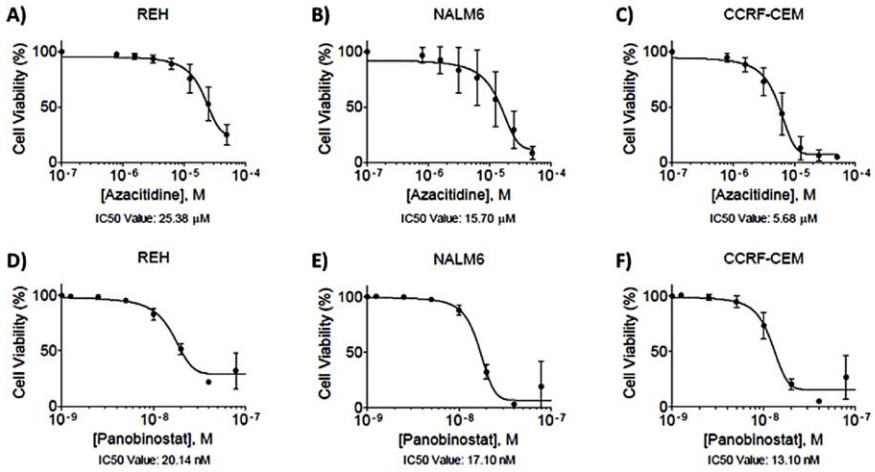

Figure 2.2 EC50 calculations for aza and pano REH, Nalm6, and CCRF-CEM were treated with different concentrations of azacitidine and panobinostat. Cell viabilities were determined using flow cytometry. Azacitidine EC50s were determined to be A) 25.38 µM B) 15.70 µM and C) 5.68 µM, whereas panobinostat EC50s were D) 20.14 nM E) 17.10 nM and F) 13.10 nM for REH, Nalm6 and CCRF-CEM respectively. EC50 values were calculated from 3 to 4 independent experiments performed in duplicates.

I then examined if the two drugs had a synergistic killing effect in combination. EC50 concentrations of azacitidine and panobinostat were used to treat ALL cells in monoculture for 48 h both alone and in combination with one another. Synergy was calculated using a relative risk ratio (RRR). All three ALL cell lines had RRR values < 1.00, indicating a synergistic killing effect of

azacitidine and panobinostat in combination (aza/pano) (Figure 2.3; Bars 1,3, and 5).

Having developed a successful BMC model relative to Ara-C treatment, I determined if treatment with azacitidine and panobinostat would be subject to the same chemoprotection. ALL cells treated with azacitidine or panobinostat alone had varying

degrees of chemoprotection (Figure 2.3; Bars 1 and 2, 3 and 4), while those treated with aza/pano did not have significant increases in viability (Figure 2.3; Bars 5 and 6). Taken together, these data show that azacitidine and panobinostat in combination have a synergistic killing effect and unlike chemotherapeutics like Ara-C are not impacted by BMC.

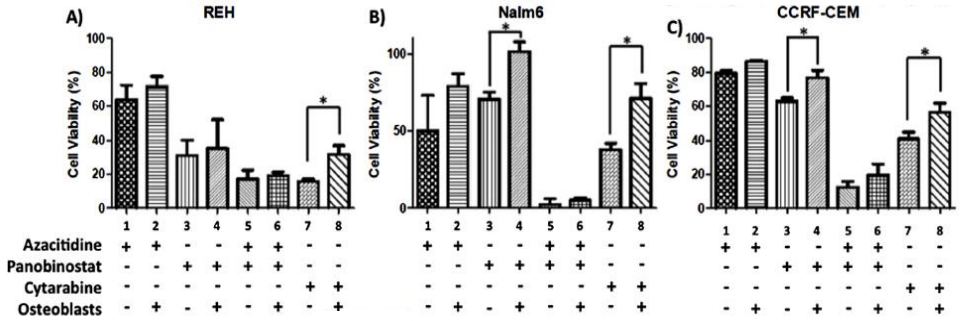

Figure 2.3 Aza/Pano have a synergistic killing effect and are more effective in overcoming BMC EC50 concentrations of azacitidine (REH: 25 µM, Nalm6: 15 µM, CCRF-CEM: 5 µM) and panobinostat (REH: 20 nM, Nalm6 and CCRF-CEM: 13 nM) were used as singular agents and in combination. Synergy was calculated using a relative risk ratio (RRR: value < 1.00 indicates synergy). REH (0.8711), Nalm6 (0.0494), and CCRF-CEM (0.2572) all exhibited synergy. Error bars denote standard deviation of the mean from 3 independent experiments. *p < 0.05 indicates statistical significance.

2.3.3 Aza/Pano Pre-Treatment Sensitizes ALL Cell to Chemotherapy Under BMC Conditions

Due to the success of aza/pano in overcoming the effects of BMC, I wanted to see if they could also be used to sensitize ALL cells to Ara-C treatment. Prior studies on the use of epigenetic modifiers have identified that minimally cytotoxic concentrations can have a potentiating effect on subsequent chemotherapy treatment. To examine this, I treated ALL cells for 48 h in monoculture with aza/pano. Following pre-treatment, ALL cells were then transferred on to monolayers of Saos-2 cells and treated with Ara-C for 48 h. Aza/pano pre-treated cells had minimal cell death (10-15%), while those that also received Ara-C treatment had a significant decrease ($p < 0.05$) in cell viability compared to those that were treated with Ara-C alone (Figure 2.4). This data shows that aza/pano pre-treatment can sensitize ALL cells to Ara-C treatment as a way to subvert the effects of BMC.

2.3.4 Synergy and Sensitizing Effects of Azacitidine/Panobinostat Are Replicable in a Variety of ALL PDX Samples

After identifying successful synergy and sensitization in multiple ALL cell lines, I investigated if these effects could be replicated in a variety of *ex vivo* patient-derived xenograft (PDX) samples. Synergy screening was performed on 21 different samples, 13 of which identified a synergistic killing effect between azacitidine and panobinostat (Table 2.1). Sensitivity screening was then performed in a cohort of 10 samples, 7 of which had increases in cell death over 10% when

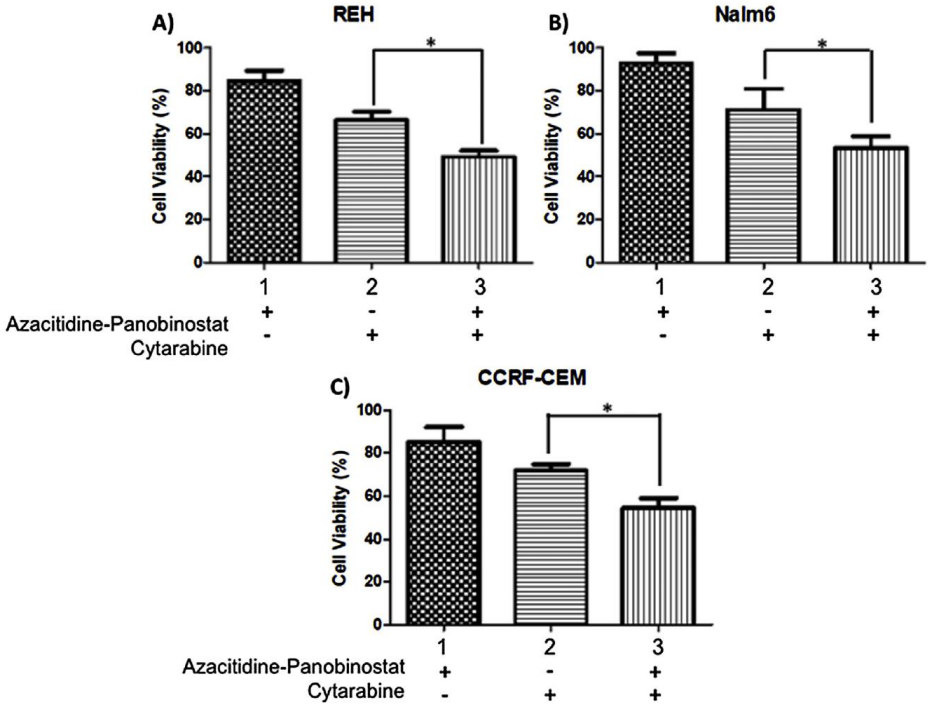

Figure 2.4 Aza/pano sensitizes ALL cells to chemotherapy under BMC conditions ALL cells were pre-treated with low-killing (10-20%) concentrations of aza/pano (REH: 3.75µM/3nM, Nalm6: 3.75µM/3.25nM, CCRF-CEM: 1.25µM/3.25nM) for 48 h in monoculture and then transferred on to monolayers of Saos-2 cells and treated with cytarabine for 48 h. Cells pre-treated with aza/pano were more sensitive to cytarabine than those that weren't pre-treated. Error bars denote standard deviation of the mean from 3 independent experiments. *$p < 0.05$ indicates statistical significance.

pre-treated with minimally cytotoxic concentrations of aza/pano prior to treatment with daunorubicin (Table 2.1). Taken together, this data supports the effectiveness of aza/pano in a variety of subtypes in ALL with different cytogenetic markers.

2.4 Summary

In this chapter, I identified that the epigenetic drug combination of azacitidine and panobinostat had a synergistic killing effect. This combination was more successful than the individual compounds or Ara-C at subverting the BMC effects of direct co-

culture with Saos-2 cells. Additionally, minimally cytotoxic concentrations sensitized ALL cells to chemotherapy under BMC conditions. Together, these findings offer a new method to circumventing the chemoprotective effects of the BM.

Sample	RRR Value	Sensitization	Cytogenetics
NTPL-20	0.6888		BCR-ABL, P16 deletion
NTPL-24	0.6204	36.07%	T-ALL
NTPL-59	1.4461		T-ALL
NTPL-83	0.8039	9.94%	ETV6-RunX1 (TEL/AML1)
NTPL-84	0.6082		Hyperdiploid, P16 deletion
NTPL-87	0.8038		Other
NTPL-90	0.7188	40.99%	ETV6-RunX1 (TEL/AML1)
NTPL-92	1.0387		E2A-PBX
NTPL-103	0.7249		Other
NTPL-109	0.8229	26.06%	Other
NTPL-119	1.0962	21.10%	RunX amplification
NTPL-127	0.6192		RunX amplification
NTPL-137	1.2071	14.06%	Hyperdiploid
NTPL-138	1.3442	26.56%	Hyperdiploid, P16 deletion
NTPL-150	0.6905		Hyperdiploid, P16 deletion
NTPL-155	0.9502		P16 deletion
NTPL-164	0.5992	14.75%	P16 deletion
NTPL-300	1.1260		Other
NTPL-313	0.9444	5.15%	ETV-RunX1 (TEL/AML1)
NTPL-454	1.4300	6.91%	T-ALL
NTPL-515	1.1597		Other

Table 2.1 Aza/pano synergy and sensitization effects can be replicated in a variety of PDX samples. EC50 concentrations for each individual sample were used to determine RRR value. 1 µM azacitidine and 1 nM panobinostat were used for sensitivity assay (24 h pre-treatment in co-culture with Saos-2 cells, then transferred to fresh monolayer and treated with 20 nM of daunorubicin for 48 h). 13 of 21 samples had synergy. 7 of 10 had sensitization > 10%.

Chapter 3

AZACITIDINE/PANOBINOSTAT MODULATES TETRASPANIN CD81 SURFACE EXPRESSION AND DISRUPTS ASSOCIATED BTK PRO-SURVIVAL SIGNALING

3.1 Introduction

In chapter 2, I identified that the epigenetic drug combination of aza/pano could successfully subvert the effects of BMC to sensitize ALL cells to chemotherapy. In order to better understand these effects, I determined the specific mechanism of sensitization.

As mentioned in chapter 1, cell surface proteins like CAMs can be responsible for mediating BMC effects. Additionally, other cell surface protein families, like TSPANs, are known to mediate interactions with the BM via cell surface organization of CAMs in nanodomains called TEMs. While TSPANs haven't been extensively studied in hematologic malignancies, preliminary indications suggest their role in mediating BMC and prolonging the survival of malignant cells. Due to their role in TEM formation and function, downregulating TSPAN expression could be a potent mechanism for disrupting BM interactions to augment the effectiveness of subsequent chemotherapy treatments in patients.

Aberrant B-cell receptor signaling in B-cell malignancies can be a potent contributor to disease progression and chemoresistance. Overactivation of this pathway can often occur via microenvironmental crosstalk, causing increased phosphorylation of Bruton's tyrosine kinase (BTK). Downstream effects of this

increase can have a plethora of effects such as augmented cellular adhesion through "inside-out" signaling, increased cell proliferation, and inhibition of cell death pathways. Contributing to these effects is the B-cell co-receptor, which is composed of CD19/CD21/CD81. The B-cell co-receptor functions to lower the threshold of B-cell receptor activation through CD19 by prolonging and amplifying the phosphorylation of BTK. Due to the role BTK plays in oncogenesis and chemoresistance, BTK is a strong therapeutic target in B-cell malignancies.

In this chapter, I elucidate that aza/pano-mediated sensitization occurs via modulation of the TSPAN protein CD81, which I also identify as a mediator of BMC, and a disruption of BTK signaling, thereby prohibiting BTK inhibition of p53-mediated cell death.

3.2 Materials and Methods

3.2.1 Antibodies

Anti-human CD81 (5A6), CD19 (4G7), CD10 (HI10a), mouse IgG1κ isotype, anti-mouse CD45 (30-F11), and purified CD81 antibodies were purchased from BioLegend (San Diego, CA). Anti-human mitochondria (113-1) and goat anti-mouse Cy5 antibodies were purchased from Abcam (Cambridge, MA). Phospho-BTK (D9T6H), p53 (7F5), Bax (D2E11), cleaved caspase-3 (5A1E), and PARP (46D11) antibodies were purchased from Cell Signaling Technology (Danvers, MA).

3.2.2 Adhesion Assay

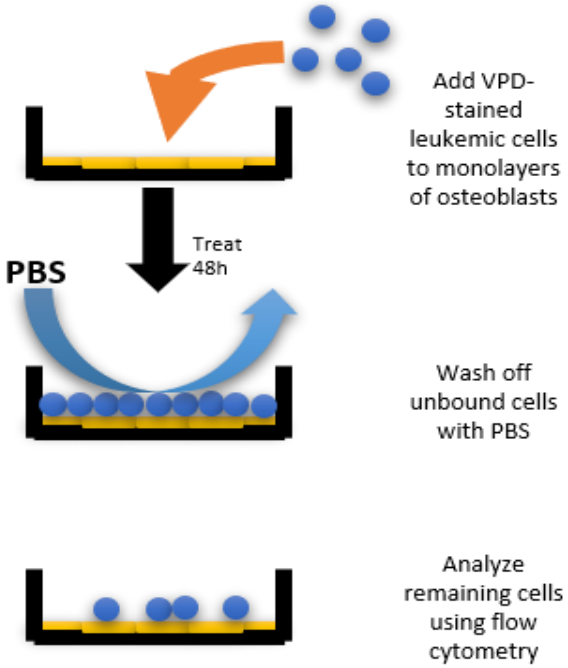

Figure 3.1 Diagram of adhesion assay protocol Pictorial representation of the protocol for performing an adhesion assay on ALL cells treated with aza/pano

For aza/pano-treated cells, 10,000 Saos-2 cells were plated in well of a 96-well plate and left to adhere overnight. 50,000 leukemic cells per well were then stained with VPD450 (BD Biosciences) according to the manufacturer's protocol and plated on Saos-2 monolayers in the presence or absence of azacitidine (1 μM) and panobinostat (1 nM) for 48 h in RPMI1640. Media was then removed and unbound cells were washed away twice with phosphate-buffered saline (PBS). 50 μL of trypsin-EDTA was then added to the wells and cells were suspended by adding 100 μL of RPMI-1640 and pipetting up and down. Cell suspensions from quadruplicate wells were analyzed using flow cytometry. 100 μL of each well was collected to detect the presence of VPD450+ leukemic cells. Samples were then

normalized to input (wells that were not washed with PBS) before comparing treated and untreated samples. For analysis of CD81KO adhesion, co-culturing was performed for only 24 h in the absence of aza/pano.

3.2.3 Lyoplate Screening and Determination of Cell Surface/Total Expression

The human cell surface marker screening panel was purchased from BD Biosciences (560747). 1 x 10^8 Nalm6 cells were treated with azacitidine (3.75 μM) and panobinostat (3.25 nM) or left untreated for 48 h. Cells were collected and stained with anti-human antibodies specific for each marker included in the plate according to the manufacturer's protocol. A minimum of 10,000 live cells were analyzed per sample. Mean fluorescence intensity (MFI) of each marker was determined following subtraction of isotype-control MFI.

For cell surface expression analysis of specific markers, treated and untreated cells were collected from culture and pelleted at 500 g for 5 min, washed, and resuspended in FACS buffer (1 x 10^6 cells/mL). 2 x 10^5 cells were stained with fluorophore tagged primary antibody or isotype control antibody for 15 min at room temperature (RT) in the dark. Samples were then washed twice and resuspended in PBS for analysis by flow cytometry. 10,000 live events were collected per sample and MFI was determined following subtraction of isotype-control MFI. Modulation was determined by dividing final expression values in treated samples by final expression values in untreated.

For total expression analysis, cells were fixed using 4% paraformaldehyde for 30 min at RT. Samples were then washed twice and then permeabilized with 0.1% saponin in PBS for 15 min prior to staining.

3.2.4 Endocytosis/Exocytosis Assay

Cells were treated with aza/pano for 24 h and centrifuged for 5 min at 350 g. Culture media was carefully aspirated and stored at 37^{o} C for later use. Cells were washed, resuspended in FACS buffer (1 x 10^{6} cells/mL), and stained with unconjugated anti-CD81 antibody (1:100) for 1 h at RT. Following incubation, cells were washed twice with FACS buffer and then resuspended in saved culture media. Cells were then returned to 37^{o} C for denoted times, collected by centrifugation at 500 g for 5 min, washed, and stained with either APC-tagged CD81 antibody (to detect newly synthesized CD81 protein – exocytosis) or Cy5-tagged goat anti-mouse secondary antibody (to detect CD81 protein retained on the cell surface – endocytosis) for 15 min at RT in the dark. Samples were then washed twice and resuspended in PBS for analysis by flow cytometry. 10,000 live cells were collected per sample. Newly synthesized CD81 appearing on the cell surface was calculated by: $Timepoint\ MFI - ZeroPoint\ MFI$. Rate of exocytosis was determined on GraphPad Prism 6 by taking the slope of a linear regression line of best fit. Percentage of internalized CD81 was determined by this formula: $\frac{(ZeroPoint\ MFI - Timepoint\ MFI)}{ZeroPoint\ MFI} \times 100$. The time taken to internalize 50% of CD81

protein was calculated on GraphPad Prism 6 by analyzing a non-linear regression curve fit constrained for the top to equal exactly 100.

3.2.5 Generation of a CD81 Knockout (KO) Nalm6 Cells by CRISPR Mutagenesis

pSpCas9(BB)-2A-GFP (PX458) (Addgene plasmid #48138), a generous gift from Dr. Feng Zhang was used to clone the guide sequence (GGCGCTGTCATGATGTTCGT) targeting CD81 exon 3 (Ran et al., 2013). Transfection was performed using a 4D nucleofector system (Lonza; Basel, Switzerland) and solution SF with 10 x 10^6 Nalm6 cells and 0.5 μg of plasmid. Transfected cells were single cell sorted using BD FACSAria III (BD Biosciences; Franklin Lake, NJ) into 96-well plates containing 20% FBS RPMI-1640 medium. Clones were initially screened by analysis of CD81 surface expression by flow cytometry. Clones that exhibited CD81 surface expression similar to isotype control antibody stained sample were then subjected to DNA extraction. Genomic DNA flanking the guide sequence was amplified from WT and KO cells and sequenced by Sanger sequencing. Sequences were analyzed using the equences were analyzed using the **T**racking of **I**ndels by **De**composition (TIDE) webtool (Desktop Genetics; London, UK)(Brinkman et al., 2014) to identify insertions/deletions at the cut site.

3.2.6 Determination of BMC

10,000 Saos-2 cells were plated in wells of a 96-well plate and left to adhere overnight. WT and KO cells were then plated in RPMI1640 media on top of

confluent Saos-2 monolayers in monoculture and treated with varying concentrations of Ara-C for 48 h. Viabilities were determined using flow cytometry and EC50 values in monoculture and co-culture with Saos-2 cells were determined as mentioned above. Drug resistance index (DRI) was calculated by taking the $EC50_{co}/EC50_{mono}$ of both CD81KO and WT cells.

3.2.7 Homing and Engraftment Analysis

For homing analysis, 1 x 10^7 cells of WT or KO were injected into NSG-SGm3 (n = 2 per cohort) mice via the tail vein. After 72 h, mice were euthanized, and femurs were collected for IHC analysis (performed as previously described using anti-human mitochondria antibody for human leukemic cell detection)(Gopalakrishnapillai et al., 2015).

For competitive homing analysis, 1 x 10^7 cells of both WT and KO were stained independently with VPD450 (WT) or CFSE (KO)(ThermoFisher) according to the manufacturer's protocol. Cell mixtures were then injected into NSG-SGm3 mice (n = 6) via the tail vein. After 72 h, mice were euthanized, and femurs were flushed with PBS to collect cells. Collected samples were then analyzed for the presence of VPD+ or CFSE+ human leukemic cells.

For engraftment and survival, 5 x 10^6 cells of WT or KO were injected into NSG-SGm3 mice (n = 2 per cohort) via the tail vein. Disease progression was monitored as previously described (Gopalakrishnapillai et al., 2016) by staining mouse peripheral blood with FITC-conjugated human CD10 and APC-conjugated mouse CD45 antibodies. Mice were monitored daily for disease symptoms and

predetermined experimental endpoints: increased leukemic burden, persistent weight loss or hind-limb paralysis. Mice were maintained in the Nemours Life Science Center following the guidelines and approval from Nemours Institutional Animal Care and Use Committee. Euthanasia was performed with method consistent with the euthanasia guidelines of the American Veterinary Medical Association when mice reached experimental endpoint.

3.2.8 Western Blot

Nalm6 cells were treated with 500 nM azacitidine and 1.5 nM panobinostat or left untreated for 48 h. Cells were then transferred onto monolayers of VPD450-labeled Saos-2 cells and treated with 30 nM of Ara-C or left untreated for 16 h. Nalm6 cells were then collected by gentle washing wells with culture media to disrupt interactions with Saos-2 cells. All samples were confirmed to be > 70% viable following treatment and enriched in leukemic cells (> 99%). Collected samples were then pelleted at 500 g for 5 min and washed with ice cold PBS. CD81KO cells were co-cultured on monolayers of Saos-2 cells in RPMI1640 and treated with 30 nM of Ara-C for 16 h. For analysis of BTK inhibition, Nalm6 cells were cultured alone in the absence or presence of the BTK inhibitors fenebrutinib (25 nM) or LFM-A13 (10 μM) for 16 h. Phosphorylation status of BTK in WT and CD81KO cells was determined after 4 h of serum starvation.

Protein was extracted from cells using RIPS lysis buffer (25 mM Tris-HCl pH 7.6, 150 mM NaCl, 1% Triton X-100, 1% deoxycholate, 0.1% SDS, 1:100 HALT^{TM} [ThermoFisher] protease and phosphatase inhibitor cocktail, 1 mM

PMSF) and lysing on ice for 30 min. Protein was then estimated using DC™ protein assay (BioRad) according to the manufacturer's protocol. 50 μg of protein were loaded for each sample on a 10% gel and resolved for 1 h and 30 min at 100 V. Samples were then transferred to a nitrocellulose membrane for 1 h at 100 V at 4°C. Membranes were then blocked for 20 minutes in 5% non-fat milk (in TBST) at 37°C. Primary antibody (1:1000 dilutions except GAPDH [1:5000]) stains were performed overnight at 4°C. Primary antibody was then detected with specific secondary antibody (1:2500 dilution) for 1 h at RT. Chemiluminescence was detected using ECL™ or ECL prime detection kits (GE healthcare) for 3 min at RT and captured using a LI-COR C-digir blot scanner (Lincoln, NE). Three independent trials were performed for each protein analysis. Raw density values were obtained from LI-COR analysis and relative expression was quantitated by normalizing to GAPDH expression.

3.2.9 RNAseq Analysis

Saos-2 cells were plated in a 6-well plate and left to adhere overnight. Nalm6 cells were added to resulting monolayers in RPMI1640 and left untreated or treated with aza/pano (800 nM and 800 pM) for 48 h. Total RNA was extracted using an RNAeasy mini kit from Qiagen (Hilden, Germany) according to the manufacturer's protocol, and subjected to reverse transcription to generate cDNA. A 1ug aliquot of cDNA was washed with Qiagen's QIAquick PCR Purification Kit and sheared to a median size of 300 bp with Covaris's AFA technology. DNA libraries prepared using Illumina's TruSeq Nano DNA Sample Prep Kit, were

sequenced via Illumina HiSeq X10, with paired end reads, 150 bp read lengths, and 30x coverage in regions around gene bodies. Fastq files were aligned to genome build hg19 using BWA and bowtie2 and alignment files were processed via GATK best practices.

3.2.10 qPCR Analysis

Nalm6 cells were left untreated or treated with aza/pano (500 μM and 1.5 nM) for 48 h.

RNA was extracted using Trizol. A cDNA library was generated using using an iScript cDNA synthesis kit from BioRad (Hercules, CA) according to the manufacturer's protocol. Transcript levels were analyzed by performing a qPCR on an ABI 7900 Real Time PCR system using SYBR Green (ThermoFisher; Waltham, MA). WIPF1 (Forward: GTTACCTTCGCCAGGACGTTCA; Reverse: TGCCGTTTCTGCTTACTGGAGG) and ACTB (Forward: CACCATTGGCAATGAGCGGTTC; Reverse: AGGTCTTTGCGGATGTCCACGT) primers were used for analysis. CT and RQ values were determined using the RQ Analyzer software.

3.3 Results

3.3.1 Aza/Pano Reduces Cellular Adhesion of ALL Cells to Saos-2 Cells

Having identified that my BMC model was reliant upon direct cell-cell contact, I wanted to examine if treatment with aza/pano was disrupting these interactions in order to induce chemosensitization. Five separate ALL PDX samples and cell lines

were stained with VPD450 prior to co-culture with Saos-2 cells. Following 48 h treatment with aza/pano, unbound cells were washed away with PBS and remaining cells were analyzed on flow cytometry. Cell that had been treated with aza/pano had a marked reduction in cellular adhesion to Saos-2 cells compared to those that were left untreated (Figure 3.2). This data indicates that aza/pano is successfully disrupting cell-cell interactions between ALL cells and Saos-2 cells as a part of sensitization.

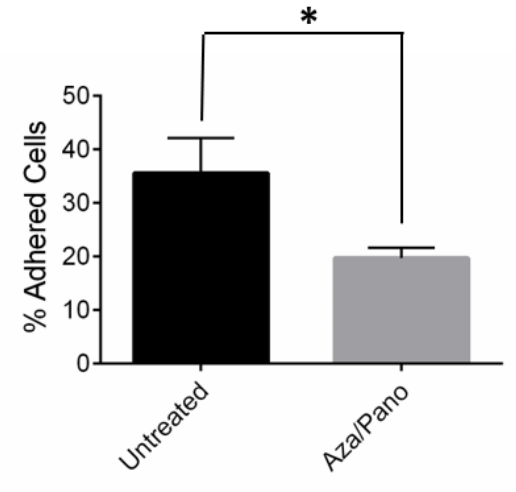

Figure 3.2 Aza/pano reduces cellular adhesion to Saos-2 cells ALL PDX samples were stained with VPD450, plated on monolayers of Saos-2, and treated for 48 h with aza/pano (1 µm and 1 nM respectively). After washing off unbound cells, flow cytometric analysis revealed a decrease in bound cells following treatment.

3.3.2 Cell Surface Marker Screening Reveals TSPAN CD81 is Significantly Downregulated by Aza/Pano

Due to the observed disruption of cellular adhesion in my sensitization model, I hypothesized that this effect could be caused by a modulation of the expression of proteins on the cell surface that are involved with cell-cell contacts. To examine

this hypothesis, I performed a Lyoplate™ screening assay of untreated and aza/pano-treated Nalm6 cells. The screening assay compared the surface expression of 242 different proteins following 48 h of treatment with aza/pano. One of the most markedly downregulated proteins was a member of the TSPAN superfamily, CD81. Follow-up analysis confirmed CD81 to be significantly ($p < 0.05$) downregulated by 65% compared to untreated cells (Figure 3.3A). While both azacitidine and panobinostat alone were able to induce downregulation of CD81 compared to untreated, maximal downregulation was only achievable via the combination treatment (Figure 3.3B).

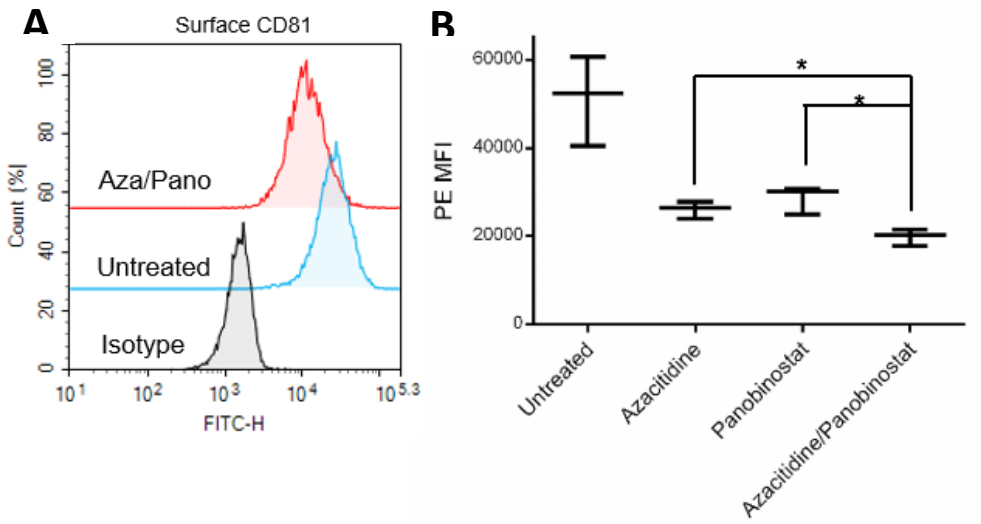

Figure 3.3 Aza/pano reduces cell surface expression of CD81 A) Flow cytometry plot overlays showing the surface expression of CD81 in untreated cells or cells treated with aza (500 nM)/pano (1.5 nM) for 48h. Isotype control antibody plots are included for reference. Representative plots from three independent experiments are shown. B) Column graph of CD81 downregulation following treatment with azacitidine and panobinostat alone and in combination. Error bars denote standard deviation of the mean from 3 independent experiments. *$p < 0.05$ indicates statistical significance.

3.3.3 CD81 Surface Downregulation is Not Caused by Anti-Leukemic Agent-Induced Stress and is Reversible Upon Cessation of Aza/Pano Treatment

To determine if CD81 downregulation in response to aza/pano treatment was specific and not due to anti-leukemic agent-induced stress, I investigated how CD81 surface expression was affected by a traditional chemotherapeutic in Ara-C. Following 16 h treatment with Ara-C, CD81 surface expression remained unchanged, supporting the specific effects of aza/pano on CD81 surface expression (Figure 3.4A).

I then wanted to determine if the downregulatory effects of aza/pano treatment were reversible. Nalm6 cells were first treated for 48 h and confirmed to have maximum downregulation of CD81 surface expression. Old media containing aza/pano was then removed from cells prior to adding fresh serum containing no drug. After 48 h, CD81 surface expression was again analyzed. In cells that had been treated and then had old media removed, CD81 surface expression had begun to recover to normal levels (Figure 3.4B). Taken together, these data suggest that CD81 downregulation is specific to aza/pano and can only be sustained while being exposed to the drug combination.

3.3.4 Aza/Pano Disrupts the Exocytosis of CD81

In order to understand how CD81 surface expression was being modulated by aza/pano, I first examined the total expression of CD81. However, total expression of CD81 unexpectedly remained unchanged following aza/pano treatment (Figure

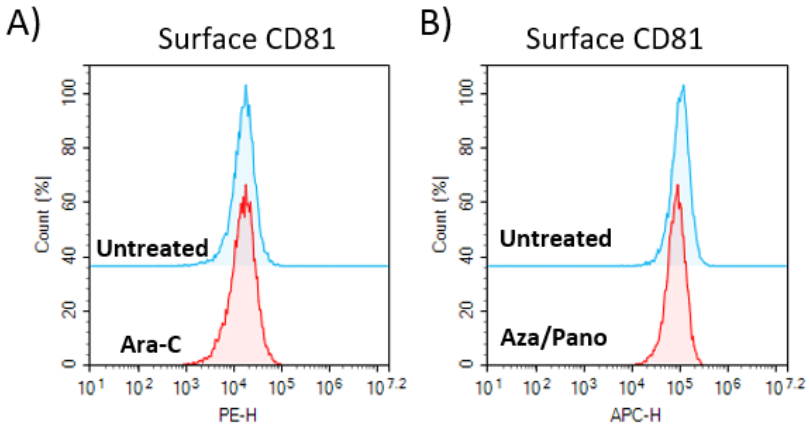

Figure 3.4 CD81 downregulation is specific to aza/pano and is reversible A) Flow cytometry plot overlays showing the surface expression of CD81 in untreated cells or cells treated with cytarabine (30 nM) for 16 h. B) Flow cytometry plot overlays showing the surface expression of CD81 in untreated cells or cells treated with aza/pano for 48 h and then allowed to recover for 48 h. Representative plots from three independent experiments are shown.

3.5A). I then hypothesized that CD81 surface expression was being modulated via an increase in endocytosis from the cell surface or a defect in exocytosis. To examine this, I performed an endocytosis/exocytosis assay using flow cytometry. Nalm6 treated with aza/pano had similar rates of endocytosis between treated and untreated cells (time to 50% internalization: 44.4±4.4 and 46.1±3.3 min respectively) (Figure 3.5B). However, the appearance of new CD81 on the cell surface (exocytosis) was markedly decreased in treated cells (60.23 MFI/min) compared to untreated (106.3 MFI/min) (Figure 3.5C). This data highlights that a defect in the exocytosis of CD81 to the cell surface is responsible for the decreased surface expression observed following aza/pano treatment.

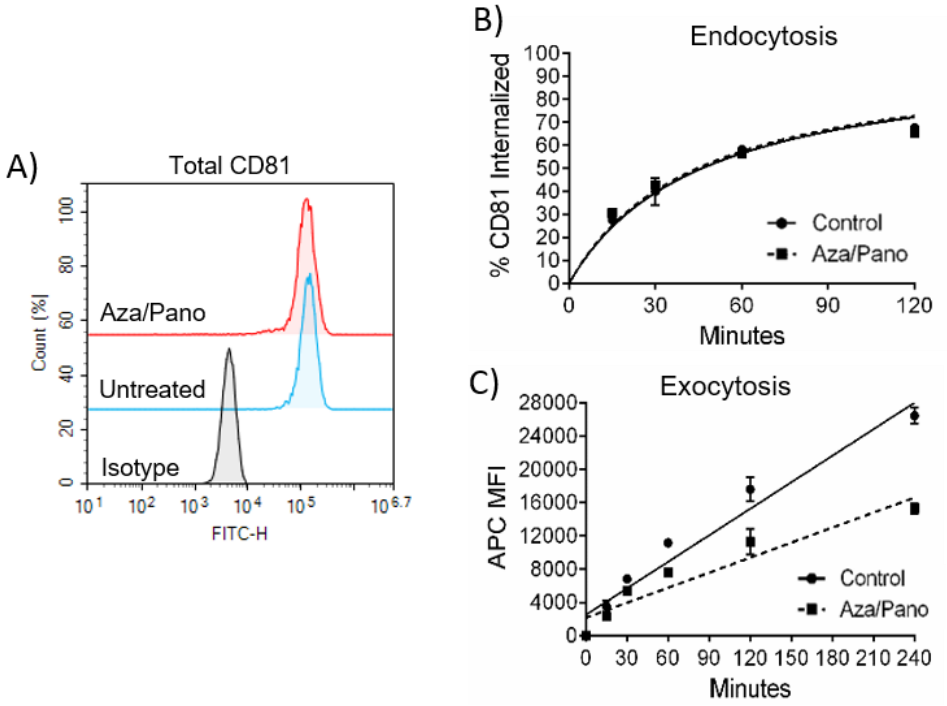

Figure 3.5 Exocytosis of CD81 is disrupted by aza/pano A) Flow cytometry plot overlays showing the total expression of CD81 in untreated or aza/pano-treated cells. Isotype control antibody plots are included for reference. Representative plots from three independent experiments are shown. B) Nalm6 cells treated with aza/pano for 24 h were blocked with unconjugated CD81 antibody. Newly appearing CD81 protein at the cell surface was captured at indicated time intervals using an APC conjugated CD81 antibody by flow cytometry. The rate of CD81 exocytosis was calculated based on the best fit line (Control rate: 106.3 MFI/min; aza/pano rate: 60.23 MFI/min). Error bars denote standard deviation from the mean of two independent experiments. C) Nalm6 cells treated with aza/pano for 24 h were incubated with unconjugated CD81 antibody. Cy5-tagged anti-mouse secondary antibody staining was performed to determine the percentage of CD81 protein internalized at a given time point. Time to 50% internalization was calculated based on the non-linear regression curve (Control: 46.1 min and Aza/Pano: 44.4 min). Error bars denote standard deviation from the mean calculated from two independent experiments.

3.3.5 CD81 Mediates BMC and Its Downregulation by Aza/Pano is Responsible for Sensitization

While I had identified CD81 to be significantly and specifically downregulated by aza/pano treatment, the role of CD81 in ALL, and specifically with respect to BMC, had previously been uncharacterized. To study its effects, I generated CD81KO clones in the Nalm6 cell line via CRISPR/Cas9 mutagenesis (Figure 3.6).

To determine if CD81 is a mediator of BMC, I treated wild-type (WT) and CD81KO cells with varying concentrations of Ara-C to determine their EC50 in both monoculture (WT: 1.86 x 10^{-8}M; KO Clone 1: 1.42 x 10^{-8}M; KO Clone 2: 1.55 x 10^{-8}M) and in co-culture with Saos-2 cells (6.37 x 10^{-8}M; KO Clone 1: 2.75 x 10^{-8}M; KO Clone 2: 2.76 x 10^{-8}M). A drug resistance index (DRI: $EC50_{co}/EC50_{mono}$) was then calculated to ascertain each sample's ability to induce chemoprotection. Both CD81KO clones had over a 1-fold reduction in DRI (Clone 1: 1.93; Clone 2: 1.78) compared to WT cells (3.43) (Figure 3.7). This data provides evidence that CD81 plays a role in mediating the effects of BMC.

After identifying CD81's role in initiating BMC, I needed to confirm that aza/pano-mediated CD81 downregulation was responsible for my sensitization effects. To examine this, I pre-treated CD81KO cells with aza/pano for 48 h prior to transferring them onto monolayers of Saos-2 cells and treating them with Ara-C for 48 h. Unlike WT cells, aza/pano-treated CD81KO cells did not have a significant reduction in cell viability following Ara-C treatment compared to

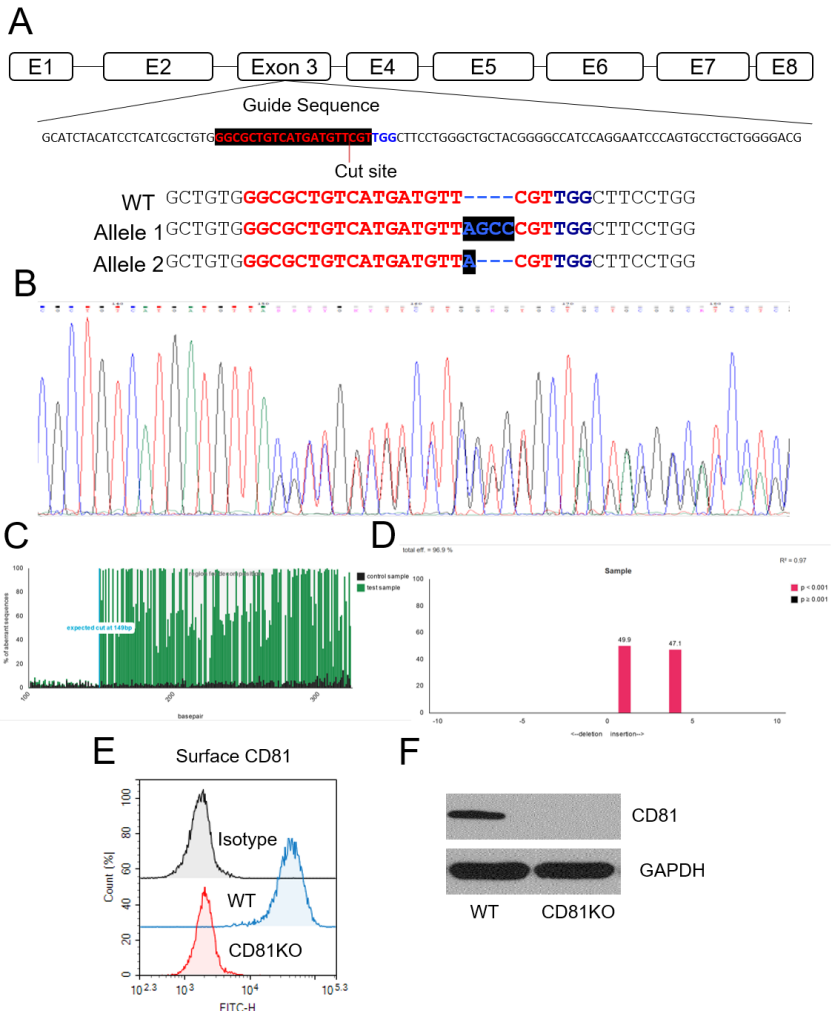

Figure 3.6 Generation of a CD81KO model via CRISPR/Cas9 mutagenesis A) CRISPR guide sequence within the targeted exon 3 of *CD81* gene is shown. The biallelic mutant clone had 4 bp insertion in one allele and 1 bp insertion in the other, each generating a premature stop codon. B) Sanger sequencing chromatogram showing location and sequence of nucleotide insertion into the CD81 gene. C) TIDE analysis confirms the cut site and insertion location within the CD81 gene. D) TIDE analysis confirms a single bp insertion in one allele and a 4 bp insertion in the other allele of CD81. E) Flow cytometry analysis of CD81 surface expression in WT and KO cells. F) Western blot analysis of CD81 in WT and KO cell lysates. GAPDH was used as a loading control.

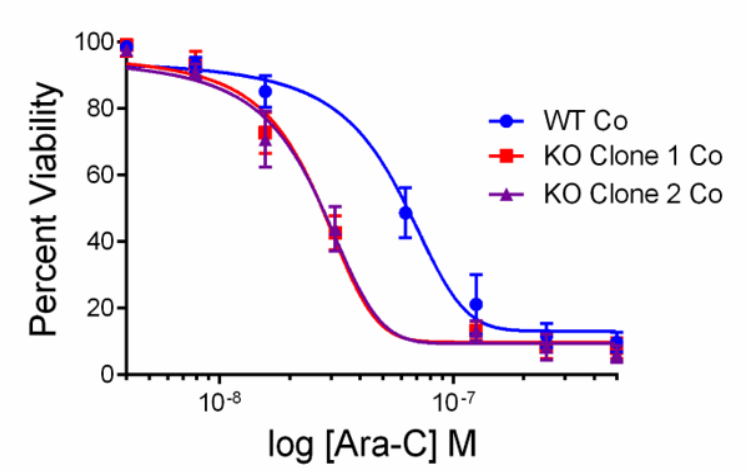

Sample	EC50 Mono	EC50 Co	DRI
WT	1.86 x 10^{-8} M	6.37 x 10^{-8} M	3.43
CD81KO Clone 1	1.42 x 10^{-8} M	2.75 x 10^{-8} M	1.93
CD81KO Clone 2	1.55 x 10^{-8} M	2.76 x 10^{-8} M	1.78

Figure 3.7 CD81 mediates BMC Graph depicting survival of cells treated with Ara-C in both and co-culture (co) with Saos-2 cells to determine. EC50s for monoculture (mono) and co-culture were determined for calculation of Drug Resistance Index (DRI). Data was generated across 4 independent trials.

Ara-C treatment alone (Figure 3.8). Taken together, this data confirms the role of CD81 in BMC and its downregulation by aza/pano is responsible for chemosensitization under BMC conditions.

3.3.6 CD81KO Cells Have Reduced Adhesion to Saos-2 Cells and Perturbed Homing and Engraftment *In Vivo*

Since my BMC model is reliant upon direct cell-cell contact, I wanted to investigate if CD81KO's increased sensitivity to Ara-C in co-culture with Saos-2 cells was due to a reduction in adhesion. WT and CD81KO cells were stained with VPD450 and then co-cultured with Saos-2 monolayers for 24 h. Following a

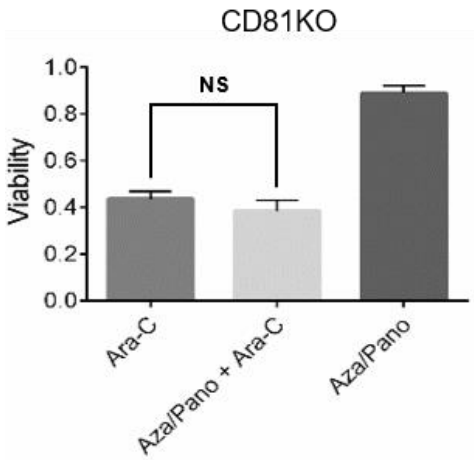

Figure 3.8 Aza/pano does pre-treatment does not further sensitize CD81KO cells to Ara-C CD81KO cells were pre-treated with aza/pano for 48h before transfer onto Saos-2 monolayers and treatment with Ara-C. Viability of ALL cells was determined using flow cytometry. Error bars denote standard deviation from the mean. NS stands for non-significant $p > 0.05$.

washing away of unbound cells, CD81KO had a marked reduction in their remaining cell counts compared to WT cells (Figure 3.9). This data confirms a reduced adhesion ability of CD81KO cells.

To understand how this reduced adhesion affected interactions with the *in vivo* BM, mice were transplanted with WT or CD81KO cells. After 72 h, mice were euthanized and femurs were collected. BMs of WT mice had significantly higher ($p < 0.01$) and uniformly distributed leukemic cells, whereas BM of CD81KO cell transplanted mice had very few leukemic cells (Figure 3.10 A and B).

To confirm this finding, I then performed a competitive homing assay by injecting equal numbers of VPD450-labeled WT cells and CFSE-labeled CD81KO cells into mice. After 72 h, mice were euthanized and femurs were flushed. There was a significant increase ($p < 0.05$) in the presence of VPD450+ WT cells

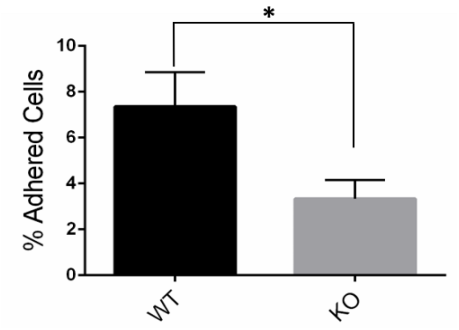

Figure 3.9 CD81KO cells have reduced cellular adhesion to Saos-2 cells Bar graph showing the average percentage of CD81KO cells bound to Saos-2 cells with respect to WT Nalm6 cells (normalized to 100%). Data from two independent experiments in quadruplicates is plotted. Error bar signifies SD of the Mean.

compared to CFSE+ CD81KO cells in the BM samples (Figure 3.10C). This data confirms my previous finding that there is a homing defect in CD81KO cells.

I then wanted to determine how this homing defect would impact engraftment. Varying numbers of WT and CD81KO (0.5×10^6 and 5×10^6) cells were injected into separate mouse cohorts and monitored for disease progression. Consistent with the reduced BM homing, mice injected with CD81KO cells had a slower appearance and progression of CD10+ leukemic cells in the peripheral blood compared to WT cells (Figure 3.10D). Additionally, mice injected with CD81KO cells survived significantly longer ($p < 0.05$) than those injected with corresponding numbers of WT cells (Figure 3.10E). Taken together with the BM homing data, this data identifies a critical role that CD81 plays in B-ALL BM homing and engraftment.

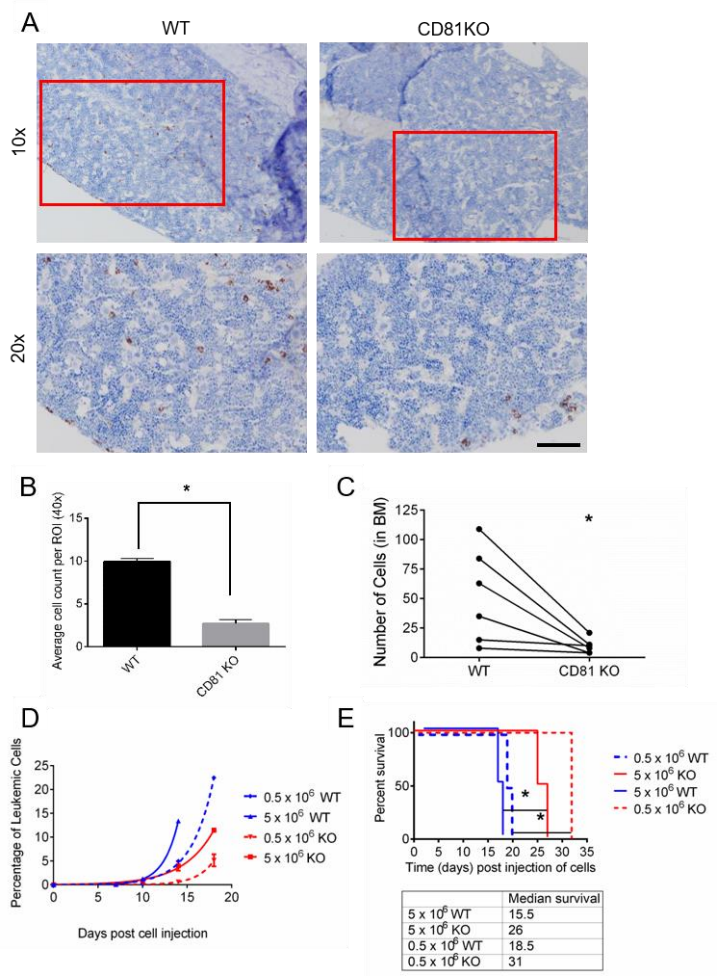

Figure 3.10 CD81KO cells have reduced homing and engraftment *in vivo* A) Representative images of mouse femurs harvested three days post injection (10 x 10^6 cells) in NSG-SM3 mice and stained using anti-human mitochondria antibody to detect the presence of leukemic cells (brown). Bar = 100 microns. B) Individual stained cells were counted in six images from each mouse femur in the cohort (n=2) to quantitate the presence of human cells. Mean $\pm$ standard deviation was plotted. *$p < 0.01$. C) For competitive homing assay, NSG-SGM3 mice were injected with WT and CD81KO cells, and three days later mouse femurs (n=6) were harvested and flushed. CFSE+ (CD81KO) and VPD450+ (WT) cells were detected by flow cytometry. *$p < 0.05$. D) Peripheral blood monitoring of human CD10+ leukemic cells in a separate cohort of NSG-SGM3 mice transplanted with 0.5 x 10^6 or 5 x 10^6 cells. E) Kaplan-Meier survival plot shows NSG-SGM3 mice xenografted with CD81KO cells live significantly (*$p<0.05$) longer than WT cell-transplanted mice.

3.3.7 BTK is Controlled via the CD81/CD19 Axis and is Diminished by CD81KO and Aza/Pano Treatment

Having identified CD81 as a mediator of BMC, I then wanted to investigate the associated signaling that contributed to this chemoprotection. CD81 is critical for the proper membrane trafficking of CD19, which has a prominent role in B-cell signaling. Prior studies identified transgenic $CD81^{-/-}$ mice to have depleted CD19 surface expression and a disruption of B-cell associated signaling. In my CD81KO cells, CD19 was completely knocked out on the cell surface, consistent with these previous reports (Figure 3.11A). CD19 along with CD21 forms the B-cell co-receptor, which lowers the threshold of B-cell receptor activation. Specifically, CD19 is responsible for prolonging and amplifying the phosphorylation of Burton's tyrosine kinase (BTK), a known leukemic cell and chemoresistance promoter. Due to their lack of CD19 surface expression, CD81KO cells had a 62% reduction in BTK compared to WT cells (Figure 3.11B). These data suggest that CD81 controls BTK signaling via its regulation of CD19 trafficking to the cell surface.

Decreased CD19 surface expression was also observed in Nalm6 cells treated with aza/pano for 48 h Figure 3.12A). To see if this alteration in CD19 expression also affected BTK, Nalm6 cells were treated with aza/pano in monoculture for 48 h before being transferred onto monolayers of Saos-2 cells and being treated with Ara-C for 16 h. While Ara-C treatment did reduce BTK by 18%, aza/pano treatment alone diminished BTK by 63%. Aza/pano-treated cells that also received

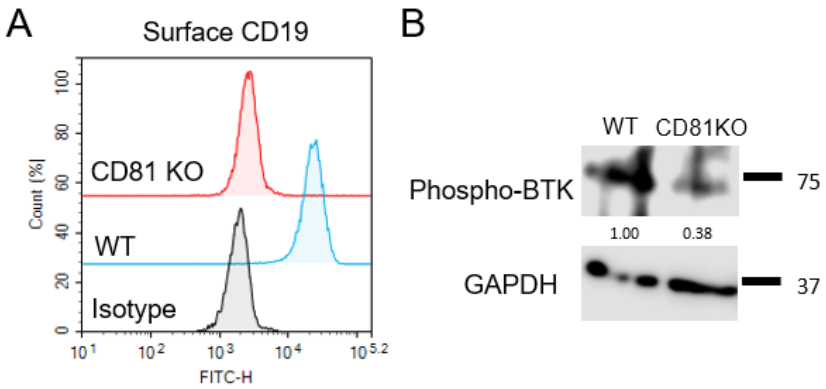

Figure 3.11 CD19 surface expression is depleted and subsequent BTK expression is decreased in CD81KO cells A) Flow cytometry plot overlays showing the surface expression of CD19 in CD81KO compared to WT. Isotype control antibody plot is included for reference. Representative plot of three independent trials is shown. B) Western blot analysis of phosphorylated BTK in CD81KO cells compared WT.

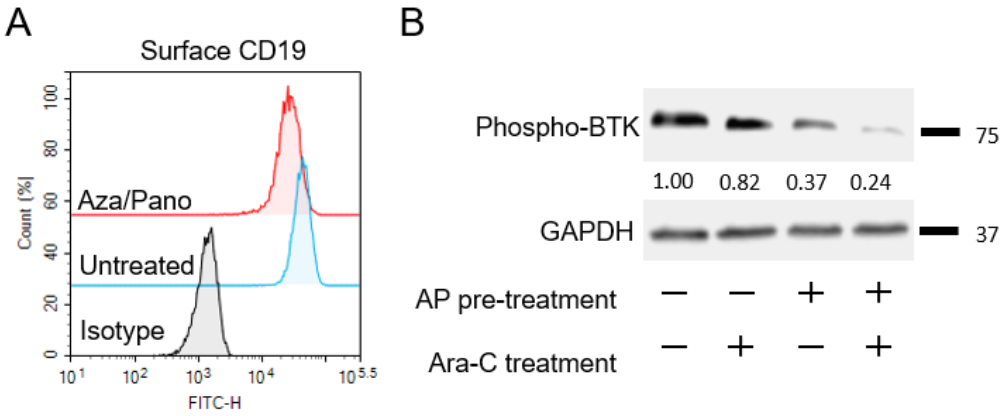

Figure 3.12 Aza/pano reduces CD19 surface expression and expression of BTK A) Flow cytometry plot overlays showing the surface expression of CD19 in aza/pano-treated cells compared to untreated. Isotype control antibody plots are included for reference. Representative plots of three independent trials are shown. B) Western blot analysis of phosphorylated BTK WT, WT pre-treated with aza/pano for 48h and/or treated with Ara-C for 16h in co-culture with Saos2. ALL cells collected from co-culture were confirmed to be a pure leukemic cell population (>99%) and all viabilities following treatment were > 70%. The numbers below the blots indicate average fold change of protein normalized to GAPDH (loading control) with respect to control (assigned value = 1.00) from three independent experiments.

Ara-C treatment had an even further decrease in BTK phosphorylation of 76% (Figure 3.12B). This data supports the role that aza/pano-mediated CD81 downregulation plays in sensitization via disruption of BTK signaling.

3.3.8 Disruption of BTK Signaling by CD81KO and Aza/Pano Leads to Augmented Activation of p53-Mediated Cell Death

Ara-C is known to induce leukemic cell death via the p53-mediated cell death pathway, culminating in the increased expression of the pro-apoptotic BCL2 associated X protein (Bax). As expected, Ara-C treatment of WT cells had induced both p53 and Bax expression. However, CD81KO cells treated with Ara-C had markedly increased expression of p53 and Bax compared to WT cells. Intriguingly, untreated CD81KO cells also showed increased levels of p53 and Bax compared to Ara-C treated WT cells (Figure 3.13A). This could suggest that CD81KO cells were already more predisposed to cell death prior to chemotherapy treatment.

To confirm that diminished BTK signaling was responsible for the activation of this p53-mediated cell death, WT cells were treated with the BTK inhibitors fenebrutinib or LFM-A13. Treated cells had a 1.7-fold and 2.3-fold increase in p53 expression respectively and a 2.8-fold and 3.3-fold increase in Bax expression compared to untreated cells (Figure 3.13B). Taken together with the CD81KO data, these data indicate that CD81-mediated control of BTK signaling can inhibit p53-mediated cell death.

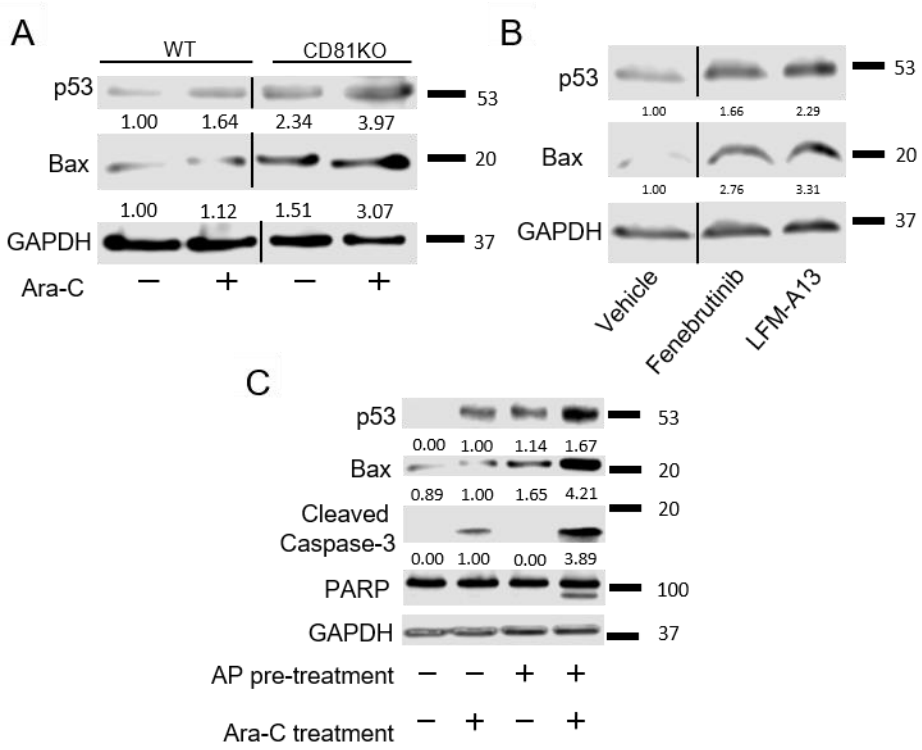

Figure 3.13 Disruption of BTK signaling by CD81KO and aza/pano augments activation of p53-mediated cell death A) Western blot analysis of p53 and Bax in untreated and Ara-C treated CD81KO cells compared to untreated and Ara-C treated WT cells. B) Western blot analysis of p53 and Bax in WT cells treated with fenebrutinib (25nM) or LFM-A13 (10μM) for 16h. C) Western blot analysis of phosphorylated BTK, p53, Bax, caspase-3 and PARP in WT, WT pre-treated with aza/pano for 48h and/or treated with Ara-C for 16h in co-culture with Saos2. Representative blots of three independent trials are shown. Numbers below the blot indicate average fold change of protein normalized to GAPDH (loading control) with respect to control (assigned value = 1.00) from three independent experiments.

I examined this pattern of p53 induction in aza/pano-treated cells. Aza/pano was able to induce p53 expression, which was further augmented following Ara-C treatment, however, the effect was less than additive. Bax expression was also increased by aza/pano, but when also treated with Ara-C it had a 4.2-fold increase in expression compared to cells that only received Ara-C. This increase in p53/Bax

was accompanied by a 3.9-fold increase in the cleavage of caspase-3 compared to Ara-C alone and it culminated in a cleavage of Poly-ADP Ribose Polymerase (PARP) (Figure 3.13C). This data suggests that aza/pano sensitizes ALL cells by disrupting BTK-mediated inhibition of p53-mediated cell death via modulating CD81 surface expression.

3.3.9 Aza/Pano Reduces WIPF1 Transcript Levels

Having identified CD81 surface downregulation via decreased exocytosis and a depletion of associated BTK signaling to be responsible for sensitization, I wanted to better understand how CD81 exocytosis was being affected. I performed an RNAseq analysis by co-culturing Nalm6 cells with Saos-2 monolayers and treating with aza/pano for 48 h. One of the most highly modulated transcripts was WIPF1 (Table 3.1). Previously, transgenic WIPF1$^{-/-}$ mice were shown to have decreased CD81 surface expression and disrupted CD19-associated signaling. This would suggest a role of WIPF1 in CD81 exocytosis. To confirm my RNAseq data, I performed a qPCR analysis. The WIPF1 transcript was continually downregulated, consistent with the data from RNAseq (Figure 3.14). This data provides further insight into how CD81 surface expression is possibly being diminished due to a defect in exocytosis.

Gene	Log_2 Fold Change	P-Value
TTN-AS1	-5.50449137	3.387E-182
PHKA2	-4.18524399	1.7405E-22
FAM86B3P	-3.86193953	3.7367E-33
TSIX	-3.51341057	2.3848E-34
PRPF40B	-3.18636419	1.5627E-08
SSC5D	-3.15828171	1.5336E-12
CELF2	-3.02214161	3.3093E-14
DIO2-AS1	-2.97474278	7.0938E-08
LINC00861	-2.95576401	1.4306E-16
ZNF224	-2.8738103	2.1277E-14
PRSS55	-2.832244	1.2278E-05
VPS9D1-AS1	-2.82858785	5.5573E-07
WIPF1	-2.78978229	1.3182E-07
LIX1	-2.77970747	2.0942E-05
SH3PXD2A	-2.74572905	4.6868E-08

Gene	Log_2 Fold Change	P-Value
IQCD	2.529500168	3.5237E-06
SERINC5	2.134718584	0.00035882
C10orf76	2.066493906	0.00054917
STC2	2.034710527	5.7165E-06
RIMS3	1.994479727	6.9898E-05
TAPT1-AS1	1.92586876	0.00218053
CASC3	1.916740343	0.00220349
PHGDH	1.838165683	0.00129955
PPOX	1.815323982	0.00177212
ELFN2	1.786161461	1.6655E-11
UNC93B1	1.748692184	0.0001439
HIST1H2AJ	1.73915653	0.00017881
IGLL5	1.730970568	0.00042545
ARID5B	1.73058847	0.0009908
NEK8	1.728757299	0.00010807

Table 3.1 Top regulated genes by aza/pano identified by RNAseq

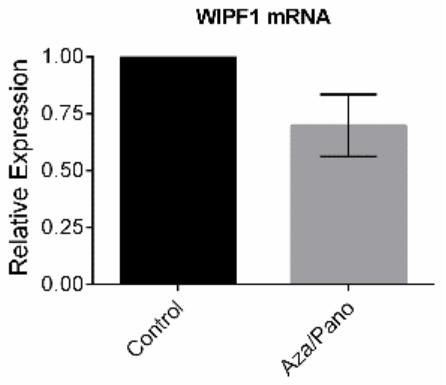

Figure 3.14 Aza/pano reduces WIPF1 transcript expression Bar graph showing the downregulation of the relative expression of WIPF1 transcript in Nalm6 cells treated with aza/pano for 48 h. Error bars denoted standard deviation from the mean across three independent trials.

3.4 Summary

In this chapter, I elucidated that the sensitizing effects of aza/pano were mediated through a reduction in cellular adhesion to Saos-2 cells. This occurs via a downregulation of the surface expression of the TSPAN protein CD81. CRISPR/Cas9 mutagenesis of CD81 confirmed its role in mediating the effects of BMC via cellular adhesion as well as homing/engraftment *in vivo*. Disruption of CD81 surface expression leads to an associated decrease in surface CD19 and a subsequent inhibition of BTK signaling. This culminates in an increased activation of p53-mediated cell death following treatment with Ara-C.

Chapter 4

AZA/PANO DECREASES *IN VIVO* BM LOAD TO POTENTIATE THE EFFECTS OF SUBSEQUENT CHEMOTHERAPY

4.1 Introduction

In chapters 2 and 3 I identified how aza/pano can successfully circumvent the effects of BMC to sensitize ALL cells to chemotherapy *in vitro*. In order for these effects to be translationally relevant, they must be examined in a disseminated leukemia model *in vivo*.

Epigenetic treatments combined with chemotherapeutics have had a good amount of success in improving patient survival in cancer. Often times, this sensitization occurs via modulation of specific chemoresistance markers or disruption of genes involved with pro-survival/anti-apoptotic signaling pathways. However, with reference to hematologic malignancies, disruption of BM interactions can also be a method of sensitization. In chapter 3, I identified how treatment with aza/pano disrupts ALL cell adhesion to Saos-2 cells and how KO of CD81, which is decreased by aza/pano, disrupts BM homing and engraftment. This data suggests that in a disseminated leukemia model *in vivo*, aza/pano treatment could reduce BM load. This is important for chemotherapy effectiveness because it increases drug sensitivity in ALL cells, resulting in better ALL cell elimination from the BM, which is important for prevention of relapse and prolonging overall survival.

In addition to the translational aspect, *in vivo* study of aza/pano treatment could provide crucial information related to treatment markers. The ability to identify

markers for treatment or ways to monitor efficacy is important in the age of personalized medicine as we try to best match patients with the specific treatments that will have the most success against their malignancy.

In this chapter, I affirm the effectiveness of aza/pano in potentiating the effects of subsequent chemotherapy in a disseminated leukemia model. I then confirm these effects are mediated through a decrease in CD81 surface expression and a decreased BM load, culminating in an increase in p53 expression following chemotherapy treatment.

4.2 Materials and Methods

4.2.1 Aza/Pano Xenograft Model

1 x 10^6 cells of NTPL-87, a B-ALL PDX sample described previously (Gopalakrishnapillai et al., 2016), or Nalm6 cells were engrafted into NSG-B2m mice (n = 5 per cohort) via tail-vein injection. Following a 72 h engraftment period (10 days in Nalm6), mice were then randomly assorted into four separate groups: control (vehicle; 5% dextrose), pre-treated (aza/pano 2.5 mg/kg each Qdx5i.p), chemotherapy (Ara-C 50 mg/kg Qdx5i.p and daunorubicin 1.5 mg/kg Qdx3i.v.), or combination (aza/pano followed by Ara-C/daunorubicin) and treated according to the plan diagrammed in figure 4.1. Disease progression was monitored by periodically collecting peripheral blood via submandibular bleeding. Blood was stained with FITC anti-human CD10 and APC anti-mouse CD45 for 10 min at RT. Red blood cells (RBC) were then lysed using a multispecies RBC lysis buffer (Affymetrix eBioscience) containing ammonium chloride. Following a 10 min

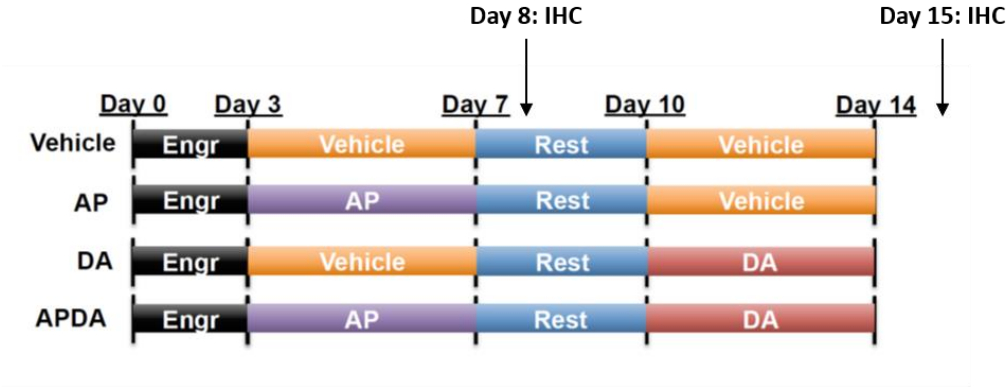

Figure 4.1 Diagram of *in vivo* treatment plan for mice engrafted with NTPL-87 cells NSG-B2M mice were transplanted with NTPL-87 cells, engrafted for three days, and then treated according to this plan. For Nalm6 mice, engraftment occurred over the course of 10 days.

lysis, samples were spun down at 800 g for 10 min and resuspended in 100 µL of PBS + propidium iodide (PI) for analysis on flow cytometry. Leukemic load was determined by gating on PI- cells to determine the counts of FITC+ (human) and APC+ (mouse) cells and calculated by: $\frac{Human\ CD10}{(Human\ CD10+Mouse\ CD45)}$. The increase in percentage was plotted over time and fitted to a non-linear regression curve in GraphPad.

Mice were monitored daily for disease symptoms and predetermined endpoints: reduced mobility, sustained weight loss, and hind-limb paralysis. Mice were maintained in the Nemours Life Science Center following the guideline and approval from Nemours Institutional Animal Care and Use Committee. Euthanasia was performed with a method consistent with the euthanasia guidelines of the American Veterinary Medical Association when mice reach experimental endpoints. Upon termination of studies, Kaplan-Meier survival curves were generated using GraphPad.

4.2.2 IHC Analysis of BM Load

Femurs were collected from mice at indicated timepoints following euthanasia. Femurs were fixed in 10% NBF for 24-48 h and then demineralized in RegularCal™ Immuno (BBC Biochemical, Mt. Vernon, WA) and checked for end point decalcification before washing with running water. The samples were processed on a routine clock and parrafin embedded Histoplast LP (Leica Biosystems) and floated onto Superfrost® Plus Gold slides (Thermo Fisher Scientific). Sections were heat immobilized for 60 minutes at 60°C and then stored at -20°C until ready to stain. Slides were equilibrated to room temperature and then deparaffinized in xylene and re-hydrated to deionized water prior to antigen retrieval. Heat retrieval was performed 60°C oven with a sodium citrate buffer at pH 6 overnight and then allowed to cool to room temperature. Slides were placed on Bond RX IHC stainer (Leica Biosystems) for staining with the anti-human mitochondria antibody. The slides were then moved through the Bond Polymer Refine Detection solutions consisting of a post primary solution, a peroxide block, a polymer, and DAB chromogen. When finished, the slides were dehydrated, cleared, and mounted in Permount® (Thermo Fisher Scientific). Separate sections were mounted onto slides and counterstained with hematoxylin and eosin. Images were captured using an Olympus BX51 microscope and DP74 microscope camera..

4.2.3 Protein Expression in Peripheral Blood and Bone Marrow

Peripheral blood for CD81 surface expression analysis was collected via cardiac puncture following euthanasia. BM samples were collected from the same mouse by collecting femurs and flushing with 1 mL of PBS. Samples were then incubated with Fc block (BD Biosciences) for 15 min at RT followed by a triple antibody cocktail of FITC anti-human CD10, Pacific Blue anti-mouse CD45, and APC anti-human CD81 for 15 min at RT. Red blood cells were lysed using RBC lysis buffer and samples were spun down at 800 g for 10 min before being resuspended in 100 μL of PBS for analysis on flow cytometry. CD81 MFI was calculated by gating on the FITC+ (human) event population.

Staining for the expression of p53, Ki-67, and geminin was performed on IHC samples as described above. Quantitation of p53 expression in samples was determined using the IHC toolbox from Image J.

4.3 Results

4.3.1 One Cycle of Aza/Pano Potentiates Subsequent Chemotherapy in Mice Engrafted with an ALL PDX Sample

Aza/pano was successful in overcoming the BMC effects of my Saos-2 model, however, in order to better understand the efficiency of aza/pano to overcome BMC, I wanted to study it in a disseminated leukemia model *in vivo*. 1 x 10^6 cells of the highly refractory and poor prognosis PDX sample NTPL-87 (B-ALL) were engrafted into NSG-B2m mice via tail vein injection. Mice were then separated into four separate treatment groups: control (dextrose), pre-treated (aza/pano), chemotherapy (Ara-C/daunorubicin), and pre-treated chemotherapy (aza/pano

prior to Ara-C/daunorubicin), and were treated according to the diagram in figure 4.1.

Following completion of all treatments, the pre-treated chemotherapy group (AP->DA) had the slowest return of CD10+ human leukemic cells into the peripheral blood (Figure 4.2A). This correlated with the largest rise in median survival (19 days over vehicle) and a significant increase compared to chemotherapy alone (DA, +11.5 days, $p < 0.05$) or those in the pre-treatment group (AP, +12.5 days) (Figure 4.2B). These effects were also replicated in mice engrafted with Nalm6 (Figure 4.3), highlighting the potentiating effect of aza/pano on chemotherapy treatment in disseminated ALL xenograft models.

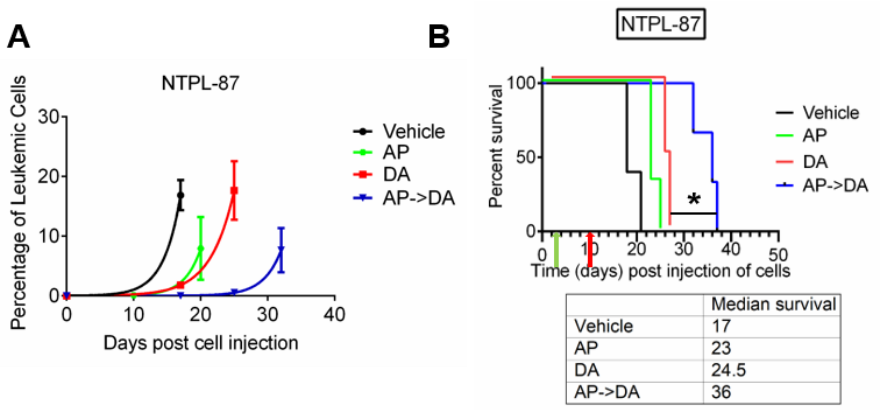

Figure 4.2 One cycle of aza/pano potentiates subsequent chemotherapy treatment *in vivo* in NTPL-87 mice A) Peripheral blood was monitored for the presence of human CD10+ cells to determine change in leukemic percentage over time. B) Kaplan-Meier survival curves show mice pre-treated with AP prior to DA live significantly longer than mice treated with DA alone (*$p < 0.05$). Green and red arrows indicate time when aza/pano or DA treatment began respectively.

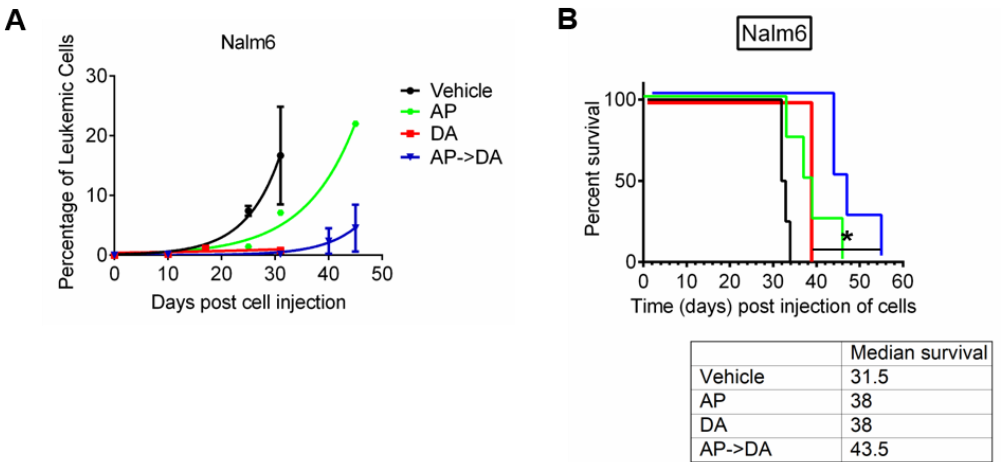

	Median survival
Vehicle	31.5
AP	38
DA	38
AP->DA	43.5

Figure 4.3 One cycle of aza/pano potentiates subsequent chemotherapy treatment *in vivo* in Nalm6 mice A) Peripheral blood analysis of the presence of human CD10+ leukemic cells. B) Kaplan-Meier survival plot shows mice treated with AP prior to chemotherapy survive longer than mice who receive chemotherapy alone.

4.3.2 Aza/Pano Reduces *In Vivo* BM Load Due to Leukemic Cell Mobilization and Increases BM Clearance by Chemotherapy

Due to aza/pano's ability to reduce cellular adhesion, I hypothesized that the potentiating effects observed *in vivo* could be a result of disrupting ALL BM interactions. To examine this, I engrafted a separate cohort of NSG-B2m mice and treated them in accordance with figure 4.1. On day 8 post-injection (following completion of aza/pano treatment), peripheral blood in aza/pano-treated mice had a higher percentage of CD10+ human leukemic cells compared to vehicle-treated mice (Figure 4.4A). However, IHC analysis of femurs identified a marked reduction in the presence of leukemic cells within the BM of aza/pano-treated mice (Figure 4.4B), suggesting that ALL cell interactions had been disrupted by aza/pano, consistent with the decreased cellular adhesion observed *in vitro*.

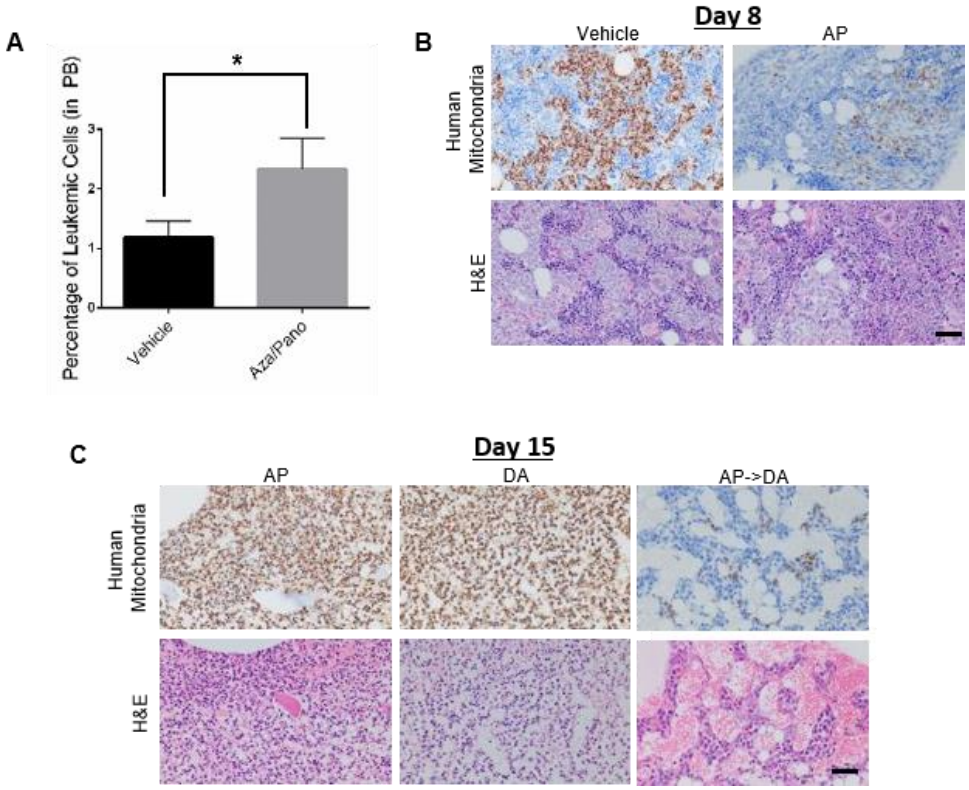

Figure 4.4 Aza/pano reduces *in vivo* BM load by mobilizing leukemic cells to increase BM clearance by chemotherapy A) Peripheral blood analysis of vehicle-treated and aza/pano-treated mice identifying CD10+ human leukemic cells. p* <0.05. B) Mouse femur sections collected at day 8 (following completion of AP treatment; Figure 6A) were stained with hematoxylin/eosin or anti-human mitochondria antibody to detect human cells (brown). Bar = 50 microns. C) D) Following completion of DA treatments (15 days post cell injection; Figure 6A), femur sections were stained with hematoxylin/eosin or anti-human mitochondria antibody. Bar=50 microns.

I then investigated if this reduced BM was responsible for the potentiating effects on chemotherapy treatment. On day 15 (following chemotherapy treatment), IHC analysis of femurs revealed similar, fully invade BMs in pre-treated and chemotherapy mice. However, the pre-treated chemotherapy mice had

a minimal presence of leukemic cells in their BM, indicating an improved clearance due to aza/pano pre-treatment (Figure 4.4C).

4.3.3 *In Vivo* Surface Expression of CD81 is Reduced on Leukemic Cells Following Aza/Pano Treatment and Leads to Increased p53-Mediated Cell Death

Having identified aza/pano treatment to be responsible for potentiating chemotherapy treatment *in vivo* due to a reduced BM load, I wanted to investigate if these effects were also due to CD81 downregulation that I had observed *in vitro*. Following completion of aza/pano treatment, NTPL-87 leukemic cells were collected from both the peripheral blood and from the BM and stained for CD81 expression. Aza/pano-treated mice had a 43% and 68% reduction in CD81 surface expression in the peripheral blood and BM respectively compared to vehicle-treated mice ($p < 0.05$, Figure 4.5A, bars 1-2; 3-4). This reduction in CD81 correlates with a reduced presence of NTPL-87 cells in the BM, consistent with the perturbed homing and engraftment that was observed with CD81KO cells *in vivo* (Figure 3.10).

With CD81 surface expression being downregulated *in vivo*, I then wanted to see if subsequent chemotherapy was able to potentiate p53-mediated cell death, as observed *in vitro*. Following chemotherapy treatment, femurs were collected from

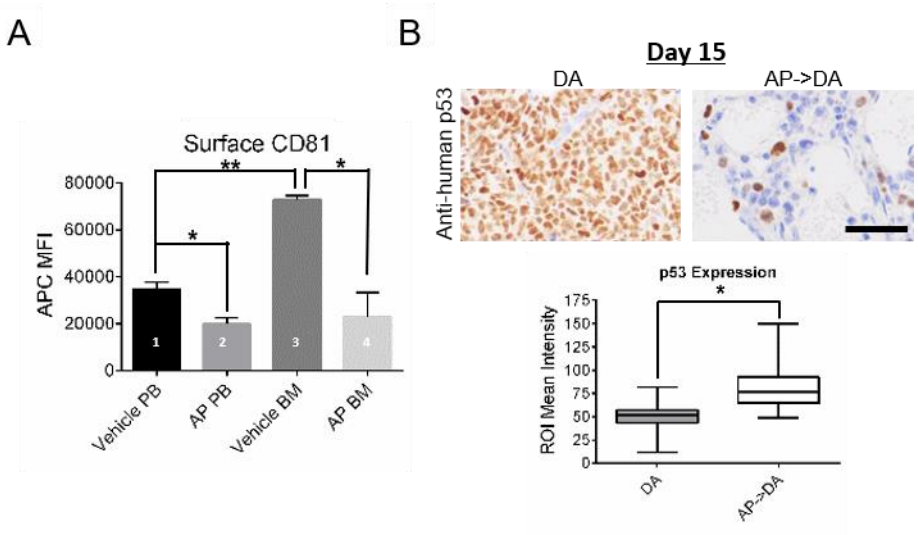

Figure 4.5 Aza/pano reduces *in vivo* CD81 surface expression and augments p53 expression following chemotherapy A) Graphical representation of CD81 surface expression on human leukemic cells from peripheral blood (PB) and bone marrow (BM) in mice transplanted with WT (n=2) or CD81KO (n=4) cells; *p < 005, **p < 0.01. B) Following completion of DA treatments (15 days post cell injection), mouse femur sections were stained with anti-human p53 antibody. Bar=50 microns. Average p53 expression per cell was quantified using the IHC toolbox from Image J (n=60-120). Average values with standard deviation and min/max are presented in the graph (*p < 0.001).

mice for IHC analysis of p53 expression and revealed a 1.6-fold increase ($p < 0.001$) in the pre-treated chemotherapy group compared to chemotherapy alone (Figure 4.5B). Analysis of the proliferation markers Ki-67 and geminin revealed no significant differences (Figure 4.6). These data support the role that aza/pano-mediated downregulation of CD81 surface expression plays in increasing sensitivity to subsequent chemotherapy treatment *in vivo* via increase of p53 expression.

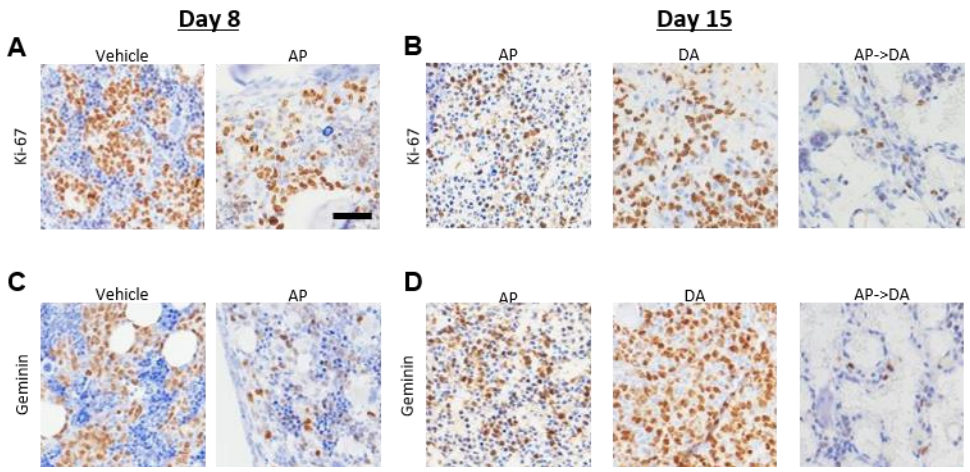

Figure 4.6 Expression of the proliferation markers Ki-67 and geminin remain unchanged following *in vivo* treatment with aza/pano A) IHC staining of Ki-67 following completion of aza/pano treatment (Day 8). B) IHC staining of Ki-67 following completion of chemotherapy treatment (Day 15). C) IHC staining of Geminin following completion of aza/pano treatment (Day 8). D) IHC staining of Geminin following completion of chemotherapy treatment (Day 15). Bar = 50 microns.

4.4 Summary

In this chapter, I replicated the sensitization effects observed *in vitro* in a disseminated leukemia model. Sensitization *in vivo* occurs via disruption of BM interactions and mobilization of leukemic cells into the peripheral blood. This mobilization is in response to a decrease in CD81 surface expression, and thereby potentiates the effects of subsequent chemotherapy treatment through augmented p53-mediated cell death.

Chapter 5

DISCUSSION

5.1 Novel and Significant Findings

Chemoresistance remains a consistent impediment to improving survival rates in pediatric hematologic malignancies like ALL. In this study, I identify that the epigenetic modifying drugs aza and pano in combination have a synergistic killing effect and can sensitize ALL cells to chemotherapy under BMC conditions. This sensitization is driven by a disruption of cellular adhesion via decreased exocytosis of the TSPAN protein CD81, which was identified for the first time to mediate BMC in ALL. Decreased expression of CD81 disrupts the CD19/BTK signaling axis to increase the activation of p53-mediated cell death (Figure 5.1). *In vivo a*za/pano treatment reduces BM load through CD81 downregulation to potentiate the effects of subsequent chemotherapy and improve median survival.

5.2 Using Epigenetic Modifiers to Overcome Chemoresistance

The prevalence of epigenetic alterations during oncogenesis leading to the development of chemoresistance has prompted the use of epigenetic drugs in an effort to circumvent these effects (Quagliano, 2020). This study focuses on the potential of epigenome modifying drugs to overcome the effects of BMC in hematologic malignancies like ALL. While there has been some evidence of the role played by epigenetic modifiers in mitigating microenvironmental interactions in solid tumors, very little information on their effects on hematologic cell interactions with the BM is available. Previous studies have noted the role that epigenetics can play in activation

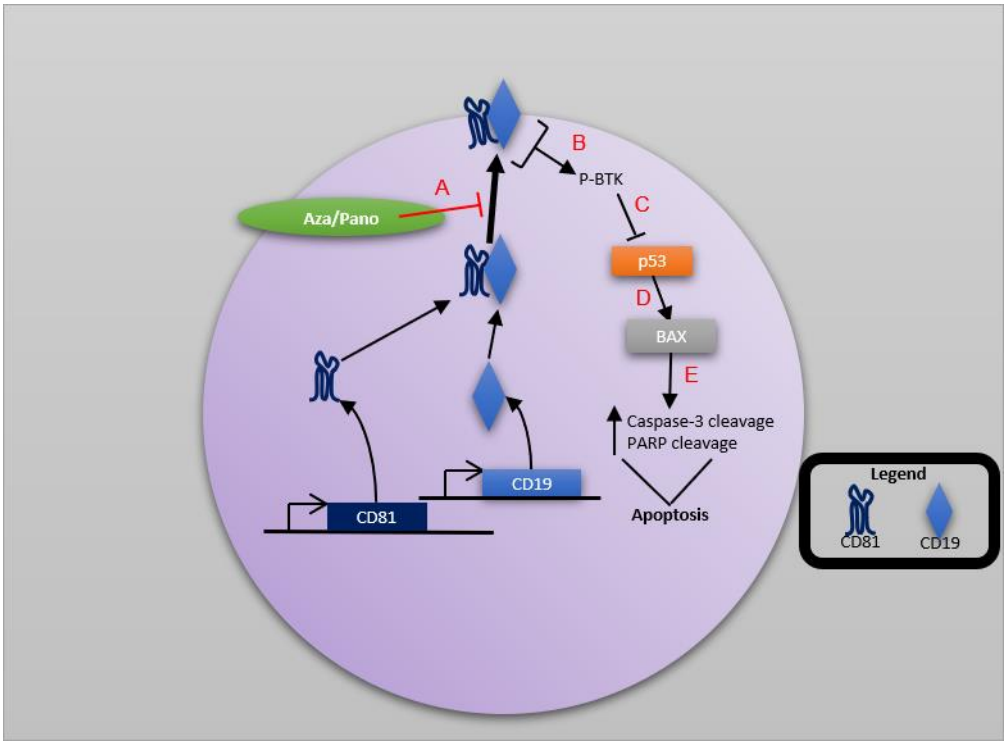

Figure 5.1 Representation of aza/pano sensitization mechanism Cartoon model of the mechanism of sensitization following aza/pano treatment. A) Aza/pano disrupts CD81 exocytosis, thereby preventing translocation of CD19 to the cell surface. B) Phosphorylation of BTK is disrupted, leading to an C) increase in the expression of p53 and D) the protein Bax. E) This causes the rapid cleavage of caspase-3 and culminates in PARP cleavage and apoptosis.

of CAM-mediated BMC via increased activation of adhesion-related pathways (Furukawa and Kikuchi, 2016; Zampini et al., 2018). This study identifies for the first time how epigenetic modifiers can revert these effects, offering a novel method to overcoming BMC and encouraging their use in BMC models in other hematologic malignancies.

While many studies utilizing epigenetic modifiers in cancer have focused on the use of just one drug in conjunction with chemotherapy, this study highlights the potential of modifier combinations in sensitizing cancer cells to treatment. Currently,

very few clinical trials have prioritized the use of a combination of epigenetic drugs along with chemotherapy (Table 5.1). The findings presented here should emphasize the need for further pre-clinical and clinical studies that incorporate multiple epigenetic drugs together as a mechanism to improve anti-cancer therapies.

Malignancy	Epigenetic Modifiers	Other Therapeutics	NCT Identifier
ALL	Decitabine/Vorinostat	Vincristine/Dexamethasone/Mitoxantrone/Pegasparagase/Methotrexate	01483690
AML	Azacitidine/Vorinostat	Gemtuzumab	00895934
AML	Azacitidine/Valproic Acid	All-trans retinoic acid/Hydroxyurea	01369368
AML/MDS	Azacitidine/Valproic Acid	All-trans retinoic acid	00339196
Breast	Decitabine/Panobinostat	Tamoxifen	01194908
Lymphoma	Azacitidine/Vorinostat	Gemcitabine/Busulfan/Melphalan/Dexamethasone/Caphosol/Glutamine/Pyridoxine/Rituximab	01983969
MDS	Azacitidine/Valproic Acid	All-trans retinoic acid	00326170
MDS	Decitabine/Vorinostat	CD3-/CD19- NK cell infusion	01593670
MDS	Azacitidine/Valproic Acid	All-trans retinoic acid	00439673
Melanoma	Decitabine/Panobinostat	Temozolomide	00925132
NSCLC	Azacitidine/Entinostat	Docetaxel/Gemcitabine/Irinotecan	01935947
NSCLC	Azacitidine/Entinostat	Nivolumab	01928576

Table 5.1: List of clinical trials utilizing multiple epigenetic modifiers in combination with traditional therapy

5.3 Specificity and Non-Specificity of Epigenetic Modifiers

On the surface, epigenetic modifiers are considered to be “non-specific” in that they alter the epigenome on a global scale rather than affecting specific gene expression. However, the effects of epigenetic modifier treatment can be felt in a “specific” manner in malignant cells. This is due to the epigenetic alterations that are accumulated during oncogenesis. Due to aberrant activity of epigenetic machinery, treatment with epigenetic modifiers can reverse these associated gene expression

changes. Thus, epigenetic modifier treatment can elicit “specific” effects within cancer cells based on the certain subsets of genes altered by epigenetic mechanisms. Additionally, the three-dimensional chromatin structure could also be responsible for conferring sensitivity to epigenetic therapies within specific genomic loci (Farhy et al., 2019; Zhang et al., 2020).

5.4 The Importance Aza/Pano-Mediated Mobilization of ALL Cells

Treatment with aza/pano was able to sensitize ALL cells to chemotherapy under BMC conditions in part by reducing their ability to adhere to BM cells. *In vivo*, this leads to a decreased BM load immediately following treatment. However, despite this decrease in BM load, there was an increase in the percentage of human leukemic cells in the peripheral blood. Considering that BM load and peripheral blood are typically correlated with one another, this finding suggests that leukemic cells were mobilized from the BM, uncovering a novel mechanism of chemosensitization by aza/pano. This observation in conjunction CD81KO cell deficiencies in homing and engraftment supports the role that aza/pano-mediated reduction in CD81 surface expression plays in mobilizing leukemic cells.

This finding is supported by a previous study which identified abundant CD81 expression on healthy progenitor B-cells and loss of CD81 on mature B-cells prepared to exit the BM (Barrena et al., 2005). Differences in CD81 surface expression between blood and BM were detected *in vivo* ($p < 0.01$, Figure 4.5A, bars 1 and 3), further supporting a BM homing role of CD81 in ALL. Together, these data suggest that

CD81 downregulation by aza/pano is an efficient mechanism for increasing leukemic cell mobilization, thus enhancing response to chemotherapy and improving survival.

One of the key contributors to relapse in hematologic malignancies like ALL is the continued presence of malignant cells in the BM following completion of treatment (Buccisano et al., 2006). This is known as minimal residual disease (MRD), and its elimination is critical to preventing secondary recurrences in patients (Health Quality, 2016). Consolidation therapy aims to reduce or eliminate MRD levels altogether, however, its effectiveness can be limited due to the development of chemoresistance and/or BM homing/evasion of leukemic cells (Barwe et al., 2017). As demonstrated in this study, aza/pano successfully mobilizes leukemic cells from the BM into the peripheral blood, thereby potentiating subsequent treatments. These findings highlight the potential use of aza/pano as an adjunct to consolidation therapy in order to potentiate its effects to reduce or eliminate MRD and prevent relapse. However, current study of the use of epigenetic modifiers in pediatric ALL utilizes them during induction therapy and not consolidation, potentially reducing their effectiveness. Further study of the protocol of aza/pano treatment is required to determine if its use in consolidation therapy could prove beneficial.

5.5 CD81's Role in ALL and Its Use in MRD Detection

Prior to this study, CD81's role in ALL had not been identified. However, CD81 downregulation was a way to distinguish leukemic cells from hematogones, recovering BM cells, for MRD measurement (Muzzafar et al., 2009; Nagant et al., 2018; Theunissen et al., 2017). This would suggest that CD81 expression on ALL

blasts was lower than normal BM precursor cells and there is a reliance of healthy BM progenitor cells on CD81 expression for B-cell development. However, transgenic $CD81^{-/-}$ mice were shown to have relatively normal B-cell development despite aberrant B-cell responses (Tsitsikov et al., 1997). Additionally, it is known that CD81 expression on mature cells is lower than ALL blasts (Barrena et al., 2005). It is also worth mentioning that aza/pano-mediated downregulation of CD81 was reversible upon removal of the drug, thus suggesting any long-term effects on B-cell development would be minimal. Thus, the data presented in this study clearly identifies CD81 as an attractive target in ALL.

5.6 TSPANs and TEMs Potent Targets in Hematologic Malignancies

CD81 and other TSPANs mediate many of their microenvironmental interactions through the formation of dynamic membrane nanoplatforms called TEMs (Barreiro et al., 2005; Hemler, 2005; Tarrant et al., 2003; van Deventer et al., 2017). Through the formation of these membrane microdomains, TSPANs are able to control the expression, density, and activation of adhesion molecules like those of the integrin family and the immunoglobulin superfamily. Such interactions with integrins like VLA-4 can improve its stability, and thereby its adhesion to targets like VCAM-1 (Feigelson et al., 2003). By augmenting interactions with microenvironments such as the BM, associated intracellular signaling pathways can be aberrantly activated, culminating in a resistance to chemotherapy via BMC.

Therefore, targeting TSPAN expression on the surface of hematologic malignant cells offers a new avenue to inhibit BM interactions and activation of BMC.

Contrary to anti-CAM therapies which target specific adhesion molecules, therapies that target TSPAN expression could prove more successful due to the disruption of TEM formations. These effects could be more broadly felts than CAM-specific inhibitors because of the dynamic formation and function of TEMs in microenvironmental interactions.

It is important to note that while targeting specific TSPANs could be beneficial, it does not guarantee success. Due to the redundancies built into TSPAN proteins (EC2 loops and transmembrane domains specifically), different TSPANs can interact with the same surface proteins to bring about similar effects (specifically interactions with integrins). This "compensatory mechanism" allows for functional TEM activity even in the absence of a specific TSPAN. Both CD9 and CD82 have been studied in leukemia previously and are known leukemia promoters, making them additional targets for inhibition studies in my BMC model (Arnaud et al., 2015; Marjon et al., 2016).

While the exact epigenetic mechanism of CD81 downregulation requires further study, preliminary indications show that WIPF1 downregulation may be responsible for defects in CD81 exocytosis. This presents another mechanism for inhibiting TSPAN surface expression. While WIPF1 is only known to mediate CD81 surface expression, it is possible that it could also control the expression of other TSPANs. Additionally, there could be other proteins involved with the actin cytoskeleton, like WIPF1, or chaperone proteins that interact with specific TSPANs whose expression could be modulated in an epigenetic manner. More study on TSPAN

translocation to the cell surface is needed to understand not only how it can be inhibited, but it could also shed more light on TEM formation and function.

5.7 "Inside-Out" Signaling of BTK and Effects on Adhesion

In addition to regulating cell survival, BTK signaling can also control cellular adhesion. Upon stimulation from the B-cell receptor, BTK activates PLCγ2, leading to IP3R-mediated Ca^{2+} release and augmented PKC activity (Spaargaren et al., 2003). This culminates in cytoskeletal reorganization, integrin clustering, and integrin activation, and is known as "inside-out" signaling. Thereby, inhibition of BTK activity has been shown to have significant effects on both integrin-mediated cellular adhesion as well as integrin expression (like VLA-4).

Since both BTK and CD81 are known to control integrin-mediated adhesion, and BTK signaling is associated with CD81 surface expression, it remains unclear if CD81 downregulation or diminished BTK signaling is responsible for the observed decreases in cellular adhesion and BM homing in this study. It is possible that the combination of CD81 and BTK signaling downregulation is the cause of the diminished adhesion, and not just one or the other. More study on this CD81/BTK axis is required to elucidate how it affects adhesion.

5.8 The BTK/p53 Axis in Cancer

The effect of BTK on cell death can be pleiotropic and cancer specific (Rada et al., 2018). In solid tumors, BTK induces p53-mediated cell death by blocking the inhibitory effects of MDM2. However, in B-cell malignancies, BTK is considered to

be oncogenic. In this study, I identify that the oncogenic role of BTK in B-ALL is due at least in part to its inhibition of p53-mediated cell death.

While this study has identified BTK's control of p53-mediated cell death, the exact mechanism by which this occurs remains unknown. It is unclear whether or not BTK interacts directly with p53 in order to achieve inhibition, or if it works indirectly via a third party. One possible connection may be through ATM-Traf6. ATM is known to be phosphorylated via BTK and can activate Traf6, an E3 ubiquitin ligase responsible for ubiquitylation of p53, thus inhibiting its pro-apoptotic activity (Althubiti et al., 2016; Chen et al., 2019). More study of the BTK/p53 connection is still required to understand how diminished BTK signaling leads to p53-mediated cell death.

5.9 Issues Facing Targeted BTK Therapies in Hematologic Malignancies

BTK is a rising therapeutic target in B-cell malignancies like B-ALL. However, patients often present with or develop resistance to BTK inhibitors. One of the most recurrent BTK mutations is C481S, which prevents covalent binding of the classical BTK inhibitor ibrutinib to induce resistance (Woyach et al., 2014). Therefore, non-covalent inhibitors such as fenebrutinib, which was used in this study to combat a C481S mutation in the Nalm6 cell line, have been developed in order to circumvent these resistant phenotypes.

In addition to BTKi resistance, concerns have risen about the long-term side effects of using tyrosine kinase inhibitors (TKI). Cardiotoxicity and skeletal/muscular defects have been discovered as possible lasting detriments to TKI usage (Caldemeyer et al., 2016; Tauer et al., 2015). Having identified the effectiveness of aza/pano in

mitigating BTK signaling, treatment with epigenetic drugs could provide an additional route to inhibit TKI activity in an effective manner while also reducing long-term negative effects.

5.10 Additional Effects of Aza/Pano Treatment in ALL

Based on the data presented in this study, the use of epigenetic modifiers could be a mechanism of disrupting TSPAN expression. However, the effects of these drugs must be studied on specific TSPANs, as downregulation is not guaranteed. CD9 surface expression increases following aza/pano treatment in contrast with CD81 downregulation (Figure 5.2). While previous data would suggest that this effect is inhibitory to sensitization, it will require further study.

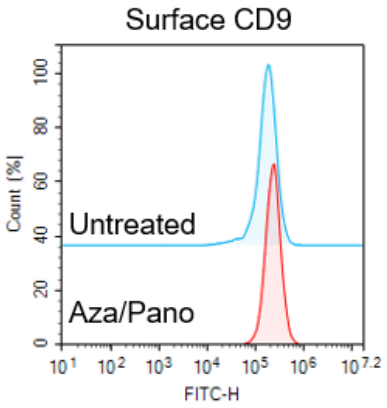

Figure 5.2 Surface expression of TSPAN protein CD9 is upregulated following treatment with aza/pano Flow cytometry plot comparing CD9 surface expression between untreated and aza/pano-treated Nalm6 cells after 48 h. Representative plot of three independent experiments is shown.

While this study identified CD81 downregulation by aza/pano to be responsible for sensitization, further mechanistic investigation is still warranted in order to elucidate additional effects of aza/pano treatment. As mentioned in chapter 3, an RNAseq analysis was performed on Nalm6 cells treated with aza/pano. Analysis of this data by

the “Key Pathway Advisor” software identified the transcription factor protein GATA-4 to be a key downregulated hub (Figure 5.3). GATA-4 is known to be highly expressed in pediatric ALL, augmenting cellular proliferation and suppressing apoptosis (Han et al., 2017). While there are no known connections of GATA-4 to BTK signaling, ATM, a BTK target, can inhibit p62 to increase GATA-4 expression levels and activity (Kang et al., 2015). The downstream BTK target, ERK, is also known to activate GATA-4 (Liang et al., 2001). This data makes GATA-4 an intriguing target for future study following the use of aza/pano.

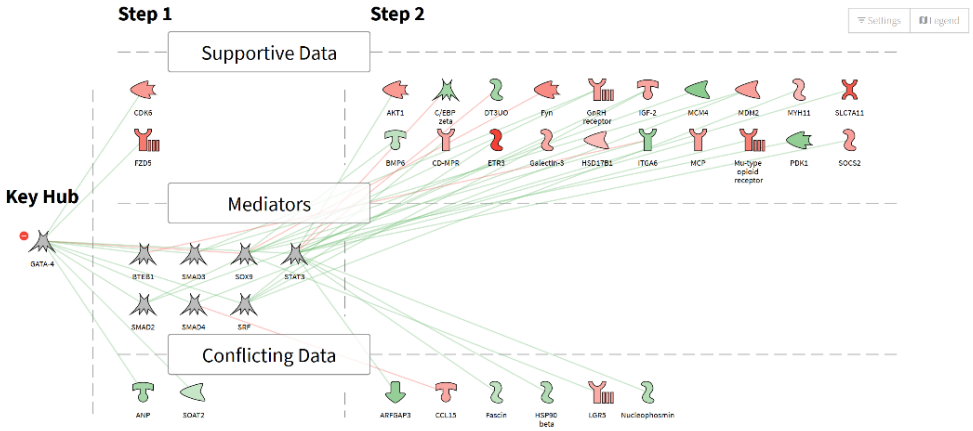

Figure 5.3 Key Pathway Advisor identified GATA-4 as a key hub downregulated by aza/pano Importing RNAseq data following treatment with aza/pano into the software “Key Pathway Advisor” identified GATA-4 as a key hub that is being downregulated following treatment. Red highlights are downregulated transcripts, while green highlights are upregulated transcripts. The more intense the color, the further the modulation of the transcript.

Another gene of interest that was highly modulated by aza/pano is ARID5B (Table 3.1). ARID5B genetic variants are known to be risk factors for pediatric ALL (Kreile et al., 2018). Recent studies have also identified low ARID5B expression to be

associated with a high risk of relapse, and its downregulation is correlated with an increased resistance to antimetabolites (Ge et al., 2018; Xu et al., 2020). This would suggest that treatment with aza/pano could restore antimetabolite sensitivity via ARID5B-induced expression. However, the exact mechanism of induced expression by aza/pano requires further analysis.

In addition to discovering CD81 downregulation by aza/pano, data from the Lyoplate™ screening assay identified CD38 to be over 4-fold increased in expression (Figure 5.4). Previously, B-cell malignancies like multiple myeloma have been treated with anti-CD38 mAbs to target malignant cells (Morandi et al., 2018). Due to CD38's significant increase following aza/pano treatment, combination with anti-CD38 therapies could provide a potent mechanism for inducing cell death and improving patient survival in B-ALL.

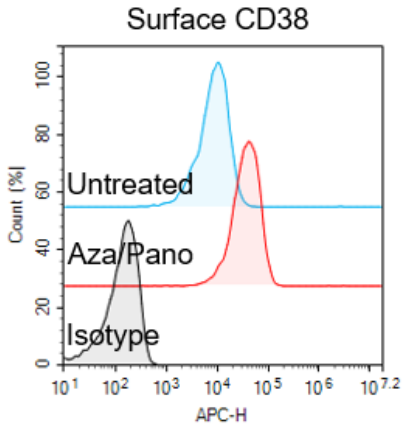

Figure 5.4 CD38 surface expression is increased following treatment with aza/pano Flow cytometry plot of untreated or aza/pano-treated Nalm6 cells for 48 h. Plot is from one trial of a Lyoplate™ screening assay. Isotype shown for reference

5.11 Exocytosis: Epigenetically Controlled and a Target to Overcome BMC?

Having identified a defect in CD81 exocytosis following treatment with aza/pano, a new question arises about epigenetic control of exocytosis. Currently, there is very little information available on the effect of epigenetics on exocytosis. However, in this study I identify WIPF1 transcript to be decreased, possibly causing the defect in CD81 exocytosis. This data could suggest that epigenetics can affect exocytosis through modulation of genes involved with the secretory pathway or actin cytoskeleton (like WIPF1).

In addition to WIPF1, other genes from the RNAseq data may suggest alterations in the epigenetic control on exocytosis. Two genes in particular, PITPNM3 and ITPKA, are known to play a role in calcium homeostasis and phosphoinositide formation, two key components in the process of exocytosis (Barclay et al., 2005; Schink et al., 2016). However, more study on these specific genes and others involved with exocytosis is required to better understand the process prior to attempting to decipher how epigenetics modulates exocytosis. Once key hubs/genes are identified, they could possibly represent novel targets to mitigate the effects of BMC, possibly through the use of epigenetic modifiers.

Chapter 6

FUTURE DIRECTIONS

I identified aza/pano sensitization occurs via modulation of CD81 surface expression. Additional questions about this mechanism require further investigation. First, how is CD81 exocytosis disrupted specifically while the expression of other cell surface proteins is unchanged? I identified WIPF1, which has previously been shown to control CD81 surface expression, to be downregulated following aza/pano treatment. However, further mechanistic study of WIPF1-mediated CD81 regulation in aza/pano-treated cells must be performed. Additionally, the epigenetic effect of aza/pano treatment must also be identified in order to understand the complete mechanism of sensitization. Identification of specific gene(s) related to aza/pano sensitization will provide biomarkers to predict patients who are good candidates to receive epigenetic therapy.

Beyond the mechanism identified in this study, a deeper analysis of the RNAseq data should also be performed in order to identify possible additional mechanisms or markers for treatment. This data should also be combined with transcript analyses from other models as well in an attempt to find consistently modulated targets. In addition to RNAseq, analysis of microRNA (miRNA) expression should also be performed. miRNAs are important regulators of gene expression and are known to be controlled via epigenetic mechanisms as well. Therefore, studying their alterations may shed more understanding on the transcript modulations that occur and/or identify additional markers for treatment.

As previously mentioned, this study is the first to confirm the role of the TSPAN CD81 in ALL and BMC. While the role of TSPANs have been studied more so recently in hematologic malignancies, understanding is still not widespread. Therefore, continued examination of their effects must be performed. In accordance with this study, examining the interactome of CD81 in ALL could provide better insight into how CD81 mediates its specific role in BMC.

In addition to diving deeper into CD81 function, follow-up examinations of the role of other TSPANs in ALL should also be performed. Due to the redundant nature of TSPANs, it is likely that multiple TSPANs can play a role in ALL progression and the development of BMC. Identifying how other TSPANs affect these processes provides not only understanding of their specific roles, but also on how different TSPANs can possibly compensate for one another in order to maintain their effects. This information could provide insight in ways to successfully augment the effectiveness of targeted therapies against TSPANs. Continued study of TSPANs and their effects is likely to reveal more information on TEMs, including how they are formed, their compositions, and their functions.

One of the most significant findings in this study is the ability of aza/pano to mobilize ALL cells from the BM into the peripheral blood. This unlocks the potential to significantly decrease relapse rates by reducing BM load post-chemotherapy treatment. Specifically, utilizing aza/pano after the induction phase and prior to consolidation therapy could be an efficient way to reduce BM load and augment consolidation effectiveness to reduce/eliminate MRD, thereby diminishing odds of

relapse and improving overall survival. Examination of an induction/pre-consolidation (aza/pano)/consolidation model should be performed *in vivo* to determine if this approach could be successful. Following this examination, it is my hope that this study/model could be developed into a clinical trial for analysis in human patients.

While this study only focused on the deployment of aza/pano in ALL sensitization, its use in other hematologic malignancies should also be examined. In particular, studying the mobilization of malignant cells from the BM is of particular interest since the BM provides sanctuary to multiple types of hematologic malignancies. If the effects observed in ALL can also be replicated in other malignancies, this provides ample opportunity for the reduction of relapse and improvement in survival. Additionally, the use of other epigenetic modifiers and their effects should also be examined singularly and in combination. While I show aza/pano to be successful, it is possible that other modifiers and combinations may also find success, possibly even to a greater degree.

REFERENCES

Abe, M., T. Sugiura, M. Takahashi, K. Ishii, M. Shimoda, and K. Shirasuna. 2008. A novel function of CD82/KAI-1 on E-cadherin-mediated homophilic cellular adhesion of cancer cells. *Cancer Lett*. 266:163-170.

Akbari Moqadam, F., E.A. Lange-Turenhout, I.M. Aries, R. Pieters, and M.L. den Boer. 2013. MiR-125b, miR-100 and miR-99a co-regulate vincristine resistance in childhood acute lymphoblastic leukemia. *Leuk Res*. 37:1315-1321.

Althubiti, M., M. Rada, J. Samuel, J.M. Escorsa, H. Najeeb, K.G. Lee, K.P. Lam, G.D. Jones, N.A. Barlev, and S. Macip. 2016. BTK Modulates p53 Activity to Enhance Apoptotic and Senescent Responses. *Cancer Res*. 76:5405-5414.

Arnaud, M.P., A. Vallee, G. Robert, J. Bonneau, C. Leroy, N. Varin-Blank, A.G. Rio, M.B. Troadec, M.D. Galibert, and V. Gandemer. 2015. CD9, a key actor in the dissemination of lymphoblastic leukemia, modulating CXCR4-mediated migration via RAC1 signaling. *Blood*. 126:1802-1812.

Bannister, A.J., and T. Kouzarides. 2011. Regulation of chromatin by histone modifications. *Cell Res*. 21:381-395.

Barclay, J.W., A. Morgan, and R.D. Burgoyne. 2005. Calcium-dependent regulation of exocytosis. *Cell Calcium*. 38:343-353.

Barreiro, O., M. Yanez-Mo, M. Sala-Valdes, M.D. Gutierrez-Lopez, S. Ovalle, A. Higginbottom, P.N. Monk, C. Cabanas, and F. Sanchez-Madrid. 2005. Endothelial tetraspanin microdomains regulate leukocyte firm adhesion during extravasation. *Blood*. 105:2852-2861.

Barrena, S., J. Almeida, M. Yunta, A. Lopez, N. Fernandez-Mosteirin, M. Giralt, M. Romero, L. Perdiguer, M. Delgado, A. Orfao, and P.A. Lazo. 2005. Aberrant expression of tetraspanin molecules in B-cell chronic lymphoproliferative disorders and its correlation with normal B-cell maturation. *Leukemia*. 19:1376-1383.

Barwe, S.P., A. Quagliano, and A. Gopalakrishnapillai. 2017. Eviction from the sanctuary: Development of targeted therapy against cell adhesion molecules in acute lymphoblastic leukemia. *Semin Oncol*. 44:101-112.

Berditchevski, F., and E. Odintsova. 1999. Characterization of integrin-tetraspanin adhesion complexes: role of tetraspanins in integrin signaling. *J Cell Biol*. 146:477-492.

Berditchevski, F., E. Odintsova, S. Sawada, and E. Gilbert. 2002. Expression of the palmitoylation-deficient CD151 weakens the association of alpha 3 beta 1 integrin with the tetraspanin-enriched microdomains and affects integrin-dependent signaling. *J Biol Chem*. 277:36991-37000.

Berditchevski, F., K.F. Tolias, K. Wong, C.L. Carpenter, and M.E. Hemler. 1997. A novel link between integrins, transmembrane-4 superfamily proteins (CD63 and CD81), and phosphatidylinositol 4-kinase. *J Biol Chem*. 272:2595-2598.

Berger, S.L., T. Kouzarides, R. Shiekhattar, and A. Shilatifard. 2009. An operational definition of epigenetics. *Genes Dev*. 23:781-783.

Birbrair, A., and P.S. Frenette. 2016. Niche heterogeneity in the bone marrow. *Ann N Y Acad Sci*. 1370:82-96.

Boyer, T., S. Guihard, C. Roumier, P. Peyrouze, F. Gonzales, C. Berthon, B. Quesnel, C. Preudhomme, H. Behal, A. Duhamel, C. Roche-Lestienne, and M. Cheok. 2016. Tetraspanin CD81 is an adverse prognostic marker in acute myeloid leukemia. *Oncotarget*. 7:62377-62385.

Brinkman, E.K., T. Chen, M. Amendola, and B. van Steensel. 2014. Easy quantitative assessment of genome editing by sequence trace decomposition. *Nucleic Acids Res*. 42:e168.

Buccisano, F., L. Maurillo, V. Gattei, G. Del Poeta, M.I. Del Principe, M.C. Cox, P. Panetta, M.I. Consalvo, C. Mazzone, B. Neri, L. Ottaviani, D. Fraboni, A. Tamburini, F. Lo-Coco, S. Amadori, and A. Venditti. 2006. The kinetics of reduction of minimal residual disease impacts on duration of response and survival of patients with acute myeloid leukemia. *Leukemia*. 20:1783-1789.

Burke, M.J., and T. Bhatla. 2014. Epigenetic modifications in pediatric acute lymphoblastic leukemia. *Front Pediatr*. 2:42.

Caldemeyer, L., M. Dugan, J. Edwards, and L. Akard. 2016. Long-Term Side Effects of Tyrosine Kinase Inhibitors in Chronic Myeloid Leukemia. *Curr Hematol Malig Rep*. 11:71-79.

Campana, D. 2010. Minimal residual disease in acute lymphoblastic leukemia. *Hematology Am Soc Hematol Educ Program*. 2010:7-12.

Cao, L., T. Yoshino, N. Kawasaki, I. Sakuma, K. Takahashi, and T. Akagi. 1997. Anti-CD53 monoclonal antibody induced LFA-1/ICAM-1-dependent and -independent lymphocyte homotypic cell aggregation. *Immunobiology*. 197:70-81.

Carloni, V., A. Mazzocca, and K.S. Ravichandran. 2004. Tetraspanin CD81 is linked to ERK/MAPKinase signaling by Shc in liver tumor cells. *Oncogene*. 23:1566-1574.

Catts, V.S., M.L. Farnsworth, M. Haber, M.D. Norris, L.H. Lutze-Mann, and R.B. Lock. 2001. High level resistance to glucocorticoids, associated with a dysfunctional glucocorticoid receptor, in childhood acute lymphoblastic leukemia cells selected for methotrexate resistance. *Leukemia*. 15:929-935.

Charrin, S., S. Jouannet, C. Boucheix, and E. Rubinstein. 2014. Tetraspanins at a glance. *J Cell Sci*. 127:3641-3648.

Charrin, S., S. Manie, M. Oualid, M. Billard, C. Boucheix, and E. Rubinstein. 2002. Differential stability of tetraspanin/tetraspanin interactions: role of palmitoylation. *FEBS Lett*. 516:139-144.

Chen, S., H. Xing, S. Li, J. Yu, H. Li, S. Liu, Z. Tian, K. Tang, Q. Rao, M. Wang, and J. Wang. 2015. Up-regulated A20 promotes proliferation, regulates cell cycle progression and induces chemotherapy resistance of acute lymphoblastic leukemia cells. *Leuk Res*. 39:976-983.

Chen, Y.L., C. Tang, M.Y. Zhang, W.L. Huang, Y. Xu, H.Y. Sun, F. Yang, L.L. Song, H. Wang, L.L. Mu, M.H. Li, W.W. Zheng, Y. Miao, L.X. Ding, B.S. Li, S.H. Shen, S.L. Liu, H. Li, Z.Q. Zhu, H.W. Chen, Z.H. Tang, J. Chen, D.L. Hong, H.Z. Chen, C.W. Duan, and B.S. Zhou. 2019. Blocking ATM-dependent NF-kappaB pathway overcomes niche protection and improves chemotherapy response in acute lymphoblastic leukemia. *Leukemia*. 33:2365-2378.

Cherukuri, A., T. Shoham, H.W. Sohn, S. Levy, S. Brooks, R. Carter, and S.K. Pierce. 2004. The tetraspanin CD81 is necessary for partitioning of coligated CD19/CD21-B cell antigen receptor complexes into signaling-active lipid rafts. *J Immunol*. 172:370-380.

Chiaretti, S., G. Zini, and R. Bassan. 2014. Diagnosis and subclassification of acute lymphoblastic leukemia. *Mediterr J Hematol Infect Dis.* 6:e2014073.

Delaguillaumie, A., C. Lagaudriere-Gesbert, M.R. Popoff, and H. Conjeaud. 2002. Rho GTPases link cytoskeletal rearrangements and activation processes induced via the tetraspanin CD82 in T lymphocytes. *J Cell Sci*. 115:433-443.

Delandre, C., T.R. Penabaz, A.L. Passarelli, S.K. Chapes, and R.J. Clem. 2009. Mutation of juxtamembrane cysteines in the tetraspanin CD81 affects palmitoylation and alters interaction with other proteins at the cell surface. *Exp Cell Res*. 315:1953-1963.

Dupont, C., D.R. Armant, and C.A. Brenner. 2009. Epigenetics: definition, mechanisms and clinical perspective. *Semin Reprod Med*. 27:351-357.

Farhy, C., S. Hariharan, J. Ylanko, L. Orozco, F.Y. Zeng, I. Pass, F. Ugarte, E.C. Forsberg, C.T. Huang, D.W. Andrews, and A.V. Terskikh. 2019. Improving drug discovery using image-based multiparametric analysis of the epigenetic landscape. *Elife*. 8.

Feigelson, S.W., V. Grabovsky, R. Shamri, S. Levy, and R. Alon. 2003. The CD81 tetraspanin facilitates instantaneous leukocyte VLA-4 adhesion strengthening to vascular cell adhesion molecule 1 (VCAM-1) under shear flow. *J Biol Chem*. 278:51203-51212.

Figueroa, M.E., S.C. Chen, A.K. Andersson, L.A. Phillips, Y. Li, J. Sotzen, M. Kundu, J.R. Downing, A. Melnick, and C.G. Mullighan. 2013. Integrated genetic and epigenetic analysis of childhood acute lymphoblastic leukemia. *J Clin Invest*. 123:3099-3111.

Fujimoto, M., J.C. Poe, A.B. Satterthwaite, M.I. Wahl, O.N. Witte, and T.F. Tedder. 2002. Complementary roles for CD19 and Bruton's tyrosine kinase in B lymphocyte signal transduction. *J Immunol*. 168:5465-5476.

Furukawa, Y., and J. Kikuchi. 2016. Epigenetic mechanisms of cell adhesion-mediated drug resistance in multiple myeloma. *Int J Hematol*. 104:281-292.

Ge, Z., Q. Han, Y. Gu, Q. Ge, J. Ma, J. Sloane, G. Gao, K.J. Payne, L. Szekely, C. Song, and S. Dovat. 2018. Aberrant ARID5B expression and its association with Ikaros dysfunction in acute lymphoblastic leukemia. *Oncogenesis*. 7:84.

Geley, S., B.L. Hartmann, M. Hala, E.M. Strasser-Wozak, K. Kapelari, and R. Kofler. 1996. Resistance to glucocorticoid-induced apoptosis in human T-cell acute lymphoblastic leukemia CEM-C1 cells is due to insufficient glucocorticoid receptor expression. *Cancer Res*. 56:5033-5038.

Gillette, J.M., and J. Lippincott-Schwartz. 2009. Hematopoietic progenitor cells regulate their niche microenvironment through a novel mechanism of cell-cell communication. *Commun Integr Biol*. 2:305-307.

Gonzales, F., T. Boyer, P. Peyrouze, S. Guihard, C. Roumier, C. Berthon, C. Preudhomme, and M. Cheok. 2017a. Targeting Aberrant Expression of CD81 Impacts Cell Adhesion and Migration, Drug Resistance and Prognosis of Acute Myeloid Leukemia. *Blood*. 130:2675-2675.

Gonzales, F., T. Boyer, P. Peyrouze, S. Guihard, C. Roumier, C. Berthon, C. Preudhomme, and M. Cheok. 2017b. Targeting Aberrant Expression of CD81 Impacts Cell Adhesion and

Migration, Drug Resistance and Prognosis of Acute Myeloid Leukemia. *Blood*. 130:2675-2675.

Gopalakrishnapillai, A., E.A. Kolb, P. Dhanan, A.S. Bojja, R.W. Mason, D. Corao, and S.P. Barwe. 2016. Generation of Pediatric Leukemia Xenograft Models in NSG-B2m Mice: Comparison with NOD/SCID Mice. *Front Oncol*. 6:162.

Gopalakrishnapillai, A., E.A. Kolb, P. Dhanan, R.W. Mason, A. Napper, and S.P. Barwe. 2015. Disruption of Annexin II /p11 Interaction Suppresses Leukemia Cell Binding, Homing and Engraftment, and Sensitizes the Leukemia Cells to Chemotherapy. *PLoS One*. 10:e0140564.

Grudowska, A., D. Czaplinska, W. Polom, M. Matuszewski, R. Sadej, and A.C. Skladanowski. 2017. Tetraspanin CD151 mediates communication between PC3 prostate cancer cells and osteoblasts. *Acta Biochim Pol*. 64:135-141.

Gustafson-Wagner, E., and C.S. Stipp. 2013. The CD9/CD81 tetraspanin complex and tetraspanin CD151 regulate alpha3beta1 integrin-dependent tumor cell behaviors by overlapping but distinct mechanisms. *PLoS One*. 8:e61834.

Hahnel, P.S., B. Enders, D. Sasca, W.P. Roos, B. Kaina, L. Bullinger, M. Theobald, and T. Kindler. 2014. Targeting components of the alternative NHEJ pathway sensitizes KRAS mutant leukemic cells to chemotherapy. *Blood*. 123:2355-2366.

Han, Q., X. Xu, J. Li, J. Wang, L. Bai, A. Wang, W. Wang, and B. Zhang. 2017. GATA4 is highly expressed in childhood acute lymphoblastic leukemia, promotes cell proliferation and inhibits apoptosis by activating BCL2 and MDM2. *Mol Med Rep*. 16:6290-6298.

Hazlehurst, L.A., and W.S. Dalton. 2001. Mechanisms associated with cell adhesion mediated drug resistance (CAM-DR) in hematopoietic malignancies. *Cancer Metastasis Rev*. 20:43-50.

He, J., O. Abdel-Wahab, M.K. Nahas, K. Wang, R.K. Rampal, A.M. Intlekofer, J. Patel, A. Krivstov, G.M. Frampton, L.E. Young, S. Zhong, M. Bailey, J.R. White, S. Roels, J. Deffenbaugh, A. Fichtenholtz, T. Brennan, M. Rosenzweig, K. Pelak, K.M. Knapp, K.W. Brennan, A.L. Donahue, G. Young, L. Garcia, S.T. Beckstrom, M. Zhao, E. White, V. Banning, J. Buell, K. Iwanik, J.S. Ross, D. Morosini, A. Younes, A.M. Hanash, E. Paietta, K. Roberts, C. Mullighan, A. Dogan, S.A. Armstrong, T. Mughal, J.A. Vergilio, E. Labrecque, R. Erlich, C. Vietz, R. Yelensky, P.J. Stephens, V.A. Miller, M.R. van den Brink, G.A. Otto, D. Lipson, and R.L. Levine. 2016. Integrated genomic DNA/RNA profiling of hematologic malignancies in the clinical setting. *Blood*. 127:3004-3014.

Health Quality, O. 2016. Minimal Residual Disease Evaluation in Childhood Acute Lymphoblastic Leukemia: A Clinical Evidence Review. *Ont Health Technol Assess Ser*. 16:1-52.

Hemler, M.E. 2005. Tetraspanin functions and associated microdomains. *Nat Rev Mol Cell Biol*. 6:801-811.

Higginbottom, A., E.R. Quinn, C.C. Kuo, M. Flint, L.H. Wilson, E. Bianchi, A. Nicosia, P.N. Monk, J.A. McKeating, and S. Levy. 2000. Identification of amino acid residues in CD81 critical for interaction with hepatitis C virus envelope glycoprotein E2. *J Virol*. 74:3642-3649.

Hiroshima, K., M. Shiiba, N. Oka, F. Hayashi, S. Ishida, R. Fukushima, K. Koike, M. Iyoda, D. Nakashima, H. Tanzawa, and K. Uzawa. 2019. Tspan15 plays a crucial role in metastasis in oral squamous cell carcinoma. *Exp Cell Res*:111622.

Hong, I.K., H.J. Byun, J. Lee, Y.J. Jin, S.J. Wang, D.I. Jeoung, Y.M. Kim, and H. Lee. 2014. The tetraspanin CD81 protein increases melanoma cell motility by up-regulating metalloproteinase MT1-MMP expression through the pro-oncogenic Akt-dependent Sp1 activation signaling pathways. *J Biol Chem*. 289:15691-15704.

Hong, I.K., D.I. Jeoung, K.S. Ha, Y.M. Kim, and H. Lee. 2012. Tetraspanin CD151 stimulates adhesion-dependent activation of Ras, Rac, and Cdc42 by facilitating molecular association between beta1 integrins and small GTPases. *J Biol Chem*. 287:32027-32039.

Horvath, G., V. Serru, D. Clay, M. Billard, C. Boucheix, and E. Rubinstein. 1998. CD19 is linked to the integrin-associated tetraspans CD9, CD81, and CD82. *J Biol Chem*. 273:30537-30543.

Hosono, N., S. Kishi, S. Iho, Y. Urasaki, A. Yoshida, H. Kurooka, Y. Yokota, and T. Ueda. 2010. Glutathione S-transferase M1 inhibits dexamethasone-induced apoptosis in association with the suppression of Bim through dual mechanisms in a lymphoblastic leukemia cell line. *Cancer Sci*. 101:767-773.

Hsieh, Y.T., E.J. Gang, H. Geng, E. Park, S. Huantes, D. Chudziak, K. Dauber, P. Schaefer, C. Scharman, H. Shimada, S. Shojaee, L. Klemm, R. Parameswaran, M. Loh, E.S. Kang, H.H. Koo, W.K. Hofmann, J. Andrade, G.M. Crooks, C.L. Willman, M. Muschen, T. Papayannopoulou, N. Heisterkamp, H. Bonig, and Y.M. Kim. 2013. Integrin alpha4 blockade sensitizes drug resistant pre-B acute lymphoblastic leukemia to chemotherapy. *Blood*. 121:1814-1818.

Hu, X., H. Xuan, H. Du, H. Jiang, and J. Huang. 2014. Down-regulation of CD9 by methylation decreased bortezomib sensitivity in multiple myeloma. *PLoS One*. 9:e95765.

Hunger, S.P., and C.G. Mullighan. 2015. Acute Lymphoblastic Leukemia in Children. *N Engl J Med*. 373:1541-1552.

Hur, J., J.I. Choi, H. Lee, P. Nham, T.W. Kim, C.W. Chae, J.Y. Yun, J.A. Kang, J. Kang, S.E. Lee, C.H. Yoon, K. Boo, S. Ham, T.Y. Roh, J.K. Jun, H. Lee, S.H. Baek, and H.S. Kim. 2016. CD82/KAI1 Maintains the Dormancy of Long-Term Hematopoietic Stem Cells through Interaction with DARC-Expressing Macrophages. *Cell Stem Cell*. 18:508-521.

Hwang, S., T. Takimoto, and M.E. Hemler. 2019. Integrin-independent support of cancer drug resistance by tetraspanin CD151. *Cell Mol Life Sci*. 76:1595-1604.

Ji, H., L. Chen, Y. Xing, S. Li, J. Dai, P. Zhao, and Y. Wang. 2019. CD82 supports survival of childhood acute myeloid leukemia cells via activation of Wnt/beta-catenin signaling pathway. *Pediatr Res*. 85:1024-1031.

Jin, B., Y. Li, and K.D. Robertson. 2011. DNA methylation: superior or subordinate in the epigenetic hierarchy? *Genes Cancer*. 2:607-617.

Kang, C., Q. Xu, T.D. Martin, M.Z. Li, M. Demaria, L. Aron, T. Lu, B.A. Yankner, J. Campisi, and S.J. Elledge. 2015. The DNA damage response induces inflammation and senescence by inhibiting autophagy of GATA4. *Science*. 349:aaa5612.

Kawahara, M., T. Hori, K. Chonabayashi, T. Oka, M. Sudol, and T. Uchiyama. 2008. Kpm/Lats2 is linked to chemosensitivity of leukemic cells through the stabilization of p73. *Blood*. 112:3856-3866.

Khan, N.S., D.P. Lukason, M. Feliu, R.A. Ward, A.K. Lord, J.L. Reedy, Z.G. Ramirez-Ortiz, J.M. Tam, P.V. Kasperkovitz, P.E. Negoro, T.D. Vyas, S. Xu, M.M. Brinkmann, M. Acharaya, K. Artavanis-Tsakonas, E.M. Frickel, C.E. Becker, Z. Dagher, Y.M. Kim, E. Latz, H.L. Ploegh, M.K. Mansour, C.K. Miranti, S.M. Levitz, and J.M. Vyas. 2019. CD82 controls CpG-dependent TLR9 signaling. *FASEB J*:fj201901547R.

Kharabi Masouleh, B., H. Geng, C. Hurtz, L.N. Chan, A.C. Logan, M.S. Chang, C. Huang, S. Swaminathan, H. Sun, E. Paietta, A.M. Melnick, P. Koeffler, and M. Muschen. 2014. Mechanistic rationale for targeting the unfolded protein response in pre-B acute lymphoblastic leukemia. *Proc Natl Acad Sci U S A*. 111:E2219-2228.

Kitadokoro, K., D. Bordo, G. Galli, R. Petracca, F. Falugi, S. Abrignani, G. Grandi, and M. Bolognesi. 2001. CD81 extracellular domain 3D structure: insight into the tetraspanin superfamily structural motifs. *EMBO J*. 20:12-18.

Komada, Y., and M. Sakurai. 1994. Shedding of CD9 antigen in acute lymphoblastic leukemia. *Leuk Lymphoma*. 12:365-372.

Kreile, M., D. Rots, A. Zarina, L. Rautiainen, Z. Visnevska-Preciniece, Z. Kovalova, and L. Gailite. 2018. Association of ARID5B Genetic Variants with Risk of Childhood B Cell Precursor Acute Lymphoblastic Leukaemia in Latvia. *Asian Pac J Cancer Prev*. 19:91-95.

Kwon, H.Y., J. Bajaj, T. Ito, A. Blevins, T. Konuma, J. Weeks, N.K. Lytle, C.S. Koechlein, D. Rizzieri, C. Chuah, V.G. Oehler, R. Sasik, G. Hardiman, and T. Reya. 2015. Tetraspanin 3 Is Required for the Development and Propagation of Acute Myelogenous Leukemia. *Cell Stem Cell*. 17:152-164.

Lachambre, S., C. Chopard, and B. Beaumelle. 2014. Preliminary characterisation of nanotubes connecting T-cells and their use by HIV-1. *Biol Cell*. 106:394-404.

Lagaudriere-Gesbert, C., F. Le Naour, S. Lebel-Binay, M. Billard, E. Lemichez, P. Boquet, C. Boucheix, H. Conjeaud, and E. Rubinstein. 1997. Functional analysis of four tetraspans, CD9, CD53, CD81, and CD82, suggests a common role in costimulation, cell adhesion, and migration: only CD9 upregulates HB-EGF activity. *Cell Immunol*. 182:105-112.

Lapalombella, R., Y.Y. Yeh, L. Wang, A. Ramanunni, S. Rafiq, S. Jha, J. Staubli, D.M. Lucas, R. Mani, S.E. Herman, A.J. Johnson, A. Lozanski, L. Andritsos, J. Jones, J.M. Flynn, B. Lannutti, P. Thompson, P. Algate, S. Stromatt, D. Jarjoura, X. Mo, D. Wang, C.S. Chen, G. Lozanski, N.A. Heerema, S. Tridandapani, M.A. Freitas, N. Muthusamy, and J.C. Byrd. 2012. Tetraspanin CD37 directly mediates transduction of survival and apoptotic signals. *Cancer Cell*. 21:694-708.

Layani-Bazar, A., I. Skornick, A. Berrebi, M.H. Pauker, E. Noy, A. Silberman, M. Albeck, D.L. Longo, Y. Kalechman, and B. Sredni. 2014. Redox modulation of adjacent thiols in VLA-4 by AS101 converts myeloid leukemia cells from a drug-resistant to drug-sensitive state. *Cancer Res*. 74:3092-3103.

Lazo, P.A., L. Cuevas, A. Gutierrez del Arroyo, and E. Orue. 1997. Ligation of CD53/OX44, a tetraspan antigen, induces homotypic adhesion mediated by specific cell-cell interactions. *Cell Immunol*. 178:132-140.

Le Naour, F., M. Andre, C. Boucheix, and E. Rubinstein. 2006. Membrane microdomains and proteomics: lessons from tetraspanin microdomains and comparison with lipid rafts. *Proteomics*. 6:6447-6454.

Lee, J., H.J. Byun, M.S. Lee, Y.J. Jin, D. Jeoung, Y.M. Kim, and H. Lee. 2017. The metastasis suppressor CD82/KAI1 inhibits fibronectin adhesion-induced epithelial-to-mesenchymal transition in prostate cancer cells by repressing the associated integrin signaling. *Oncotarget*. 8:1641-1654.

Lee, M.S., J. Lee, Y.M. Kim, and H. Lee. 2019. The metastasis suppressor CD82/KAI1 represses the TGF-beta 1 and Wnt signalings inducing epithelial-to-mesenchymal transition linked to invasiveness of prostate cancer cells. *Prostate*. 79:1400-1411.

Leung, K.T., K.Y. Chan, P.C. Ng, T.K. Lau, W.M. Chiu, K.S. Tsang, C.K. Li, C.K. Kong, and K. Li. 2011. The tetraspanin CD9 regulates migration, adhesion, and homing of human cord blood CD34+ hematopoietic stem and progenitor cells. *Blood*. 117:1840-1850.

Leung, K.T., K. Li, Y.T.S. Wong, K.Y.Y. Chan, X.-B. Zhang, A.W.K. Leung, T.Y. Leung, K.S. Tsang, P.C. Ng, and C.K. Li. 2015. The Tetraspanin CD9 Regulates Engraftment and Mobilization of Human CD34+ Hematopoietic Stem/Progenitor Cells and Modulates VLA-4 Activity. *Blood*. 126:1169-1169.

Li, Z.W., and W.S. Dalton. 2006. Tumor microenvironment and drug resistance in hematologic malignancies. *Blood Rev*. 20:333-342.

Liang, Q., R.J. Wiese, O.F. Bueno, Y.S. Dai, B.E. Markham, and J.D. Molkentin. 2001. The transcription factor GATA4 is activated by extracellular signal-regulated kinase 1- and 2-mediated phosphorylation of serine 105 in cardiomyocytes. *Mol Cell Biol*. 21:7460-7469.

Lin, K.K., L. Rossi, N.C. Boles, B.E. Hall, T.C. George, and M.A. Goodell. 2011. CD81 is essential for the re-entry of hematopoietic stem cells to quiescence following stress-induced proliferation via deactivation of the Akt pathway. *PLoS Biol*. 9:e1001148.

Liu, J., A. Masurekar, S. Johnson, S. Chakraborty, J. Griffiths, D. Smith, S. Alexander, C. Dempsey, C. Parker, S. Harrison, Y. Li, C. Miller, Y. Di, Z. Ghosh, S. Krishnan, and V. Saha. 2015. Stromal cell-mediated mitochondrial redox adaptation regulates drug resistance in childhood acute lymphoblastic leukemia. *Oncotarget*. 6:43048-43064.

Liu, T., R.J. Kishton, A.N. Macintyre, V.A. Gerriets, H. Xiang, X. Liu, E.D. Abel, D. Rizzieri, J.W. Locasale, and J.C. Rathmell. 2014. Glucose transporter 1-mediated glucose uptake is limiting for B-cell acute lymphoblastic leukemia anabolic metabolism and resistance to apoptosis. *Cell Death Dis*. 5:e1470.

Liu, W.M., F. Zhang, S. Moshiach, B. Zhou, C. Huang, K. Srinivasan, S. Khurana, Y. Zheng, J.M. Lahti, and X.A. Zhang. 2012. Tetraspanin CD82 inhibits protrusion and retraction in cell movement by attenuating the plasma membrane-dependent actin organization. *PLoS One*. 7:e51797.

Liu, W.M., and X.A. Zhang. 2006. KAI1/CD82, a tumor metastasis suppressor. *Cancer Lett*. 240:183-194.

Locatelli, F., M. Schrappe, M.E. Bernardo, and S. Rutella. 2012. How I treat relapsed childhood acute lymphoblastic leukemia. *Blood*. 120:2807-2816.

Machado-Pineda, Y., B. Cardenes, R. Reyes, S. Lopez-Martin, V. Toribio, P. Sanchez-Organero, H. Suarez, J. Grotzinger, I. Lorenzen, M. Yanez-Mo, and C. Cabanas. 2018. CD9 Controls Integrin alpha5beta1-Mediated Cell Adhesion by Modulating Its Association With the Metalloproteinase ADAM17. *Front Immunol*. 9:2474.

Mannion, B.A., F. Berditchevski, S.K. Kraeft, L.B. Chen, and M.E. Hemler. 1996. Transmembrane-4 superfamily proteins CD81 (TAPA-1), CD82, CD63, and CD53 specifically associated with integrin alpha 4 beta 1 (CD49d/CD29). *J Immunol*. 157:2039-2047.

Marjon, K.D., C.M. Termini, K.L. Karlen, C. Saito-Reis, C.E. Soria, K.A. Lidke, and J.M. Gillette. 2016. Tetraspanin CD82 regulates bone marrow homing of acute myeloid leukemia by modulating the molecular organization of N-cadherin. *Oncogene*. 35:4132-4140.

Meads, M.B., L.A. Hazlehurst, and W.S. Dalton. 2008. The bone marrow microenvironment as a tumor sanctuary and contributor to drug resistance. *Clin Cancer Res*. 14:2519-2526.

Mizoshiri, N., T. Shirai, R. Terauchi, S. Tsuchida, Y. Mori, D. Hayashi, T. Kishida, Y. Arai, O. Mazda, T. Nakanishi, and T. Kubo. 2019. The tetraspanin CD81 mediates the growth and metastases of human osteosarcoma. *Cell Oncol (Dordr)*.

Morandi, F., A.L. Horenstein, F. Costa, N. Giuliani, V. Pistoia, and F. Malavasi. 2018. CD38: A Target for Immunotherapeutic Approaches in Multiple Myeloma. *Front Immunol*. 9:2722.

Muzzafar, T., L.J. Medeiros, S.A. Wang, A. Brahmandam, D.A. Thomas, and J.L. Jorgensen. 2009. Aberrant underexpression of CD81 in precursor B-cell acute lymphoblastic leukemia: utility in detection of minimal residual disease by flow cytometry. *Am J Clin Pathol*. 132:692-698.

Nagant, C., D. Casula, A. Janssens, V.T.P. Nguyen, and B. Cantinieaux. 2018. Easy discrimination of hematogones from lymphoblasts in B-cell progenitor acute lymphoblastic leukemia patients using CD81/CD58 expression ratio. *Int J Lab Hematol*. 40:734-739.

Navarrete-Meneses, M.D.P., and P. Perez-Vera. 2017. [Epigenetic alterations in acute lymphoblastic leukemia]. *Bol Med Hosp Infant Mex*. 74:243-264.

Newton, T.P., C.T. Cummings, D.K. Graham, and K.M. Bernt. 2014. Epigenetics and chemoresistance in childhood acute lymphoblastic leukemia. *International Journal of Hematologic Oncology*. 3:19-30.

Nishioka, C., T. Ikezoe, A. Takeuchi, A. Nobumoto, M. Tsuda, and A. Yokoyama. 2015a. The novel function of CD82 and its impact on BCL2L12 via AKT/STAT5 signal pathway in acute myelogenous leukemia cells. *Leukemia*. 29:2296-2306.

Nishioka, C., T. Ikezoe, J. Yang, A. Nobumoto, S. Kataoka, M. Tsuda, K. Udaka, and A. Yokoyama. 2014. CD82 regulates STAT5/IL-10 and supports survival of acute myelogenous leukemia cells. *Int J Cancer*. 134:55-64.

Nishioka, C., T. Ikezoe, J. Yang, and A. Yokoyama. 2015b. Tetraspanin Family Member, CD82, Regulates Expression of EZH2 via Inactivation of p38 MAPK Signaling in Leukemia Cells. *PLoS One*. 10:e0125017.

Nowak, D., N.L. Liem, M. Mossner, M. Klaumunzer, R.A. Papa, V. Nowak, J.C. Jann, T. Akagi, N. Kawamata, R. Okamoto, N.H. Thoennissen, M. Kato, M. Sanada, W.K. Hofmann, S. Ogawa, G.M. Marshall, R.B. Lock, and H.P. Koeffler. 2015. Variegated clonality and rapid emergence of new molecular lesions in xenografts of acute lymphoblastic leukemia are associated with drug resistance. *Exp Hematol*. 43:32-43 e31-35.

Park, H.S., S. Lee, J. Lee, H.B. Shin, S.M. Yoo, M.S. Lee, and J. Park. 2019. Suppression of CD81 promotes bladder cancer cell invasion through increased matrix metalloproteinase expression via extracellular signal-regulated kinase phosphorylation. *Investig Clin Urol*. 60:396-404.

Pfeifer, H., B. Wassmann, A. Pavlova, L. Wunderle, J. Oldenburg, A. Binckebanck, T. Lange, A. Hochhaus, S. Wystub, P. Bruck, D. Hoelzer, and O.G. Ottmann. 2007. Kinase domain mutations of BCR-ABL frequently precede imatinib-based therapy and give rise to relapse in patients with de novo Philadelphia-positive acute lymphoblastic leukemia (Ph+ ALL). *Blood*. 110:727-734.

Pillozzi, S., M. Masselli, E. De Lorenzo, B. Accordi, E. Cilia, O. Crociani, A. Amedei, M. Veltroni, M. D'Amico, G. Basso, A. Becchetti, D. Campana, and A. Arcangeli. 2011. Chemotherapy resistance in acute lymphoblastic leukemia requires hERG1 channels and is overcome by hERG1 blockers. *Blood*. 117:902-914.

Powner, D., P.M. Kopp, S.J. Monkley, D.R. Critchley, and F. Berditchevski. 2011. Tetraspanin CD9 in cell migration. *Biochem Soc Trans*. 39:563-567.

Quagliano, A., Gopalakrishnapillai, A., Barwe, S.P. 2020. Understanding the mechanisms by which epigenetic modifiers avert chemoresistance in cancer. *Frontiers in Oncology*.

Rada, M., N. Barlev, and S. Macip. 2018. BTK: a two-faced effector in cancer and tumour suppression. *Cell Death Dis*. 9:1064.

Ran, F.A., P.D. Hsu, J. Wright, V. Agarwala, D.A. Scott, and F. Zhang. 2013. Genome engineering using the CRISPR-Cas9 system. *Nat Protoc*. 8:2281-2308.

Rappa, G., T.M. Green, J. Karbanova, D. Corbeil, and A. Lorico. 2015. Tetraspanin CD9 determines invasiveness and tumorigenicity of human breast cancer cells. *Oncotarget*. 6:7970-7991.

Redner, A., S. Hegewisch, J. Haimi, P. Steinherz, S. Jhanwar, and M. Andreeff. 1990. A study of multidrug resistance and cell kinetics in a child with near-haploid acute lymphoblastic leukemia. *Leuk Res*. 14:771-777.

Rocha-Perugini, V., M. Zamai, J.M. Gonzalez-Granado, O. Barreiro, E. Tejera, M. Yanez-Mo, V.R. Caiolfa, and F. Sanchez-Madrid. 2013. CD81 controls sustained T cell activation signaling and defines the maturation stages of cognate immunological synapses. *Mol Cell Biol*. 33:3644-3658.

Rous, B.A., B.J. Reaves, G. Ihrke, J.A. Briggs, S.R. Gray, D.J. Stephens, G. Banting, and J.P. Luzio. 2002. Role of adaptor complex AP-3 in targeting wild-type and mutated CD63 to lysosomes. *Mol Biol Cell*. 13:1071-1082.

Rubinstein, E., F. Le Naour, C. Lagaudriere-Gesbert, M. Billard, H. Conjeaud, and C. Boucheix. 1996. CD9, CD63, CD81, and CD82 are components of a surface tetraspan network connected to HLA-DR and VLA integrins. *Eur J Immunol*. 26:2657-2665.

Sadej, R., A. Grudowska, L. Turczyk, R. Kordek, and H.M. Romanska. 2014. CD151 in cancer progression and metastasis: a complex scenario. *Lab Invest*. 94:41-51.

Sagi, Y., A. Landrigan, R. Levy, and S. Levy. 2012. Complementary costimulation of human T-cell subpopulations by cluster of differentiation 28 (CD28) and CD81. *Proc Natl Acad Sci U S A*. 109:1613-1618.

Saito-Reis, C.A., K.D. Marjon, E.M. Pascetti, M. Floren, and J.M. Gillette. 2018. The tetraspanin CD82 regulates bone marrow homing and engraftment of hematopoietic stem and progenitor cells. *Mol Biol Cell*. 29:2946-2958.

Schink, K.O., K.W. Tan, and H. Stenmark. 2016. Phosphoinositides in Control of Membrane Dynamics. *Annu Rev Cell Dev Biol*. 32:143-171.

Seigneuret, M., A. Delaguillaumie, C. Lagaudriere-Gesbert, and H. Conjeaud. 2001. Structure of the tetraspanin main extracellular domain. A partially conserved fold with a structurally variable domain insertion. *J Biol Chem*. 276:40055-40064.

Shallal, S., and J. Kornbluth. 2000. CD9 expression enhances the susceptibility of myeloma cell lines to cell-mediated cytolysis. *Blood*. 96:224-233.

Sheng, K.C., A.B. van Spriel, K.H. Gartlan, M. Sofi, V. Apostolopoulos, L. Ashman, and M.D. Wright. 2009. Tetraspanins CD37 and CD151 differentially regulate Ag presentation and T-cell co-stimulation by DC. *Eur J Immunol*. 39:50-55.

Shibagaki, N., K. Hanada, H. Yamashita, S. Shimada, and H. Hamada. 1999. Overexpression of CD82 on human T cells enhances LFA-1 / ICAM-1-mediated cell-cell adhesion: functional association between CD82 and LFA-1 in T cell activation. *Eur J Immunol*. 29:4081-4091.

Shoham, T., R. Rajapaksa, C. Boucheix, E. Rubinstein, J.C. Poe, T.F. Tedder, and S. Levy. 2003. The tetraspanin CD81 regulates the expression of CD19 during B cell development in a postendoplasmic reticulum compartment. *J Immunol*. 171:4062-4072.

Spaargaren, M., E.A. Beuling, M.L. Rurup, H.P. Meijer, M.D. Klok, S. Middendorp, R.W. Hendriks, and S.T. Pals. 2003. The B cell antigen receptor controls integrin activity through Btk and PLCgamma2. *J Exp Med*. 198:1539-1550.

Spring, F.A., R.E. Griffiths, T.J. Mankelow, C. Agnew, S.F. Parsons, J.A. Chasis, and D.J. Anstee. 2013. Tetraspanins CD81 and CD82 facilitate alpha4beta1-mediated adhesion of human erythroblasts to vascular cell adhesion molecule-1. *PLoS One*. 8:e62654.

Stipp, C.S., T.V. Kolesnikova, and M.E. Hemler. 2001. EWI-2 is a major CD9 and CD81 partner and member of a novel Ig protein subfamily. *J Biol Chem*. 276:40545-40554.

Stipp, C.S., T.V. Kolesnikova, and M.E. Hemler. 2003. Functional domains in tetraspanin proteins. *Trends Biochem Sci*. 28:106-112.

Stow, P., L. Key, X. Chen, Q. Pan, G.A. Neale, E. Coustan-Smith, C.G. Mullighan, Y. Zhou, C.H. Pui, and D. Campana. 2010. Clinical significance of low levels of minimal residual disease at the end of remission induction therapy in childhood acute lymphoblastic leukemia. *Blood*. 115:4657-4663.

Tai, X.G., Y. Yashiro, R. Abe, K. Toyooka, C.R. Wood, J. Morris, A. Long, S. Ono, M. Kobayashi, T. Hamaoka, S. Neben, and H. Fujiwara. 1996. A role for CD9 molecules in T cell activation. *J Exp Med*. 184:753-758.

Tarrant, J.M., L. Robb, A.B. van Spriel, and M.D. Wright. 2003. Tetraspanins: molecular organisers of the leukocyte surface. *Trends Immunol*. 24:610-617.

Tauer, J.T., L.C. Hofbauer, R. Jung, S. Gerdes, I. Glauche, R.G. Erben, and M. Suttorp. 2015. Impact of long-term exposure to the tyrosine kinase inhibitor imatinib on the skeleton of growing rats. *PLoS One*. 10:e0131192.

Tejera, E., V. Rocha-Perugini, S. Lopez-Martin, D. Perez-Hernandez, A.I. Bachir, A.R. Horwitz, J. Vazquez, F. Sanchez-Madrid, and M. Yanez-Mo. 2013. CD81 regulates cell migration through its association with Rac GTPase. *Mol Biol Cell*. 24:261-273.

Termini, C.M., M.L. Cotter, K.D. Marjon, T. Buranda, K.A. Lidke, and J.M. Gillette. 2014. The membrane scaffold CD82 regulates cell adhesion by altering alpha4 integrin stability and molecular density. *Mol Biol Cell*. 25:1560-1573.

Termini, C.M., and J.M. Gillette. 2017. Tetraspanins Function as Regulators of Cellular Signaling. *Front Cell Dev Biol*. 5:34.

Theunissen, P., E. Mejstrikova, L. Sedek, A.J. van der Sluijs-Gelling, G. Gaipa, M. Bartels, E. Sobral da Costa, M. Kotrova, M. Novakova, E. Sonneveld, C. Buracchi, P. Bonaccorso, E. Oliveira, J.G. Te Marvelde, T. Szczepanski, L. Lhermitte, O. Hrusak, Q. Lecrevisse, G.E. Grigore, E. Fronkova, J. Trka, M. Bruggemann, A. Orfao, J.J. van Dongen, V.H. van der Velden, and C. EuroFlow. 2017. Standardized flow cytometry for highly sensitive MRD measurements in B-cell acute lymphoblastic leukemia. *Blood*. 129:347-357.

Todros-Dawda, I., L. Kveberg, J.T. Vaage, and M. Inngjerdingen. 2014. The tetraspanin CD53 modulates responses from activating NK cell receptors, promoting LFA-1 activation and dampening NK cell effector functions. *PLoS One*. 9:e97844.

Tohami, T., L. Drucker, H. Shapiro, J. Radnay, and M. Lishner. 2007. Overexpression of tetraspanins affects multiple myeloma cell survival and invasive potential. *FASEB J*. 21:691-699.

Touzet, L., F. Dumezy, C. Roumier, C. Berthon, C. Bories, B. Quesnel, C. Preudhomme, and T. Boyer. 2019. CD9 in acute myeloid leukemia: Prognostic role and usefulness to target leukemic stem cells. *Cancer Med*. 8:1279-1288.

Tsitsikov, E.N., J.C. Gutierrez-Ramos, and R.S. Geha. 1997. Impaired CD19 expression and signaling, enhanced antibody response to type II T independent antigen and reduction of B-1 cells in CD81-deficient mice. *Proc Natl Acad Sci U S A*. 94:10844-10849.

Tzoneva, G., A. Perez-Garcia, Z. Carpenter, H. Khiabanian, V. Tosello, M. Allegretta, E. Paietta, J. Racevskis, J.M. Rowe, M.S. Tallman, M. Paganin, G. Basso, J. Hof, R. Kirschner-Schwabe, T. Palomero, R. Rabadan, and A. Ferrando. 2013. Activating mutations in the NT5C2 nucleotidase gene drive chemotherapy resistance in relapsed ALL. *Nat Med*. 19:368-371.

Ullah, M., A. Akbar, N.N. Ng, W. Concepcion, and A.S. Thakor. 2019. Mesenchymal stem cells confer chemoresistance in breast cancer via a CD9 dependent mechanism. *Oncotarget*. 10:3435-3450.

Uretmen Kagiali, Z.C., E. Sanal, O. Karayel, A.N. Polat, O. Saatci, P.G. Ersan, K. Trappe, B.Y. Renard, T.T. Onder, N. Tuncbag, O. Sahin, and N. Ozlu. 2019. Systems-level Analysis Reveals Multiple Modulators of Epithelial-mesenchymal Transition and Identifies DNAJB4 and CD81 as Novel Metastasis Inducers in Breast Cancer. *Mol Cell Proteomics*. 18:1756-1771.

van Deventer, S.J., V.E. Dunlock, and A.B. van Spriel. 2017. Molecular interactions shaping the tetraspanin web. *Biochem Soc Trans*. 45:741-750.

van Spriel, A.B., S. de Keijzer, A. van der Schaaf, K.H. Gartlan, M. Sofi, A. Light, P.C. Linssen, J.B. Boezeman, M. Zuidscherwoude, I. Reinieren-Beeren, A. Cambi, F. Mackay, D.M. Tarlinton, C.G. Figdor, and M.D. Wright. 2012. The tetraspanin CD37 orchestrates the alpha(4)beta(1) integrin-Akt signaling axis and supports long-lived plasma cell survival. *Sci Signal*. 5:ra82.

van Spriel, A.B., K.L. Puls, M. Sofi, D. Pouniotis, H. Hochrein, Z. Orinska, K.P. Knobeloch, M. Plebanski, and M.D. Wright. 2004. A regulatory role for CD37 in T cell proliferation. *J Immunol*. 172:2953-2961.

van Zelm, M.C., J. Smet, B. Adams, F. Mascart, L. Schandene, F. Janssen, A. Ferster, C.C. Kuo, S. Levy, J.J. van Dongen, and M. van der Burg. 2010. CD81 gene defect in humans disrupts CD19 complex formation and leads to antibody deficiency. *J Clin Invest*. 120:1265-1274.

Wang, J., W. Lei, G. Li, H. Ma, H. Guo, and S. Li. 2019. CD151 promotes proliferation and migration of SK-NEP-1 cells via the GSK-3beta/P21/cyclinD signaling pathway. *Pathol Res Pract*. 215:329-334.

Wang, X., M. Lin, J. Zhao, S. Zhu, M. Xu, and X. Zhou. 2018a. TSPAN7 promotes the migration and proliferation of lung cancer cells via epithelial-to-mesenchymal transition. *Onco Targets Ther*. 11:8815-8822.

Wang, Y., Y. Liang, G. Yang, Y. Lan, J. Han, J. Wang, D. Yin, R. Song, T. Zheng, S. Zhang, S. Pan, X. Liu, M. Zhu, Y. Liu, Y. Cui, F. Meng, B. Zhang, S. Liang, H. Guo, Y. Liu, M.K. Hassan, and L. Liu. 2018b. Tetraspanin 1 promotes epithelial-to-mesenchymal transition and metastasis of cholangiocarcinoma via PI3K/AKT signaling. *J Exp Clin Cancer Res*. 37:300.

Wang, Z., C. Wang, Z. Zhou, M. Sun, C. Zhou, J. Chen, F. Yin, H. Wang, B. Lin, D. Zuo, S. Li, L. Feng, Z. Duan, Z. Cai, and Y. Hua. 2016. CD151-mediated adhesion is crucial to osteosarcoma pulmonary metastasis. *Oncotarget*. 7:60623-60638.

Wee, J.L., K.E. Schulze, E.L. Jones, L. Yeung, Q. Cheng, C.F. Pereira, A. Costin, G. Ramm, A.B. van Spriel, M.J. Hickey, and M.D. Wright. 2015. Tetraspanin CD37 Regulates beta2 Integrin-Mediated Adhesion and Migration in Neutrophils. *J Immunol*. 195:5770-5779.

Winter, S.S., J. Ricci, L. Luo, D.M. Lovato, H.M. Khawaja, T. Serna-Gallegos, N. Debassige, and R.S. Larson. 2013. ATP Binding Cassette C1 (ABCC1/MRP1)-mediated drug efflux contributes to disease progression in T-lineage acute lymphoblastic leukemia. *Health (Irvine Calif)*. 5.

Winterwood, N.E., A. Varzavand, M.N. Meland, L.K. Ashman, and C.S. Stipp. 2006. A critical role for tetraspanin CD151 in alpha3beta1 and alpha6beta4 integrin-dependent tumor cell functions on laminin-5. *Mol Biol Cell*. 17:2707-2721.

Woyach, J.A., R.R. Furman, T.M. Liu, H.G. Ozer, M. Zapatka, A.S. Ruppert, L. Xue, D.H. Li, S.M. Steggerda, M. Versele, S.S. Dave, J. Zhang, A.S. Yilmaz, S.M. Jaglowski, K.A. Blum, A. Lozanski, G. Lozanski, D.F. James, J.C. Barrientos, P. Lichter, S. Stilgenbauer, J.J. Buggy, B.Y. Chang, A.J. Johnson, and J.C. Byrd. 2014. Resistance mechanisms for the Bruton's tyrosine kinase inhibitor ibrutinib. *N Engl J Med*. 370:2286-2294.

Xu, H., X. Zhao, D. Bhojwani, S. E, C. Goodings, H. Zhang, N.L. Seibel, W. Yang, C. Li, W.L. Carroll, W.E. Evans, and J.J. Yang. 2020. ARID5B Influences Antimetabolite Drug Sensitivity and Prognosis of Acute Lymphoblastic Leukemia. *Clin Cancer Res*. 26:256-264.

Yamazaki, H., C.W. Xu, M. Naito, H. Nishida, T. Okamoto, F.I. Ghani, S. Iwata, T. Inukai, K. Sugita, and C. Morimoto. 2011. Regulation of cancer stem cell properties by CD9 in human B-acute lymphoblastic leukemia. *Biochem Biophys Res Commun*. 409:14-21.

Yanez-Mo, M., O. Barreiro, M. Gordon-Alonso, M. Sala-Valdes, and F. Sanchez-Madrid. 2009. Tetraspanin-enriched microdomains: a functional unit in cell plasma membranes. *Trends Cell Biol*. 19:434-446.

Yang, H., C. Bueso-Ramos, C. DiNardo, M.R. Estecio, M. Davanlou, Q.R. Geng, Z. Fang, M. Nguyen, S. Pierce, Y. Wei, S. Parmar, J. Cortes, H. Kantarjian, and G. Garcia-Manero. 2014. Expression of PD-L1, PD-L2, PD-1 and CTLA4 in myelodysplastic syndromes is enhanced by treatment with hypomethylating agents. *Leukemia*. 28:1280-1288.

Yang, Y.G., I.N. Sari, M.F. Zia, S.R. Lee, S.J. Song, and H.Y. Kwon. 2016. Tetraspanins: Spanning from solid tumors to hematologic malignancies. *Exp Hematol*. 44:322-328.

Yoon, S.O., I.Y. Lee, X. Zhang, M.C. Zapata, and Y.S. Choi. 2014. CD9 may contribute to the survival of human germinal center B cells by facilitating the interaction with follicular dendritic cells. *FEBS Open Bio*. 4:370-376.

Yoon, S.O., X. Zhang, A.S. Freedman, D. Zahrieh, I.S. Lossos, L. Li, and Y.S. Choi. 2010. Down-regulation of CD9 expression and its correlation to tumor progression in B lymphomas. *Am J Pathol*. 177:377-386.

Yunta, M., and P.A. Lazo. 2003. Apoptosis protection and survival signal by the CD53 tetraspanin antigen. *Oncogene*. 22:1219-1224.

Zampini, M., C. Tregnago, V. Bisio, L. Simula, G. Borella, E. Manara, C. Zanon, F. Zonta, V. Serafin, B. Accordi, S. Campello, B. Buldini, A. Pession, F. Locatelli, G. Basso, and M. Pigazzi. 2018. Epigenetic heterogeneity affects the risk of relapse in children with t(8;21)RUNX1-RUNX1T1-rearranged AML. *Leukemia*. 32:1124-1134.

Zeng, T.D., B. Zheng, W. Zheng, and C. Chen. 2018. CD82/KAI1 inhibits invasion and metastasis of esophageal squamous cell carcinoma via TGF-beta1. *Eur Rev Med Pharmacol Sci*. 22:5928-5937.

Zhang, B., Z. Zhang, L. Li, Y.R. Qin, H. Liu, C. Jiang, T.T. Zeng, M.Q. Li, D. Xie, Y. Li, X.Y. Guan, and Y.H. Zhu. 2018. TSPAN15 interacts with BTRC to promote oesophageal squamous cell carcinoma metastasis via activating NF-kappaB signaling. *Nat Commun*. 9:1423.

Zhang, T., A. Pilko, and R. Wollman. 2020. Loci specific epigenetic drug sensitivity. *Nucleic Acids Res*.

Zhao, S.J., H.D. Zhao, J. Li, H. Zhang, D.T. Gao, and Q. Wang. 2018. CD151 promotes breast cancer metastasis by activating TGF-beta1/Smad signaling pathway. *Eur Rev Med Pharmacol Sci*. 22:7314-7322.

Zhou, B., L. Liu, M. Reddivari, and X.A. Zhang. 2004. The palmitoylation of metastasis suppressor KAI1/CD82 is important for its motility- and invasiveness-inhibitory activity. *Cancer Res*. 64:7455-7463.

Appendix A

IRB APPROVAL

Nemours Office of Human Subjects Protection
Nemours/Alfred I. duPont Hospital for Children
1600 Rockland Road
Wilmington, DE 19803
Fax: 302-651-4683
Office: 302-298-7613

DATE:	May 2, 2019
TO:	Sonali Barwe, PhD
FROM:	Nemours IRB 2
STUDY TITLE:	[1427910-1] Generation of patient-derived xenograft models of pediatric leukemia
IRB #:	1427910
SUBMISSION TYPE:	New Project
ACTION:	RESEARCH - NOT HSR
REVIEW DATE:	April 30, 2019

Thank you for your submission of New Project materials for this project. Nemours IRB 2 has determined this project does not meet the definition of human subject research under the purview of the IRB according to federal regulations.

Please note that any project modifications that may alter this non-human subject research determination must be submitted to the IRB for review.

Reviewed documents in this submission:

- Application Form - Application - Initial Review_SB_COG.docx (UPDATED: 04/15/2019)
- Application Form - Application - Barwe_COG_Exempt.docx (UPDATED: 04/15/2019)
- Investigator Agreement - Research Team Member Agreement_PI.docx (UPDATED: 04/15/2019)
- Investigator Agreement - Research Team Member Agreement_PI.docx (UPDATED: 04/15/2019)
- Protocol - Barwe_COG_IRB_Protocol.docx (UPDATED: 04/15/2019)

If you have any questions, please contact Caroline Schierle at Nemours Children's Specialty Care, 807 Children's Way, Jacksonville, FL 32207 at (904) 697-3415 or Caroline.Schierle@nemours.org. Please include your study title and reference number in all correspondence with this office.

Appendix B

IRB APPROVAL

Institutional Animal Care and Use Committee
1600 Rockland Road
Wilmington, DE 19803
p (302) 651-6826 f (302)-651-6881
IACUC@nemours.org

MEMORANDUM

DATE: July 18, 2019

TO: Sonali Barwe, PhD

FROM: Paul T. Fawcett, PhD

SUBJECT: Leukemia xenograft models for pre-clinical drug testing

The Institutional Animal Care and Use Committee (IACUC) have reviewed the submitted the submitted annual review on the above referenced project and the following decision has been made:

Action: Approved

Date of Action: 8/15/2019

Approval Period: August 15, 2019 through August 14, 2020 for annual renewal
August 16, 2018 through August 15, 2021 for three year renewal

Protocol Approval Number: NBR 2009-007

Approved Number of Animals: 1,427

Please submit your Biosafety Classification form electronically to the Alfred I. duPont Hospital for Children Institutional Biosafety Committee via the link:

http://www.nemours.org/pediatric-research/approval/biosafety-committee.html

Please note that the study cannot begin until the Office of Regulatory Compliance in Research Administration has received all approvals.

Please maintain this approval with your project records. A tally of the number of animals approved and the number ordered for the project will be maintained in the Life Science Center. If changes occur in your protocol or if you require more animals than approved, an amendment to your protocol will need to be submitted for consideration

If you have any questions regarding this memorandum, please contact Paul T. Fawcett, Ph.D. at x 6776 or email: pfawcett@nemours.org.

Appendix C

REPRINT PERMISSION POLICIES

Epigenetic drug combination overcomes osteoblast-induced chemoprotection in pediatric acute lymphoid leukemia

Author: Anthony Quagliano,Anilkumar Gopalakrishnapillai,Sonali P. Barwe
Publication: Leukemia Research
Publisher: Elsevier
Date: May 2017

Eviction from the sanctuary: Development of targeted therapy against cell adhesion molecules in acute lymphoblastic leukemia

Author: Sonali P. Barwe,Anthony Quagliano,Anilkumar Gopalakrishnapillai
Publication: Seminars in Oncology
Publisher: Elsevier
Date: April 2017

Keywords: epigenetic aberrations, chemoresistance, mechanism, cancer, epigenetic drugs, epigenetic combination therapies

Citation: Quagliano A, Gopalakrishnapillai A and Barwe SP (2020) Understanding the Mechanisms by Which Epigenetic Modifiers Avert Therapy Resistance in Cancer. *Front. Oncol.* 10:992. doi: 10.3389/fonc.2020.00992

Received: 14 March 2020; **Accepted:** 19 May 2020;
Published: 24 June 2020.

Edited by:
Atsushi Fujimura, Okayama University, Japan

Reviewed by:
Hamid Morjani, Université de Reims Champagne-Ardenne, France
Antonis Kirmizis, University of Cyprus, Cyprus

***Correspondence:** Sonali P. Barwe, **sbarwe@nemours.org**